Granulocyte-Macrophage Colony-Stimulating Factor: Linking the Adaptive and Innate Immune Systems in Autoimmune Demyelinating Disease

by

Patrick C. Duncker

A dissertation submitted in partial fulfillment
of the requirements for the degree of
Doctor of Philosophy
(Immunology)
in the University of Michigan
2019

Doctoral Committee:

Professor Benjamin M. Segal, Chair
Associate Professor Yasmina Laouar
Professor Bethany B. Moore
Professor Gabriel Nuñez
Associate Professor Michal A. Olszewski

Patrick C. Duncker

dunckerp@umich.edu

ORCiD: 0000-0002-3292-0878

DEDICATION

No person is an island entire of itself; every person
is a piece of the continent, a part of the main;
if a clod be washed away by the sea, all
are less, as well as if a promontory were, as
well as any manner of thy friends or of thine
own were; any person's death diminishes me,
because I am involved in humankind.
And therefore, never send to know for whom
the bell tolls; it tolls for thee

Without the love and support of my parents and fiancée Kendal,
nothing would be possible.

Poem adapted from Meditation XVII, Devotions Upon Emergent Occasions, John Donne, 1624.

ACKNOWLEDGMENTS

I am grateful to all who have helped me throughout my graduate career.

I thank the Program in Immunology at the University of Michigan for the opportunity to obtain my Ph.D. Members of this program have worked hard to ensure students are afforded every opportunity to pursue their interests. Without funding sources, including Rackham Travel Grants, the Immunology Training Grant, and NIH grants funding this work, I would not have been able to perform these studies or travel around the country, or to other countries, to present my work to the greater scientific community.

Dr. Benjamin Segal has been an incredible mentor and I am extremely grateful to have had the opportunity to train under his tutelage. His scientific and moral rigor, attention to detail, and care for his students, trainees, employees, and patients are exemplary and admirable. Our personalities and mentor: mentee needs/ expectations are remarkably complementary. I should be so lucky as to ever have another relationship as ours. The lessons he has taught me will not soon be forgotten.

To the members of the neuroimmunology research group, past (Josh, Amanda, Jesse, Giles, Penney, Justin, Heather, Keven, Stephen, Tina, and Lisa) and present (Ashley, Ying-Jian, Sas, Niki, Jeff, Andrew, Stephen, and Amiya), working together has not only helped me perform the work for my thesis project but also made it more enjoyable to go to work every day and put in the long hours. Several of my best friendships have formed from this group. Josh, Amanda, Giles, and Ashley, our collaborative efforts have strengthened the merit of our individual works and I am a better scientist for it. Jesse and Niki, your assistance in carrying out experiments and

troubleshooting new techniques have been invaluable in my research efforts. Ying-Jian, you always have a great attitude and it has been a great pleasure working with you. David Irani, your input into my projects is appreciated and has been taken to strengthen the quality of my work.

To the members of my thesis committee; Yasmina Laouar, Beth Moore, Gabriel Nuñez, and Michal Olszewski, I am grateful for the time you have given to help me progress my graduate career. Your critical input and advice on my projects kept me on track and contributed to the quality of my work.

To my parents Steve and Marisa, without your continued support throughout my life I would never have made it to this point. You gave me the gift of education and encouraged me to achieve my ambitions.

To my fiancée Kendal, I am grateful for your companionship, support, and encouragement through the last years of my graduate career. I would not want to take the next step in life without you and can't wait to start our family together.

TABLE OF CONTENTS

LIST OF FIGURES

ABSTRACT

Multiple sclerosis (MS) is a debilitating disorder of the central nervous system (CNS) characterized by motor, sensory, and visual deficits. Published literature supports the contention that MS is an autoimmune disease mediated by auto-reactive $CD4^+$ T-helper (Th) cells which infiltrate the CNS from circulation. Infiltrating Th cells are reactivated within the CNS in an antigen-specific manner, driving recruitment, differentiation, and activation of circulating myeloid cells, and ultimately resulting in demyelination and axonopathy. Much work has been devoted to elucidating the roles of each of the known Th cell subsets, and the inflammatory mediators they produce, in CNS autoimmune disease. One Th cell mediator, granulocyte-macrophage colony-stimulating factor (GM-CSF), has been proposed to be a critical inflammatory cytokine that connects CNS-infiltrating Th cells with the pathogenic programming of tissue-invading myeloid cells. The aim of my dissertation project was to determine the mechanism of action of GM-CSF in the initiation, progression, and maintenance of experimental autoimmune encephalomyelitis (EAE), widely used as an animal model of MS.

The Segal lab and others have previously shown that C57BL/6 mice deficient in GM-CSF are resistant to EAE. We found that lymph node cells from immunized GM-CSF deficient mice mount an impaired MOG_{35-55}-specific proliferative and cytokine response. Insufficient Th priming could explain, in part, the resistance of those mice to EAE. To study the role of GM-CSF during the effector phase, we transferred encephalitogenic T cells from MOG_{35-55}-primed wild-type (WT) mice into naïve GM-CSF receptor-deficient mice (*Csf2r*$^{-/-}$). Although *Csf2r*$^{-/-}$ recipients developed EAE with similar incidence and initial disease trajectory as their WT counterparts, they underwent

clinical remission. The total number of cells infiltrating the CNS at peak EAE were comparable between groups, but neutrophils, myeloid-derived dendritic cells (mDCs), and MOG_{35-55}-specific T cells were reduced in *Csf2r*$^{-/-}$ recipients. This suggested that either a paucity of infiltrating neutrophils, mDCs, and/ or encephalitogenic T cells could be responsible for the remitting phenotype exhibited by *Csf2r*$^{-/-}$ recipients.

To investigate the basis of the differences in the CNS infiltration, we compared chemokine expression in the spinal cords of WT and *Csf2r*$^{-/-}$ recipients during EAE. The myeloid cell chemoattractants CXCL1, CXCL2, and CCL2 were consistently comparable between groups, and CCL6 was comparable at disease onset but diverged thereafter. CCL6 levels progressively rose in the CNS of WT mice but dropped dramatically in *Csf2r*$^{-/-}$ mice by peak disease. CCR1, the sole receptor for CCL6, is expressed by subsets of leukocytes and has been detected on inflammatory cells in MS lesions. Its role in EAE remains to be elucidated. CCR1 blockade beginning at the time of T cell transfer reduced CNS-infiltration by monocytes and classical DCs (cDCs) and prevented the development of EAE. Conversely, CCR1 blockade following EAE onset triggered clinical remission associated with a reduction in CNS-infiltrating neutrophils, closely resembling the phenotype of *Csf2r*$^{-/-}$ recipients.

Together, these studies provide insight into the pleiotropic, and extensive, roles GM-CSF plays in the development and maintenance of CNS autoimmunity. We propose the following model: encephalitogenic T cells are reactivated in the CNS by cDCs and secrete GM-CSF. GM-CSF promotes the production of CCL6 within the CNS and expression of CCR1 by peripheral myeloid cells. CCL6:CCR1 interactions promote the migration of monocytes and neutrophils across the blood-brain-barrier and into the CNS parenchyma where they directly damage the myelin sheath and axons. Concurrently, GM-CSF enhances expansion of CNS-resident cDCs and

differentiation of monocytes into mDCs. cDCs and mDCs perpetuate neuroinflammation by activating myelin-reactive T cells, in a feed-forward pathway. The collective actions of GM-CSF result in sustained neuroinflammation and chronic disability. The results presented herein provide evidence to support the development of new MS therapeutics targeted at the myeloid cell compartment and the GM-CSF/ CCL6/ CCR1 pathway, in particular.

CHAPTER 1 – Introduction

Multiple sclerosis (MS) is a demyelinating disorder of the central nervous system (CNS) that presents with visual, motor, and sensory deficits (1). It is estimated that more than 2 million people have MS, at least 400,000 reside in the United States (2). The majority of people with MS initially present with a relapsing-remitting (RRMS) course, characterized by self-limited episodes of neurological dysfunction (relapses), separated by clinically quiescent periods (remissions). Within 20 years, the majority of individuals with RRMS enter a progressive stage of disease (secondary progressive MS, SPMS) during which they experience a relentless, gradual decline in neurological function. Over the past 20 years, 15 disease-modifying therapies (DMTs) have been introduced that significantly reduce the frequency of MS relapses. However, none are cures, and none reverse existing CNS damage (3–5). A significant percentage of patients are unresponsive to each of the currently available DMTs (6). MS imparts substantial financial and personal burdens to patients and society. There is a dire need for novel, more effective therapies.

Multiple Sclerosis: Pathology, Treatment, and Immunology

While the cause of MS is unknown, the pathological consequences of the disease have been appreciated for over 150 years (7). By definition, MS lesions are disseminated over space and time. Lesions can form at literally any site in the CNS, including the brain, spinal cord, and/ or optic nerves. The pathological hallmarks of MS lesions are perivascular inflammatory infiltrates, surrounded by focal demyelination and axonopathy (8, 9). CNS infiltrates in MS post-mortem tissues are composed of macrophages, DCs, B cells, and T cells (10, 11). It is widely believed that

damage to the myelin sheath causes initial neurological symptoms by reducing the efficiency of axonal signaling. While remyelination can occur in MS lesions, irreversible axonal transection has been observed even in early stage disease (8).

Multiple sclerosis is believed to be an autoimmune disease, mediated by myelin-reactive $CD4^+$ T cells. This theory is supported by the animal model, experimental autoimmune encephalomyelitis (EAE), which can be induced by the transfer of highly purified myelin peptide reactive $CD4^+$ Th1 or Th17 cell lines or clones into naïve syngeneic rodents. The majority of DMTs currently used to manage MS were first demonstrated to be effective in EAE as a proof of concept, thereby validating the translational relevance of the model. DMTs have evolved dramatically since the introduction of the immunomodulating agent, interferon (IFN) beta-1b, in 1993 (7). Each of these agents, which decrease the rate of MS relapses, is believed to primarily act by modulating immunological pathways, either broadly, such as in the case of IFNbeta-1b, or in a more targeted fashion, as in the case of B cell depleting monoclonal antibodies. The newest generation of DMTs were deliberately designed to directly target T and/ or B lymphocytes via depletion (alemtuzumab and ocrelizumab), or blockade of their migration to the CNS (natalizumab and fingolimod) (12, 13).

Further justification for targeting the immune system as a therapeutic strategy in MS comes from genome-wide association studies. Among the 200+ MS susceptibility loci thus far identified, most are immune related, and many overlap with those associated with other autoimmune diseases (14). The strongest heritable factors have been linked to major histocompatibility complex class II (MHCII) loci, which are requisite genes in activation of $CD4^+$ T lymphocytes, and genes that encode receptors for the T cell survival/ growth cytokines, IL-2 and IL-7 (15–17). Despite the contribution of genetic factors to MS pathogenesis, environmental factors are also important.

Hence, the concordance rate of MS among monozygotic twins is only 25% at most (18–20). Several studies have found comparable frequencies of myelin-reactive T cells among blood cells from healthy individuals and people with MS, and it is postulated that environmental exposures in some way enhance the priming, differentiation, and/ or CNS access of encephalitogenic T cells, or inhibit endogenous immunoregulatory pathways (21–23).

Experimental Autoimmune Encephalomyelitis

Experimental autoimmune encephalomyelitis (EAE) is an animal model which simulates many of the clinical and pathological features of MS. EAE was serendipitously discovered in the late 1920s when it was recognized that a subset of patients vaccinated against rabies developed an inflammatory demyelinating syndrome shortly thereafter (24). The vaccine was produced by infecting animals with active rabies virus and recovering the virus from CNS tissue. The virus within the isolated material was "inactivated" by a chemical procedure and then administered intramuscularly to vaccinate humans (25). It was ultimately demonstrated that the post-vaccination demyelinating syndrome resulted from the induction of an immune response against heterologous CNS myelin, which contaminated the vaccine. Rivers and Schwentker subsequently showed that immunizations of macaque monkeys with brain tissue emulsified in adjuvant reproducibly induced a demyelinating encephalitis (24, 26). Later analyses of the CNS of rhesus monkeys with experimentally induced encephalitis revealed disseminated lesion formation and CSF abnormalities reminiscent of MS (27).

These studies first suggested that MS might have an autoimmune etiology and led to the development of EAE models in a range of mammalian species, most commonly rodents. EAE can be induced in mice from different genetic backgrounds and with different immunogenic myelin

proteins or peptides. The clinical course may vary with mice strain and autoantigen. For example, B10.PL mice immunized with the N terminal region of myelin basic protein (MBP) develop a self-limited single attack of myelitis, followed by complete remission. In contrast, EAE induced in SJL mice with the immunogenic peptide of proteolipid protein ($PLP_{139-151}$), manifests as a relapse-remitting course that mirrors to RRMS (28, 29). C57BL/6 mice immunized with the immunogenic peptide of myelin-oligodendrocyte glycoprotein (MOG_{35-55}) develop a monophasic disease, often characterized by complete hindlimb paralysis and sustained disability. The latter is the most common mouse model of MS, due in large part to the wide availability of genetically engineered mice on the C57BL/6 background. All of the EAE models display clinical and pathological similarities to MS, are mediated by $CD4^+$ T cells, and require MHCII expressing antigen presenting cells (APCs) to prime the encephalitogenic T cells in the peripheral lymphoid tissues and to reactivate them in the CNS.

EAE can be induced either by active immunization with the relevant immunogenic peptides, or proteins, or by the adoptive transfer of myelin-reactive $CD4^+$ T cells to syngeneic recipients. The EAE model has not only contributed to our understanding of MS pathogenesis and guided the development of DMTs, but it has increased our understanding of target organ-specific autoimmunity and immunoregulatory pathways in general.

$CD4^+$ T cells Activation, Function, Phenotypes, and Autoimmunity

The immune system is broadly separated into innate and adaptive immune cells. Innate cells, including monocytes, macrophages, dendritic cells, and granulocytes, directly interact with highly conserved pathogen and danger associated molecular patterns (PAMPs and DAMPs) to sense pathogens and produce the appropriate pro-inflammatory cytokines and immune mediators

for their eradication. One prominent function, which is carried out most efficiently by dendritic cells, is phagocytosis of pathogens or their components, processing of foreign proteins, and presentation of the resultant peptides to T cells. $CD4^+$ T cells are a member of the adaptive immune system and respond to antigenic peptides presented bound to the MHCII complex on the surface of professional APCs by proliferating and producing effector cytokines.

Each T cell clone expresses a unique antigen-specific receptor (the T cell receptor or TCR) which is generated via genetic recombination. The rearrangement of genes at the TCR locus confers the ability to produce over 10^{15} possible TCR variants. TCR diversity allows the immune system to respond to a broad range of bacteria, viruses, and parasites, as well as mutated proteins, in a customized fashion (30). Ideally, each $CD4^+$ TCR would be specific to antigens derived from microbial pathogens, parasites, or mutated cells exclusively. However, inevitably TCRs are generated that have the capacity to recognize native host peptides (often referred to as "self" or autoantigens). The failure to delete such autoreactive T cells during negative selection in the thymus can ultimately lead to the development of autoimmune diseases such as arthritis and MS.

When the TCR is engaged on naïve $CD4^+$ T cells, they proliferate, produce growth factors such as IL-2, and upregulate homing molecules. They differentiate along a particular T-helper (Th) cell lineage and acquire a particular effector cytokine panel, depending on the polarizing cytokines they are exposed to during the course of activation. APCs express a number of T cell costimulatory molecules and secrete polarizing cytokines that guide Th cell differentiation along lineages that are commensurate with the type of pathogen eliciting the immune response. Researchers have identified a broad range of $CD4^+$ T cells that have distinct functional phenotypes. The most common of these have been designated Th1, Th2, Th17, and T regulatory (Treg) cells. Th1 cells arise largely in response to intracellular pathogens, such as viruses and some bacteria, and are

polarized by interleukin 12 (IL-12). Memory Th1 cells produce interferon gamma (IFNγ) as their signature cytokine. IFNγ has pleiotropic effects including the recruitment of monocytes/ macrophages to sites of inflammation, promotion of immunoglobulin class switching to IgG2a, induction of free radical species by myeloid cells, and elimination of pathogen-infected cells. Conversely, Th2 differentiation is driven by IL-4, secreted by accessory cells (including mast cells and innate lymphoid cells) in response to extracellular bacteria and fungi. Th2 cells produce IL-4 themselves, as well as IL-5, and IL-33, all of which promote B cell proliferation, immunoglobulin class switching to IgG1, IgE antibody release and eosinophil mobilization and activation. Extracellular bacteria and fungi elicit a Th17 phenotype via induction of IL-6, IL-23, and TGF-β by APCs. Th17 cells produce IL-17 upon reactivation which promotes infiltration of neutrophils. Lastly, TGF-β-induced Tregs are programmed via the transcription factor FoxP3 to dampen potentially destructive inflammatory responses. Collectively, $CD4^+$ T cell subsets interact in a coordinated fashion during homeostasis to protect the host from exogenous pathogens while preventing unnecessary bystander damage to healthy host tissues. When this finely balanced system becomes dysregulated, autoimmunity can ensue.

The manifestation of an autoimmune response, and its impact on the host, is dependent on the location of the autoantigen and the characteristics of the autoreactive Th subset that is dominant. MS was historically characterized as a Th1-mediated autoimmune demyelinating disease since large amounts of IFNγ and macrophage-rich infiltrates were detected in MS lesions. However, it is now believed that MS it is heterogeneous and can be driven by Th1 or Th17 cells, or a combination of both (31, 32). Unexpectedly, it has been shown that most of the Th1/ Th17 cell polarizing cytokines, transcription factors, and canonical effector cytokines are dispensable, on an individual basis, for the induction of EAE in C57BL/6 mice actively immunized with

MOG_{35-55} in CFA (33–37). These observations are consistent with the contention that EAE can be driven independently by Th1 and Th17 pathways. Granulocyte-macrophage colony-stimulating factor (GM-CSF) has been portrayed as the only T cell effector cytokine that is universally required for the development of EAE (33, 35, 38–45).

Granulocyte-Macrophage Colony-Stimulating Factor

GM-CSF is a myeloid cell growth and differentiation factor originally characterized by its ability to drive the development of granulocytes and macrophages from stimulated bone marrow cells *in vitro* (46). During homeostasis, GM-CSF promotes the development of circulating eosinophils and tissue-resident macrophages and dendritic cells, though GM-CSF deficient mice (*Csf2*$^{-/-}$) only display minor perturbations in myeloid cell development (47, 48). Under inflammatory conditions, it acts peripherally to promote the mobilization of GM-CSF receptor (GM-CSFR) expressing myeloid cells from the bone marrow, into the blood, and locally to promotes myeloid cell activation, differentiation, and survival within inflamed tissues. Although GM-CSF can be produced by a variety of cells during homeostasis and inflammation, during EAE its primary source is encephalitogenic T cells (49).

At the initiation of EAE, it is believed that encephalitogenic T cells enter the CNS where they are reactivated by local APCs presenting endogenous myelin peptides bound to MHCII molecules (50). This interaction drives the myelin-reactive $CD4^+$ T cells to secrete GM-CSF, which stimulates APCs to produce pro-inflammatory cytokines and chemokines including IL-1β, IL-6, IL-12, CCL2, TNFα, and IL-23. A feedforward loop is established whereby IL-23 signals encephalitogenic T cells to produce more GM-CSF, and GM-CSF signals APC to produce more IL-23 (38, 51–53). Circulating neutrophils, monocytes, dendritic cells, and additional lymphocytes

are secondarily recruited to the nascent EAE lesion. GM-CSF then acts on the infiltrating myeloid cells to enhance phagocytosis of myelin and production of toxic factors. GM-CSF also drives monocytes to differentiate into macrophages and monocyte-derived dendritic cells. It has been suggested that this GM-CSF dependent circular process, of T cell:APC reactivation and myeloid cell activation within the CNS, amplifies demyelination and axonopathy in mice with EAE, as summarized in the illustration by M. McGeachy in Fig. 1.1 (38).

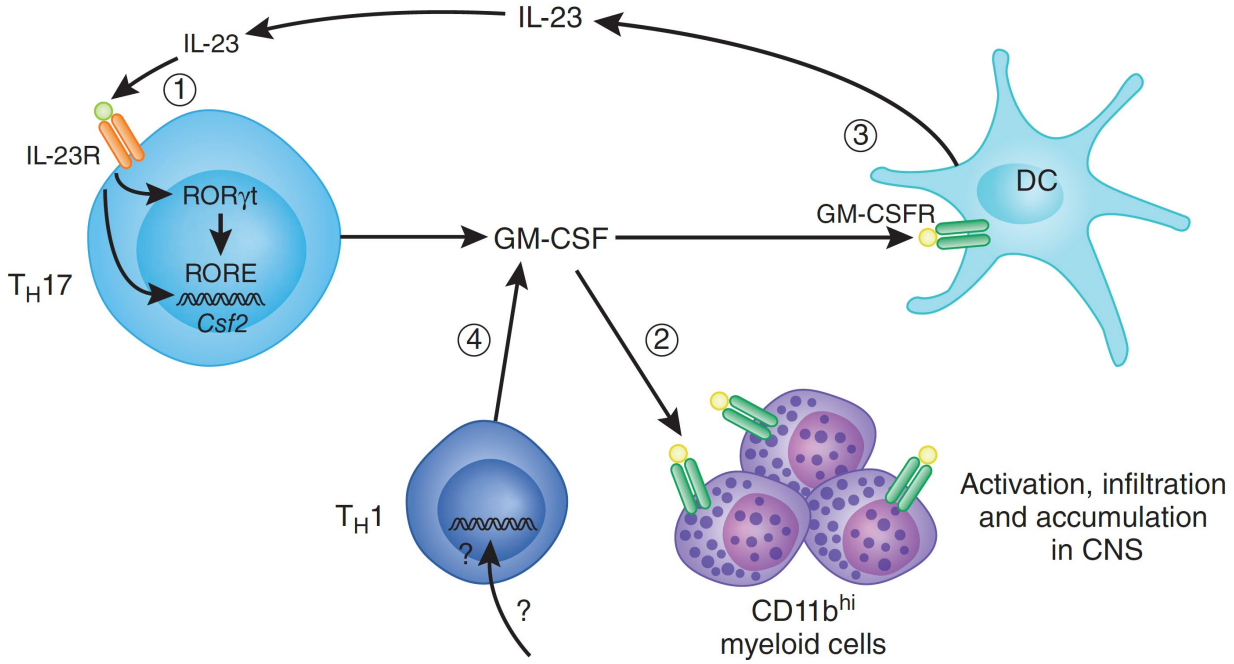

Figure 1.1 – Proposed functions of GM-CSF in CNS autoimmunity (38)**.**

Csf2$^{-/-}$ mice are resistant to EAE induced by active immunization with MOG_{35-55}. The mechanism underlying this protection is subject to debate (39, 41, 42, 44, 45, 49). Studies in active immunization and adoptive transfer EAE models have suggested that GM-CSF is required to prime encephalitogenic T cells (42), drive T cell reactivation in the CNS (39, 44), activate CNS-resident microglia (49), enhance accumulation of Ly6C^{hi} monocytes (54) in the CNS, and activate CCR2^{+} monocytes within the CNS (41). Despite their differences, these studies share certain conclusions. GM-CSF was consistently found to play a role in modulating myeloid cells (particularly

monocytes, macrophages, microglia and/ or dendritic cells) and often to have an indirect impact on the priming and/ or reactivation of encephalitogenic T cells.

Dendritic Cell Heterogeneity and Functions in EAE

Dendritic cells were originally identified in secondary lymphoid tissues and distinguished by their morphological features, having large nuclei and "abundant cytoplasm arranged in processes of varying length and width" (55). In mice, DCs are generally characterized by expression of MHCII and CD11c and are considered professional APCs, due to their ability to activate and polarize naïve $CD4^+$ T cells. DCs are a heterogeneous population of cells and have been subdivided based on their relative expression of CD11b, CD103, Langerin, CX3CR1, CD115, as well as a variety of other markers that vary with their location, ontogeny, and activation state (56). Although it is widely accepted that $MHCII^+$ APCs are required for initiation of autoimmune demyelination, there remains a lack of clarity regarding exactly which cell type is the initiating APC in EAE, and potentially MS.

In the MOG_{35-55}-induced model of EAE, B cells are dispensable for EAE pathogenesis (57, 58). In-depth analyses have been performed to compare potential APC populations during the course of EAE (59, 60). Microglia are CNS-resident cells which upregulate MHCII and CD11c upon activation and have been proposed to be the requisite APC in EAE. A recent study compared microglia to resident macrophages which populate the meninges (mMΦs), perivascular spaces (pvMΦs), and choroid plexus (cpMΦs) in the naïve CNS (61). Microglia are restricted to the CNS parenchyma, derived from cells that migrate to the CNS from the embryonic yolk sac during early development, and are self-renewed. In contrast, macrophages that exist in border areas of the CNS are of mixed origin and transcriptionally diverse. Similar to microglia; mMΦs, pvMΦs, and

cpMΦs populate the CNS early in development. However, cpMΦs are rapidly replaced during development, while mMΦs and pvMΦs are more stable into adulthood. All populations were dependent on the transcription factor Pu.1 but only mMΦs required IRF8. During autoimmune CNS inflammation, mMΦs were rapidly replaced by circulating monocytes which infiltrated the CNS while pvMΦs and microglia were each self-renewing and expanded *in situ*.

Dendritic cells are also heterogeneous. Nakano et al. showed that the surface markers CD88 and CD26 can be used to distinguish two subsets of DCs that differ based on their hematopoietic origin (62). CD88, the C5a complement receptor, is restricted to DCs derived from a common monocyte progenitor and can be used to reliably identify monocyte-derived DCs (moDCs). CD26, dipeptidyl peptidase (an enzyme that catalyzes peptide hydrolysis), is restricted to DCs derived from the common dendritic cell progenitor in the bone marrow and are termed classical DCs (cDCs). $CD88^+$ moDC development is promoted by GM-CSF signaling and the transcription factor IRF4, while $CD26^+$ cDCs are dependent on the ligation of the FLT3 receptor and the transcription factor ZBTB46 (63–65). The experimental tools necessary to study the importance of these subsets in inflammation have been developed, but they have yet to be studied in the EAE literature.

Rationale and Specific Aims

Although it is widely believed that $CD4^+$ T cells initiate inflammatory lesions in MS, their activation represents one of many steps in the pathogenesis of CNS autoimmune demyelinating disease. Myeloid cells comprise a prominent component of the immune cells in MS and EAE lesions. GM-CSF holds a prominent role in connecting the lymphocyte mediated adaptive arm with the innate arm of the immune system. It drives myeloid cells to mobilize from the bone marrow into the circulation, home to sites of inflammation and differentiate into macrophages or

dendritic cells within the target tissue. The infiltrating myeloid cells escalate neuroinflammation by secreting chemokines and cytokines and can directly destroy myelin and damage axons. Current MS therapeutics target lymphocytes, either by depletion or blockade of CNS infiltration. However, none of the currently used drugs are effective in all patients; none are cures and none reverse existing damage. Understanding the interplay between CNS-autoantigenic lymphocytes, the myeloid cells they recruit, and the functions that the different leukocytes carry out in tandem, may reveal novel approaches to target the destructive immune cells and thereby attenuate autoimmune demyelination.

In the studies outlined in this dissertation, we investigate the role of GM-CSF dependent pathways in the initiation, progression, and maintenance of autoimmune demyelination.

- **Aim 1: Chapter 2:** Interrogate the role of GM-CSF in the development of EAE. We used mice deficient in GM-CSF or GM-CSFR, and an anti-GM-CSF neutralizing antibody, to explore the impact of GM-CSF signaling on the clinical and histopathological aspects of EAE, and to elucidate its mechanism of action. We tested our hypothesis that GM-CSF plays its most important role during the effector stage of EAE, by shaping the cellular composition and spatial distribution of the inflammatory cells that infiltrate the CNS.
- **Aim 2: Chapter 3:** Investigate GM-CSF-dependent activation of the CCR1 chemokine pathway during EAE and assess the impact of CCR1 ligands on histopathological and clinical features of the disease. We interrogated the relationship between GM-CSF signaling and the expression of CCR1 and its ligands on different immune subsets during EAE. We tested our hypothesis that GM-CSF promotes EAE pathology, in part, by a CCR1/ CCL6 dependent pathway.

- **Aim 3: Chapter 4:** Compare the contribution of monocyte-derived DCs vs conventional DCs as antigen presenting cells during the initiation of EAE. We characterized DC lineages in the CNS at successive stages of EAE, compared their abilities to process myelin proteins and activate naïve and effector myelin-specific T cells, and directly investigated their importance to clinical onset and progression.

These studies provide insight into the role of GM-CSF, and its downstream mediators, in the interplay of the adaptive and innate branches of the immune system during the development of autoimmune demyelination and strongly supports further research into GM-CSF, CCR1, CCR1 ligands, and the myeloid cell compartment, as therapeutic targets in the treatment of MS.

CHAPTER 2 – GM-CSF Promotes Chronic Disability in Experimental Autoimmune Encephalomyelitis by Altering the Composition of Central Nervous System-Infiltrating Cells, but Is Dispensable for Disease Induction

Duncker PC, Stoolman JS, Huber AK, Segal BM. GM-CSF Promotes Chronic Disability in Experimental Autoimmune Encephalomyelitis by Altering the Composition of Central Nervous System-Infiltrating Cells, but Is Dispensable for Disease Induction. *J Immunol*. 2017;200(3):ji1701484.

Abstract

Granulocyte-macrophage colony-stimulating factor (GM-CSF) has been portrayed as a critical cytokine in the pathogenesis of experimental autoimmune encephalomyelitis (EAE) and, ostensibly, in multiple sclerosis. C57BL/6 mice deficient in GM-CSF are resistant to EAE induced by immunization with the 35-55 fragment of myelin oligodendrocyte glycoprotein (MOG_{35-55}). The mechanism of action of GM-CSF in EAE is poorly understood. Here we show that GM-CSF augments the accumulation of MOG_{35-55}-specific T cells in the skin-draining lymph nodes of primed mice, but is not required for the development of encephalitogenic T cells. Abrogation of GM-CSF receptor signaling in adoptive transfer recipients of MOG_{35-55}-specific T cells did not alter the incidence of EAE, or the trajectory of its initial clinical course, but limited the extent of chronic CNS tissue damage and neurological disability. The attenuated clinical course was associated with a relative dearth of MOG_{35-55}-specific T cells, myeloid dendritic cells, and neutrophils, and an abundance of B cells, within CNS infiltrates. Our data indicate that GM-CSF drives chronic tissue damage and disability in EAE via pleiotropic pathways, but is dispensable during early lesion formation and the onset of neurological deficits.

Introduction

It is widely believed that $CD4^+$ T cells mediate lesion development in individuals with Multiple Sclerosis (MS). This theory is supported by the identification of MHC Class II, and other genes that modulate T cell function, as MS risk alleles, and by the success of clinical trials of lymphocyte depleting or modulating agents in relapsing-remitting MS (66, 67). Furthermore, myelin-specific $CD4^+$ Th1 or Th17 cells induce experimental autoimmune encephalomyelitis (EAE, an animal model with clinical and histopathological similarities to MS) upon adoptive transfer into naïve syngeneic mice. Unexpectedly, expression of the signature Th1 and Th17 cytokines, IFNγ and IL-17, respectively, or their cognate receptors, were found to be dispensable for the manifestation of both active and passive EAE (33, 68, 69). The specific factors produced by myelin-reactive T cells that are required to mediate demyelination and axonopathy, and thereby cause neurological deficits, is a subject of intense research. The elucidation of those factors could have a profound translational impact on MS and other neuroinflammatory disorders by leading to the discovery of surrogate biomarkers and novel therapeutic targets.

In contrast to IFNγ and IL-17, the myeloid cell growth and mobilizing factor, granulocyte-macrophage colony-stimulating factor (GM-CSF), has been identified as playing a critical role in EAE across different strains of mice and target autoantigens (45, 54). In addition to the adoptive transfer of myelin-specific Th1 or Th17 cells, EAE can be induced in C57BL/6 mice via active immunization with myelin oligodendrocyte glycoprotein peptide 35-55 (MOG_{35-55}) suspended in CFA, and co-administration of pertussis toxin. C57BL/6 mice that are genetically deficient in GM-CSF (*Csf2*$^{-/-}$) are completely resistant to EAE induced by active immunization (45, 54). Disease susceptibility is restored by the systemic administration of recombinant GM-CSF from the day of immunization onward. Conversely, wild type (WT) mice are protected from EAE by serial

administration of a neutralizing antibody to GM-CSF from the time of active immunization with MOG_{35-55} onward (45, 54), indicating that the resistance of *Csf2*$^{-/-}$ mice is not solely attributable to the absence of GM-CSF during early development.

The mechanism of action of GM-CSF in EAE is a controversial issue. Several laboratories have reported that MOG_{35-55}-primed $CD4^+$ donor T cells, derived from *Csf2*$^{-/-}$, as opposed to WT donors, are ineffective in transferring EAE to WT hosts (39, 44). This led some investigators to conclude that GM-CSF production by CNS-infiltrating T cells directly drives the development of demyelinating lesions *in situ*. An alternative explanation is that the optimal activation and/ or differentiation of encephalitogenic T cells are dependent upon their interaction with GM-CSF modulated antigen presenting cells (APCs) within secondary lymphoid tissues. Conflicting data have been published as to whether GM-CSF plays a significant role in the priming of autoreactive Th1 and Th17 cells (42, 45, 70, 71).

In the current chapter, we revisit the mechanism of action of GM-CSF in EAE using reciprocal adoptive transfer experiments with WT donor T cells and GM-CSF receptor-deficient (*Csf2r*$^{-/-}$) hosts, versus *Csf2*$^{-/-}$ donor T cells and WT hosts. In parallel, we compare the clinical impact of administering a GM-CSF-neutralizing antibody during the priming of MOG_{35-55}-specific T cells in donors, versus during the effector phase in hosts. The results of these experiments indicate that, in the absence of GM-CSF, the frequency of MOG_{35-55}-reactive Th1 and Th17 cells is modestly diminished in immunized mice. Nevertheless, GM-CSF is not absolutely required for the generation of encephalitogenic T cells. Surprisingly, disruption of GM-CSF signaling in adoptive transfer recipients does not reduce the incidence or mitigate the early clinical course of EAE, but does curtail the extent of tissue damage at peak disease and prevents chronic disability. Unlike WT recipients of WT encephalitogenic $CD4^+$ T cells, which rarely recover function

following acute EAE, the majority of *Csf2r*$^{-/-}$ recipients undergo clinical remission. The milder chronic clinical course is associated with decreases in the number and frequencies of myelin-reactive CD4^{+} T cells, myeloid dendritic cells, and neutrophils, and an increase in the frequency of B cells, within the neuroinflammatory infiltrate.

Materials and Methods

Mice. Six- to eight-week-old CD45.1 congenic and WT C57BL/6 mice were obtained either from National Cancer Institute Frederick or Charles River Laboratories. *Csf2r*$^{-/-}$ mice (B6.129S1-Csf2rb^{1tm1Cgb}/J) mice were obtained from L. Robb (The Walter and Eliza Hall Institute), *Csf2*$^{-/-}$ mice were obtained from D. McGavern (National Institutes of Health), and mT/mG (B6.129(Cg)-*Gt(ROSA)26Sor*$^{tm4(ACTB-tdTomato,-EGFP)Luo}$/J) mice were obtained from B. Moore (University of Michigan, Ann Arbor) and bred in our facility. Mice were housed in micro-isolator cages under specific pathogen-free conditions. All animal studies were approved by the University Committee on Use and Care of Animals.

Induction and scoring of EAE. Mice were immunized s.c. with 100 μg of the MOG$_{35-55}$ peptide (MEVGWYRSP-FSRVVHLYRNGK; Biosynthesis) in CFA (Difco) at four sites over the flanks. For active immunization, mice were also administered 300 ng inactivated Bordetella pertussis toxin i.p. on days 0 and 2. For adoptive transfer EAE, inguinal, axial, and brachial dLNs were harvested from donor mice 10-14 days post-immunization, pooled, homogenized, and passed through a 70 μm strainer (Fisher Scientific). Cells were cultured under Th17-polarizing conditions: MOG$_{35-55}$ [50 μg/ml], rmIL-23 [8 ng/ml], rmIL-1α [10 ng/ml], and α-IFNγ [10 μg/ml]. Following 96 hours of culture, CD4^{+} T cells were purified by positive selection using L3T4 magnetic microbeads (Miltenyi Biotec). 3-6x10^{6} CD4^{+} T cells were injected i.p. to naïve recipients. The

recipient mice were observed daily for signs of EAE, and rated for degree of disability using a 5 point scale, as previously described (68).

Flow cytometry. For surface staining, cells were resuspended in PBS with 2% FBS and Fc Block (αCD16/32) [100 ng/ml] before 1:2 dilution with fluorochrome-conjugated Abs. For intracellular staining, cells were stimulated either; overnight with MOG_{35-55} before brefeldin A (BFA) [5 µg/ml] was added for 4-6 hours, or with PMA [50 ng/ml], ionomycin [2 µg/ml], and BFA [5 µg/ml] for 4-6 hours. Cells were stained for surface markers, as above, fixed in 4% PFA, permeabilized with 0.5% saponin, and incubated with fluorochrome-conjugated anti-cytokine mAbs. Flow gating began with comparison of SSC-A vs. FSC-A to exclude events outside the normal parameters of leukocytes followed by doublet exclusion comparing FSC-A vs. FSC-H. Dead cells were gated out using fixable viability dyes. Microglia were identified as $CD45^{int}CD11b^{+}$. CNS-infiltrating immune cells were identified as $CD45^{hi}$. Data were collected with a FACSCanto II flow cytometer using FACSDiva software (v6.1.3 and v7.0, Becton Dickinson). A FACS Aria III cell sorter was used to purify immune cells from the CNS and spleen. Data were analyzed using FlowJo software (vX 10.0, Treestar).

Antibodies and reagents. The following antibodies were obtained from eBioscience: Allophycocyanin-(αB220 [RA3-6B2], αCD11c [N418]), eFluor 450-(αCD45 [30-F11], αCD45.1 [A20]), eFluor 506-Fixable Viability, eFluor 780-Fixable Viability, FITC-(αGM-CSF [MP1-22E9], αMHCII [M5/114.15.2]), PE-αCD4 [RM4-5], PE-Cy7-(αCD44 [IM7], αCD11b [M1/70], αCD4 [RM4-5]), and PerCP-Cy5.5-(αIL-17A [eBio17B7], αCD11c [N418]). The following antibodies were obtained from BD Biosciences: Allophycocyanin-Cy7-(αIFNγ [XMG1.2], α-

Ly6G [1A8]). PE-labeled MOG_{38-49} tetramers were obtained from the NIH Tetramer Core Facility. rmIL-23 and rmIL-1α were obtained from R&D Systems. αGM-CSF (22E9.11), αIFNγ (XMG1.2), and αCD16/32 (2.4G2) were produced in-house via hybridoma. 500μg of αGM-CSF or whole rat IgG (Sigma Aldrich) was administered i.p. every other day, beginning at the time of immunization or T cell transfer, during blocking experiments. 100μg of αCD20 (clone 5D2, Genentech) or mouse IgG2a (clone C1.18.4, Bio X cell) was administered i.p. every other day, beginning at the time of T cell transfer, in B cell depleting experiments.

Isolation of inflammatory cells from the CNS, spleen, and blood. Tissue was harvested following intracardiac perfusion with 1X PBS. CNS was separated into whole brain or spinal cord, homogenized in 1 ml 1X PBS containing a protease inhibitor (Roche), and pelleted at 800 x g for 5-10 min. Supernatants were isolated and stored at -80°C. Pellets were resuspended in 3 ml collagenase A (1 mg/ml) and DNase I (1 mg/ml) in HBSS with calcium and magnesium and incubated in a 37°C water bath for 10 minutes. Samples were pelleted at 800 x g, resuspended in 27% percoll, and centrifuged for 10 minutes at 800 x g. The myelin/ debris layer and percoll were removed, and the cell pellet used for flow cytometric staining. Splenic immune cells were isolated by homogenization through a 70 μm strainer (BD Falcon). RBCs were lysed using ACK lysis buffer (Quality Biologicals). Blood was isolated into microtainers with EDTA (Becton Dickinson). Following centrifugation, plasma was isolated and stored at -80°C. Cells were resuspended in 6 ml 1X PBS with 2% FBS and underlayed with 3 ml pre-warmed Lympholyte-M (Cedarlane) before centrifugation at 1750 x g for 20 min at room temperature. White blood cells were harvested from the interface, washed, and remaining RBCs were lysed using ACK lysis buffer.

Construction of mixed bone marrow chimeric mice. Mixed bone marrow chimeras were constructed by first ablating the endogenous hematopoietic cells of congenic (CD45.1) C57BL/6 WT mice with a lethal dose of 1300 Rads, delivered in two 650 Rad doses separated by 3 hours. For experiments comparing WT to *Csf2*$^{-/-}$ myelin-reactive T cells, irradiated mice were reconstituted with a 1:1 mixture of WT CD45.1 congenic:*Csf2*$^{-/-}$ bone marrow. For experiments comparing CNS immune cell infiltrates at peak EAE, irradiated mice were reconstituted with mT/mG and *Csf2r*$^{-/-}$ bone marrow mixed at a 1:2 ratio, respectively, to obtain an approximate 50:50 composition of circulating leukocytes following reconstitution. Animals were kept on acid water for 2 weeks and allowed to reconstitute for an additional 6 weeks before induction of EAE.

Nanostring and qPCR. Mononuclear cells were isolated from the brain and spinal cord tissues of mixed bone marrow chimeric mice as detailed above. To obtain enough cells for RNA analysis, CNS immune isolates were combined from 4-5 mice before staining with myeloid cell markers for flow sorting of CD45.1^{+} or mT/mG WT vs CD45.2^{+} knock-out monocytes (CD45^{hi}CD11b^{+}Ly6G^{-} CD11c^{-}) and mDCs (CD45^{hi}CD11b^{+}Ly6G^{-}CD11c^{+}). Samples prepared for nanostring analysis were resuspended in RLT buffer at a concentration of 4,000 cells/µl, frozen, and run on the nCounter platform (Nanostring Technologies). Cells used to confirm nanostring results by qPCR were resuspended in either 300 µl RLT buffer or 1 ml Trizol (Life Technologies) before Qiagen RNeasy RNA purification. Purified RNA was converted into cDNA using the High Capacity cDNA Reverse Transcription Kit (Life Technologies). Relative RNA levels were quantified by SYBR Green qPCR performed on an iQ Thermocycler (Bio-Rad).

Multiplex cytokine analysis and ELISA. CNS cytokine levels in homogenate supernatants were measured using Luminex multiplex bead-based analysis (Millipore) using a Bio-Plex 200 system following the manufacturer's protocols. Data shown indicate levels within the linear portion of appropriate standard curves. CXCL13 Quantikine ELISA kit (R&D Systems) was used, according to manufacturer protocols, to determine the concentration of CXCL13 in CNS homogenate supernatants. Total protein was determined via Bradford assay (Thermo Scientific) and used to normalize analyte concentrations.

Immunofluorescence. Following intracardiac perfusion with Tyrode's and 4% paraformaldehyde (PFA), spinal columns were removed, post-fixed for 3 days in PFA, decalcified in 0.5 M EDTA for 4 days, cryoprotected in 30% sucrose, and embedded and frozen in OCT (Cellpath). 12 μm sections were blocked with Avidin B and biotin (Vector Labs) before staining with the following primary and secondary antibodies: goat anti-MBP (Santa Cruz Biotechnology), Alexa Fluor 488-conjugated donkey anti-goat IgG (Life Technologies), rat anti-CD45 (eBiosciences), Alexa Fluor 647-conjugated goat anti-rat (Life Technologies), mouse anti-SMI-32 (Covance), and Alexa Fluor 594 conjugated goat anti-mouse IgG. DAPI (Life Technologies) was used to label nuclei. Images were acquired on a Nikon Eclipse Ti, CoolSnap EZ camera, and NIS Elements: Basic Research v3.10. Appropriate image processing, including image merging and black level and brightness adjustments, was performed in Photoshop CC 2017 and applied equally to all samples.

Statistical analysis. Statistical analyses were performed using GraphPad Prism software (v6.05). Disease curves were compared by Two-way ANOVA and T-tests (day-by-day) without multiple comparisons. Immune parameters were compared using unpaired t-test with Welch's correction.

Leukocyte numbers and mRNA from mixed bone marrow chimera mice were analyzed via paired, parametric T-test. Outliers were identified by ROUT analysis and removed as necessary. A p-value < 0.05 (*) was considered significant, with $p < 0.01$ (**), $p < 0.001$ (***), and $p < 0.0001$ (****).

Results

MOG_{35-55}-specific T cell priming is compromised in the absence of GM-CSF. Consistent with published studies, we found that *Csf2*$^{-/-}$ and *Csf2r*$^{-/-}$ mice, as well as WT mice treated with αGM-CSF neutralizing antibodies, were resistant to EAE induced by active immunization (Fig. 2.1A, B). Bone marrow chimeric mice, constructed by reconstituting lethally irradiated WT mice with *Csf2r*$^{-/-}$ donor bone marrow cells, were also resistant to EAE (Fig. 2.1C). These findings indicate that GM-CSF signaling into hematopoietic cells is required for the development and expansion of encephalitogenic T cells in the periphery, and/ or for their function as mature effector cells within the CNS. We previously reported that the frequencies of MOG_{35-55}-reactive IFNγ- and IL-17-producing lymph node cells, measured by ELISPOT, are diminished in MOG_{35-55}-immunized *Csf2*$^{-/-}$ or *Csf2r*$^{-/-}$ versus WT mice (42). Similarly, Bernard and colleagues found that splenocytes harvested from primed *Csf2*$^{-/-}$ mice are impaired in mounting MOG_{35-55}-specific proliferative and cytokine recall responses upon antigenic challenge *ex vivo* (45). In contrast, another laboratory found that splenocytes harvested from GM-CSF sufficient or deficient 2D2 mice (which express a transgenic T cell receptor specific for MOG_{35-55}) produce comparable amounts of IFNγ and IL-17 when polarized *in vitro* and challenged with a mitogenic stimulus (44).

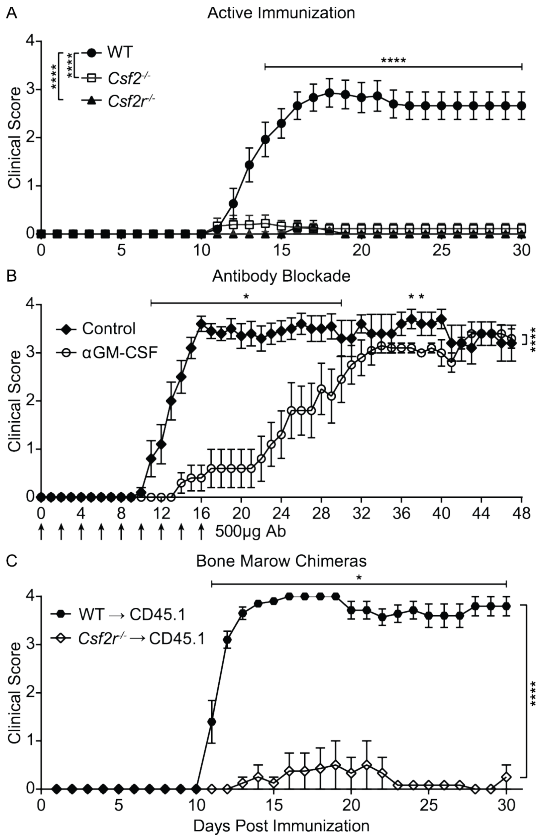

Figure 2.1 – GM-CSF is required for the development of EAE induced by active immunization.

(A) EAE was induced in WT (n=15), *Csf2*$^{-/-}$(n=18), and *Csf2r*$^{-/-}$ (n=5) mice via active immunization with MOG in CFA and administration of pertussis toxin. **(B)** WT mice were actively immunized with MOG, as in (A), and treated with αGM-CSF (n=10) or control Rat IgG (n=10) from days 0 through 16. **(C)** Bone marrow chimeras were constructed by injecting lethally irradiated WT mice with bone marrow cells from either WT (n=10) or *Csf2r*$^{-/-}$ (n=8) donors. Following reconstitution, EAE was induced by active immunization. * $p<0.05$ and **** $p<0.0001$ as determined by multiple T-tests with Welch's correction comparing daily clinical scores (significance shown above the curves). **** $p<0.0001$ as determined by Two-Way ANOVA (significance is shown to the right of curves).

In order to investigate the basis of these discrepant findings, we subjected draining lymph node (dLN) cells harvested from MOG_{35-55}/ CFA-immunized WT or *Csf2*$^{-/-}$ mice to flow cytometric analysis directly *ex vivo*. The absolute number of dLN cells, as well as the percentage of $CD4^+$ T cells among $CD45^+$ cells, were reduced in the *Csf2*$^{-/-}$ cohort (Fig. 2.2A-C). In contrast, the frequency of B cells was elevated in *Csf2*$^{-/-}$ lymph nodes (Fig. 2.2B, C). Following 96 hours of stimulation with MOG_{35-55} under Th17 polarizing conditions, *Csf2*$^{-/-}$ lymph node cells maintained

a lower frequency of $CD4^+$ T cells, of which fewer were antigen-experienced ($CD44^{hi}$) or capable of binding a MOG_{38-49}/ MHCII tetramer, when compared with their WT counterparts (Fig. 2.2D-F). The frequency of $CD4^+CD44^{hi}Tetramer^+$ T cells was approximately 1.8-fold higher in WT compared with *Csf2*$^{-/-}$ lymph node cells. Lymph node cells derived from primed *Csf2*$^{-/-}$ mice also had lower percentages of $CD4^+$ T cells that expressed IFNγ or IL-17 in response to short-term incubation with PMA/ ionomycin (Fig. 2.2G), or following rest and restimulation with MOG_{35-55} (Fig. 2.2H). Similar results were obtained when lymph node cell composition and recall responses were compared between MOG_{35-55}-immunized *Csf2r*$^{-/-}$ versus WT mice, or WT mice treated with αGM-CSF versus control antibodies (Fig. 2.3).

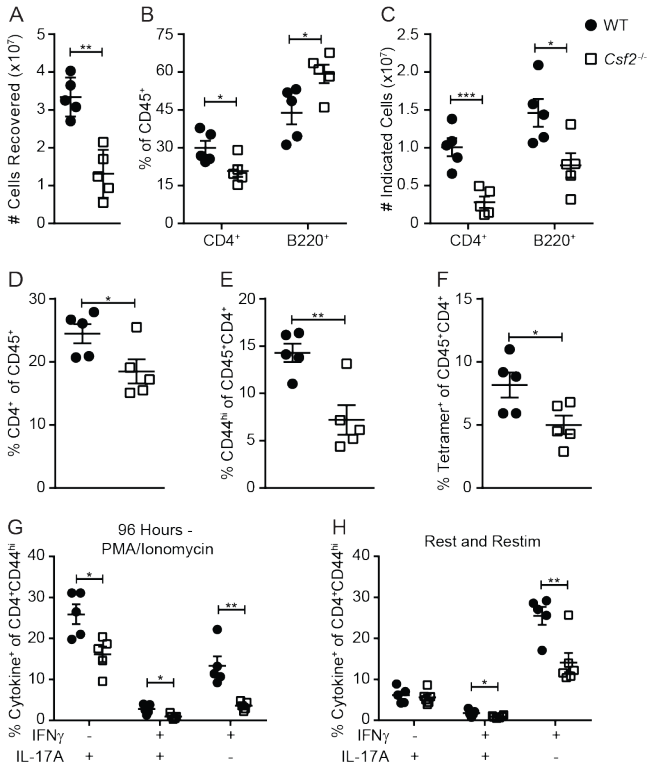

Figure 2.2 – MOG_{35-55}-specific $CD4^+$ T cell priming is diminished in *Csf2*$^{-/-}$ mice.
(A-C) dLN cells were isolated from WT and *Csf2*$^{-/-}$ C57BL/6 mice 14 days after immunization and analyzed directly *ex vivo* by flow cytometry. The total number of dLN cells was determined per mouse **(A)**, as well as the frequency **(B)** and number/ mouse **(C)** of $CD4^+$ and $B220^+$ cells. **(D-F)** dLN cells from each group were cultured with MOG_{35-55} and Th17 polarization factors. After 96 hours, cells were subjected to flow cytometric analysis to determine the frequencies of $CD4^+$ cells among $CD45^+$ cells **(D)**, $CD44^{hi}$ cells among $CD45^+CD4^+$ cells **(E)**, and MOG_{38-49} $Tetramer^+$

cells among $CD45^+CD4^+$ cells **(F)**. **(G, H)** Cells were either cultured with PMA/ ionomycin for 4 hours **(G)** or rested for 48 hours prior to overnight co-culture with MOG_{35-55}-pulsed T-depleted splenocytes **(H)**. Brefeldin A (BFA) was added at the start of culture in **(G)** and for the last 4 hours of culture in **(H)**. Cells were analyzed by intracellular cytokine staining and flow cytometry. Data (± SEM) are representative of 3 **(A-F)** or 2 **(G, H)** independent experiments with 4-7 mice per group. * $p<0.05$, ** $p<0.01$, and *** $p<0.001$.

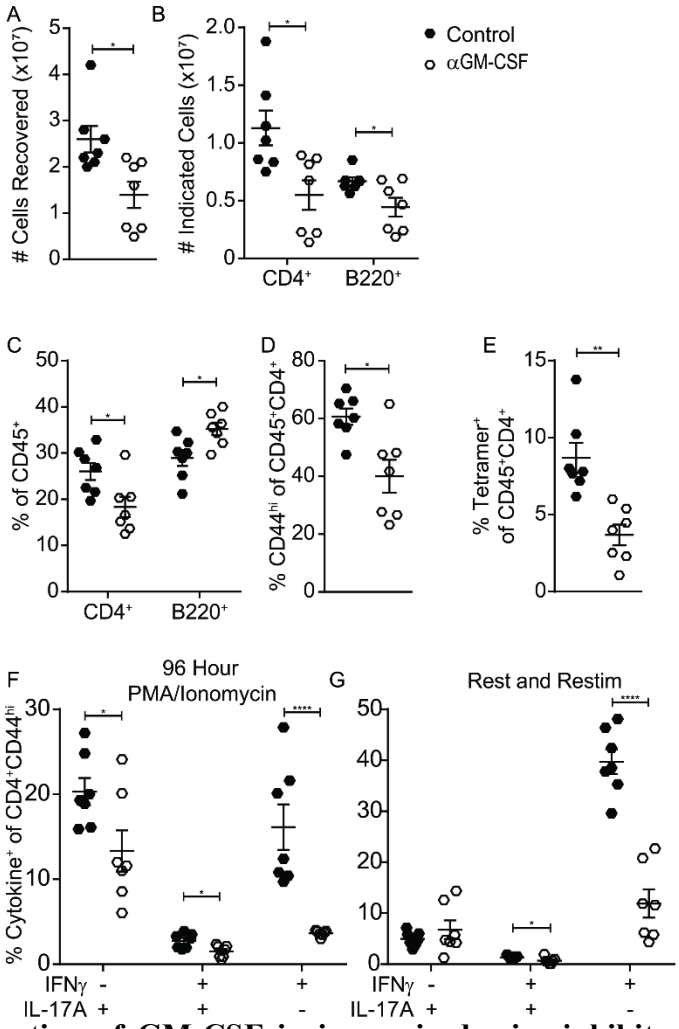

Figure 2.3. Neutralization of GM-CSF in immunized mice inhibits MOG-specific T cell priming.

(A) Total number of cells isolated from draining LNs of MOG-immunized WT mice treated with either control Rat IgG or αGM-CSF from days 0 to 14. **(B)** Number of $CD4^+$ and $B220^+$ cells in draining LNs per mouse. (**C-E)** Primed LN cells from each group were cultured with MOG in the presence of recombinant IL-23 and IL-1□. Cells were harvested after 96 hours and subjected to flow cytometric analysis to determine the frequencies of $CD4^+$ and $B200^+$ cells among $CD45^+$ cells (C), $CD44^{hi}$ cells among $CD45^+CD4^+$ cells (D), and MOG $Tetramer^+$ cells among $CD45^+CD4^+$ cells (E). **(F, G)** WT and *Csf2*$^{-/-}$ MOG-reactive, Th17-polarized LN cells were either cultured with PMA/ ionomycin for 4 hours (F) or rested for 48 hours prior to overnight co-culture with MOG-pulsed T-depleted splenocytes (G). BFA was added at the start of culture in (F) and for the last 4 hours of culture in (G). Cells were harvested and subjected to intracellular cytokine staining and

flow cytometric analysis * $p<0.05$, ** $p<0.01$, *** $p<0.001$, and **** $p<0.0001$ by T-test with Welch's correction. The figure shows 1 representative experiment of 2 with 5-7 mice per group.

We next assessed the encephalitogenicity of IL-23-polarized $CD4^+$ Th17 cells derived from MOG_{35-55}-primed *Csf2*$^{-/-}$ donors. In contrast to previous studies, we found that *Csf2*$^{-/-}$ Th17 cells readily induced EAE in WT C57BL/6 mice when injected at a dose of $3x10^6$ cells per host (Fig. 2.4A). The day of onset and incidence of disease were similar in mice injected with $3x10^6$ *Csf2*$^{-/-}$ or WT effector cells (Table I). Hence, despite a modest impairment in T cell priming, *Csf2*$^{-/-}$ mice are capable of generating encephalitogenic T cells and are competent adoptive transfer donors when a sufficient number of cells are transferred.

Donor	Host	Experiment	Day of Onset	Incidence	No. of Mice Remitting
WT	WT	1	9.6 ± 1.7	5/5	1/5
		2	7.8 ± 0.5	4/5	1/4
		3	7.4 ± 0.9	5/5	0/5
		Total	8.3 ± 1.5	14/15	2/14
Csf2$^{-/-}$	WT	1	7.9 ± 1.3	7/8	6/7
		2	7.8 ± 0.8	6/7	6/6
		3	6.8 ± 0.5	4/5	4/4
		Total	7.6 ± 1.1	17/20	16/17

Table 2.1 – *Csf2*$^{-/-}$ and WT encephalitogenic $CD4^+$ T cells induce EAE in naive WT recipients at a comparable incidence.
Shown are the results of three independent experiments. Remission is defined as a sustained decrease in clinical score by ≥2 points.

GM-CSF signaling during the effector phase augments disease severity and prevents remission. Although 85% of WT mice injected with $3x10^6$ *Csf2*$^{-/-}$ Th17 effector cells developed EAE, they experienced a slightly lower peak clinical score than recipients of the same number of WT donor cells (Fig. 2.4A). Nearly 95% (16/17) of the recipients of *Csf2*$^{-/-}$ Th17 cells underwent remission, compared with 14% (2/14) of the recipients of WT cells (Table I). Similarly, *Csf2*$^{-/-}$ $CD4^+$ Th17 cells sorted from the dLNs of primed *Csf2*$^{-/-}$:WT mixed bone marrow chimeras induced a monophasic course of EAE in WT hosts, whereas Th17-polarized WT $CD4^+$ T cells obtained from the same chimeras induced chronic EAE (Fig. 2.4B). Doubling the number of *Csf2*$^{-/-}$ donor

$CD4^+$ T cells to $6x10^6$/ host did not normalize the clinical course to that of the recipients of $3x10^6$ WT $CD4^+$ T cells (unpublished data). This suggests that the milder clinical course experienced by the *Csf2*$^{-/-}$ T cell recipients is not simply secondary to a lower frequency of MOG_{35-55}-specific donor T cells in the transferred population, but that GM-CSF production is specifically required during the effector phase for heightened clinical disease severity/ chronicity.

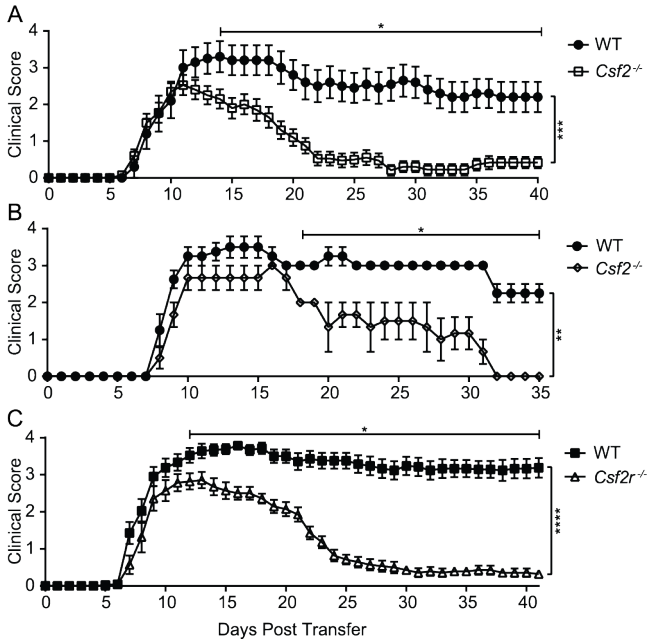

Figure 2.4 – GM-CSF signaling during the effector phase is dispensable for the induction of EAE.
(A) Purified Th17-polarized $CD4^+$ T cells from WT and *Csf2*$^{-/-}$ were injected into naïve syngeneic WT mice. The clinical courses of recipients of WT (closed circles; n=15) and *Csf2*$^{-/-}$ (open squares; n=20) cells are shown. **(B)** After 96 hours of Th17-polarization, $CD4^+$ T cells from primed mixed bone marrow chimeric mice ($CD45.1^+$*Csf2*$^{+/+}$:$CD45.2^+$*Csf2*$^{-/-}$) were flow sorted based on CD45.1 versus CD45.2 expression and transferred into naïve WT recipients. The clinical courses (mean ± SEM) of mice injected with $CD45.1^+$*Csf2*$^{+/+}$ $CD4^+$ T cells (closed circles; n=4) or $CD45.2^+$*Csf2*$^{-/-}$ $CD4^+$ T cells (open diamonds, n=3) are shown. **(C)** Th17-polarized, MOG_{35-55}-reactive, WT $CD4^+$ T cells were adoptively transferred into naïve WT (closed squares; n=21) or *Csf2r*$^{-/-}$ mice (open triangles; n=14). Data (mean ± SEM) were pooled from 3 independent experiments with similar results (A, C). * $p<0.05$, ** $p<0.01$, *** $p<0.001$, and **** $p<0.0001$

In order to focus exclusively on the role of GM-CSF during the effector phase of EAE, we transferred WT donor T cells into *Csf2r*$^{-/-}$ versus WT hosts, or into WT hosts treated with αGM-CSF versus control antibodies. As anticipated, the *Csf2r*$^{-/-}$ and αGM-CSF treated WT recipients

experienced an abbreviated clinical course, mimicking that of WT mice injected with MOG_{35-55}-reactive *Csf2*$^{-/-}$ Th17 cells (Fig. 2.4A, C, and Fig. 2.6B). Similar results were observed when Th1-polarized WT encephalitogenic $CD4^+$ T cells were transferred to naïve WT or *Csf2r*$^{-/-}$ recipients (Fig. 2.6A). Immunohistochemical analyses of spinal cord tissue revealed more extensive demyelination in WT versus *Csf2r*$^{-/-}$ adoptive transfer recipients that were matched for degree of neurological impairment (Fig. 2.5). This was particularly evident in mice with clinical scores between 2 and 3. Furthermore, inflammatory cells in the spinal cords of *Csf2r*$^{-/-}$ recipients were, in large part, restricted to the meningeal space and peripheral white matter. In contrast, inflammatory cells penetrated deep into the parenchyma of WT spinal cords.

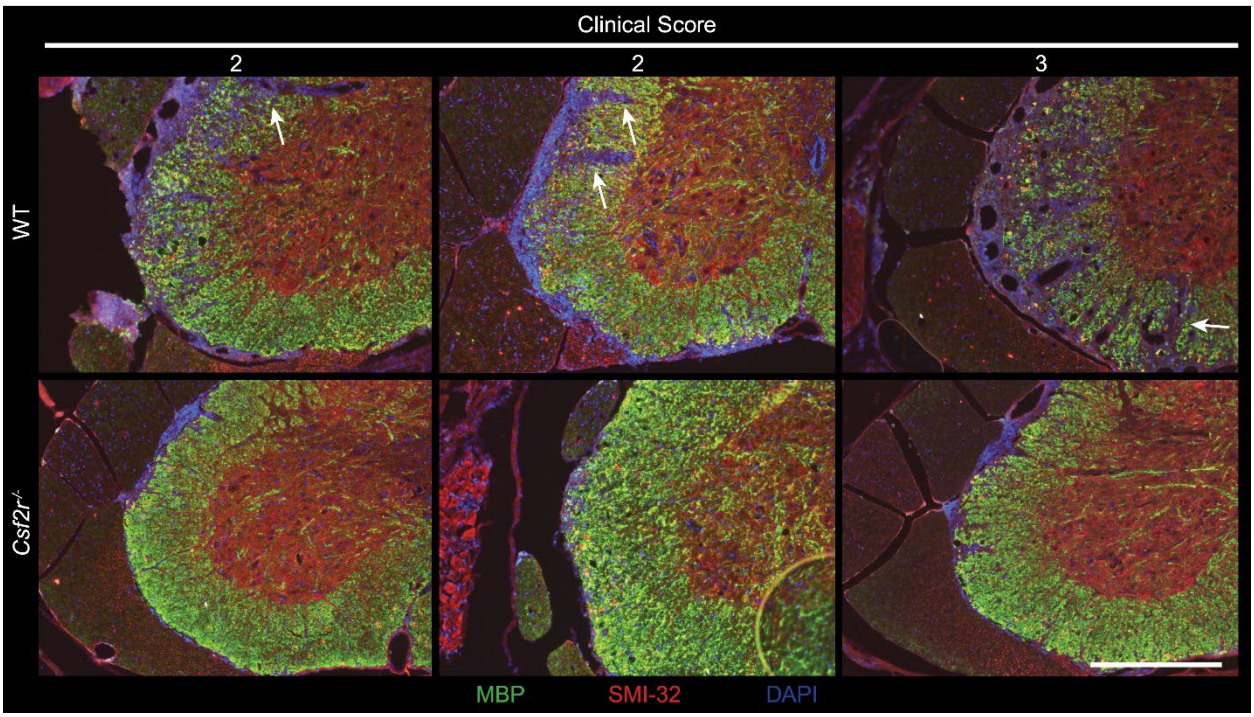

Figure 2.5 – Inflammatory infiltrates are confined to the meninges and peripheral white matter, and demyelination is sparse, in *Csf2r*$^{-/-}$ compared to WT Th17 transfer recipients. Representative spinal cord sections of WT and *Csf2r*$^{-/-}$ recipients of WT Th17 encephalitogenic T cells, matched by clinical scores. Clinical scores at the time of euthanasia are shown above each pair of panels. Sections were stained for MBP (green), SMI-32 (red), and DAPI (blue). White arrows point to immune cells penetrating into the parenchyma. Scale bar, 300 μm.

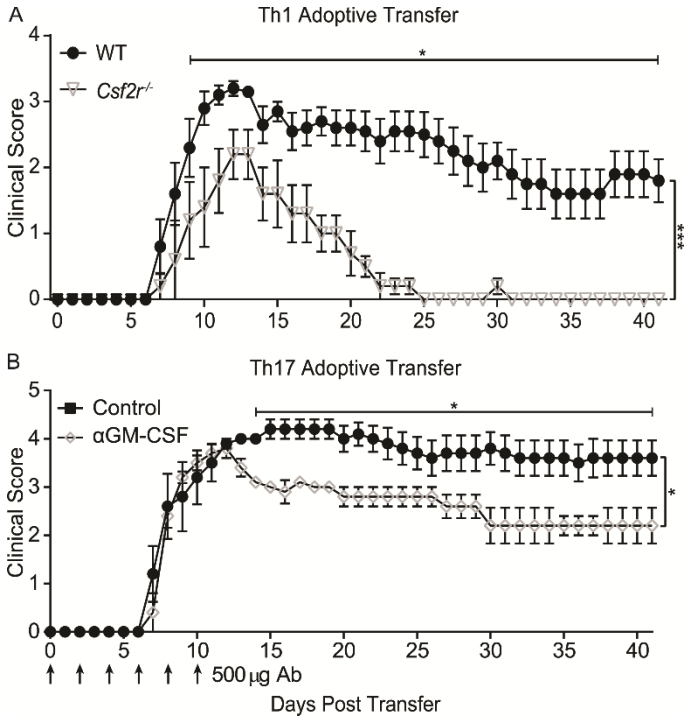

Figure 2.6 – GM-CSF disruption during adoptive transfer EAE leads to a monophasic disease course.
(A) WT MOG-primed LN cells were cultured under Th1-polarizing conditions prior to $CD4^+$ T cell isolation and transfer into naïve WT (n=10) or *Csf2r*$^{-/-}$ (n=10) mice. **(B)** WT MOG-primed LN cells were cultured under Th17-polarizing conditions prior to $CD4^+$ T cell isolation and transfer into naïve WT which were treated every other day with αGM-CSF, or control antibody, starting at the time of transfer. * $p<0.05$ as determined by multiple T-tests with Welch's correction comparing daily clinical scores (significance shown above the curves). *** $p<0.001$ as determined by Two-Way ANOVA (significance shown to the right of the curves).

GM-CSF signaling alters the composition of immune cells infiltrating the CNS during the development and progression of EAE. To investigate the impact of GM-CSF signaling on the size and composition of neuroinflammatory infiltrates, we performed flow cytometric analysis of CNS-infiltrating cells collected from *Csf2r*$^{-/-}$ or WT recipients at the pre-clinical, onset, peak, and late stages of adoptively transferred EAE. The total number of $CD45^{hi}$ cells recovered per spinal cord were comparable between the two groups at all stages of disease (Fig. 2.8A). There were no significant differences in the number of monocytes/ macrophages ($CD45^{hi}CD11b^+Ly6G^-CD11c^-$) at any of the time points (Fig. 2.8C). At pre-clinical, onset, and peak disease, the number of granulocytes ($CD45^{hi}CD11b^+Ly6G^+CD11c^-$) was significantly lower in the CNS of *Csf2r*$^{-/-}$ hosts

relative to WT hosts. Donor (CD45.1^{+}) CD4^{+} T cells were also reduced in CNS infiltrates of *Csf2r*$^{-/-}$ hosts at peak disease, and there was a consistent trend towards a lower number of myeloid DCs (mDCs) (CD45^{hi}CD11b^{+}Ly6G^{-}CD11c^{+}) at the same time point (Fig. 2.8D, F). Conversely, the number of B cells (CD45^{hi}CD11b^{-}Ly6G^{-}CD11c^{-}B220^{+}MHCII^{+}) was significantly increased in the spinal cords of *Csf2r*$^{-/-}$ hosts at onset and peak (Fig. 2.8E). These findings were recapitulated in WT transfer recipients treated with αGM-CSF (Fig. 2.7). The percentages of IFNγ- and IL-17-producers among CNS donor T cells, following short-term stimulation with PMA/ ionomycin or overnight stimulation with MOG_{35-55}, were comparable between the WT and *Csf2r*$^{-/-}$ hosts (Fig. 2.8G, H).

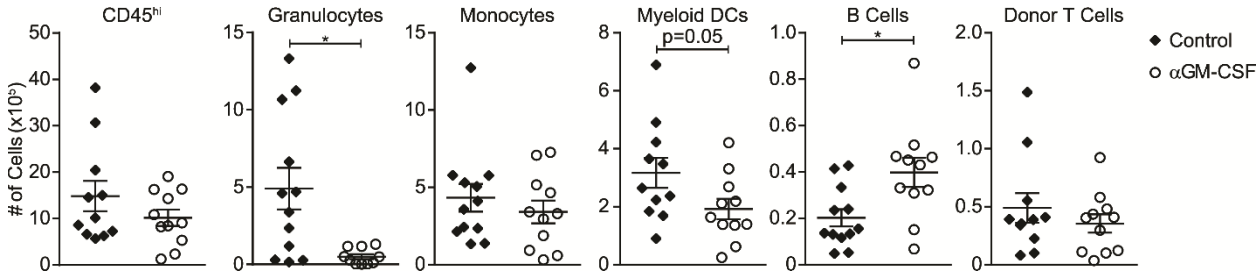

Figure 2.7 – Neutralization of GM-CSF in WT adoptive transfer recipients alters the cellular composition of CNS infiltrates.

WT adoptive transfer recipients were treated with αGM-CSF or control Rat IgG from the day of transfer onward. Spinal cord infiltrates were analyzed at peak disease via flow cytometry. The numbers of total CD45^{hi} cells, Granulocytes, Monocytes, Myeloid DCs, B cells, and donor T cells per mouse were determined. Data (mean ± SEM) is pooled from 2 experiments with 5-6 animals per group per experiment. * $p<0.05$ by T-test with Welch's correction.

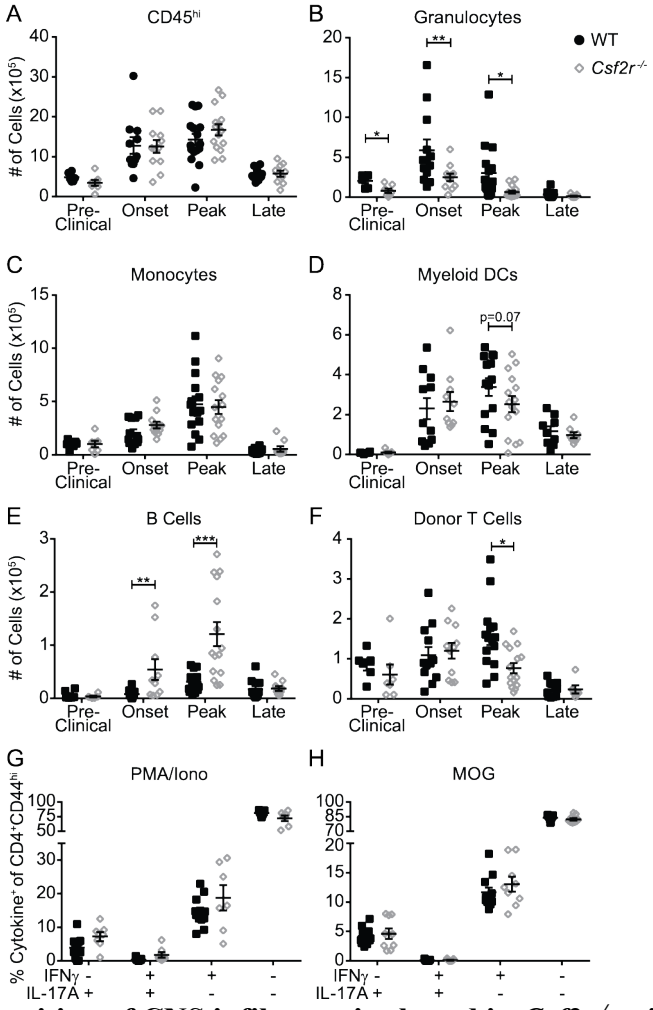

Figure 2.8 – The composition of CNS infiltrates is altered in *Csf2r*$^{-/-}$ mice with Th17-induced EAE.

(A-F) CNS inflammatory cells were harvested from WT (closed squares) and *Csf2r*$^{-/-}$ (open diamonds) Th17 recipients at pre-clinical, onset, peak, and late time-points of EAE. The total number of (A) CD45^{hi}, (B) Granulocytes, (C) Monocytes, (D) mDCs, (E) B Cells, and (F) donor T cells were determined by flow cytometric analysis. Data (± SEM) for the pre-clinical and onset time points were pooled from 2 experiments (n=3-4 and 5-7 per group, respectively), peak and late time points were pooled from 3 experiments (n=5-6 and n=3-4 per group, respectively). **(G, H)** CNS inflammatory cells were isolated at peak disease and cultured with PMA/ Ionomycin for 4-6 hours (G), or overnight with MOG_{35-55}. BFA was added at the initiation of culture (G), or during the last 4 hours of culture (H). The experiment was repeated twice with n=4-5 per group. * $p<0.05$, ** $p<0.01$, and *** $p<0.001$.

To determine whether the relative paucity of granulocytes and mDCs in the CNS infiltrates of *Csf2r*$^{-/-}$ hosts is cell intrinsic, we constructed mixed bone marrow chimeric mice by reconstituting lethally irradiated CD45.1^{+} congenic WT mice with a combination of *Csf2r*$^{-/-}$ and

WT donor bone marrow cells and induced EAE by Th17 transfer. Consistent with our earlier results (Fig. 2.8B, D), a significantly higher percentage of the granulocytes and mDCs in CNS infiltrates at peak EAE were derived from WT versus *Csf2r*$^{-/-}$ bone marrow cells (Fig. 2.9A, B). In contrast, CNS monocytes/ macrophages were preferentially derived from *Csf2r*$^{-/-}$ hematopoietic cells (Fig. 2.9C). Splenic monocytes, mDCs, and granulocytes were evenly derived from WT and *Csf2r*$^{-/-}$ hematopoietic cells (data not shown). This suggests that GM-CSF directly promotes the accumulation of granulocytes and mDCs, but not monocytes/ macrophages, in the CNS of adoptive transfer recipients.

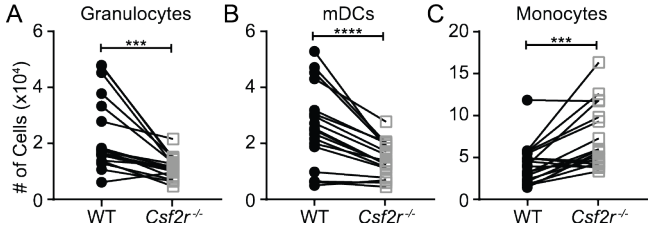

Figure 2.9 – GM-CSF promotes the accumulation of granulocytes, mDCs, and monocytes in the CNS at peak EAE.
(A-C) EAE was induced in WT:*Csf2r*$^{-/-}$ mixed bone marrow chimeras via adoptive transfer. CNS inflammatory cells were analyzed at peak EAE by flow cytometry. The numbers of WT or *Csf2r*$^{-/-}$ granulocytes (A), mDCs (B), and monocytes/ macrophages (C), were quantified per mouse. *** $p<0.001$, and **** $p<0.0001$ as determined by paired, parametric, T-test. Data were combined from 3 independent experiments with 5-7 paired points per experiment.

Loss of GM-CSF signaling alters the inflammatory milieu in the CNS of mice with EAE. The skewed cellular composition and properties of neuroinflammatory infiltrates in *Csf2r*$^{-/-}$ transfer recipients could be secondary to, as well as the cause of, an altered inflammatory milieu. Therefore, we measured the expression of a panel of cytokines, chemokines, and growth factors in spinal cord homogenates obtained from WT and *Csf2r*$^{-/-}$ transfer recipients at peak EAE, via multi-variate bead-based immunoassays or ELISA (72). Expression of the B cell-attracting chemokine CXCL13 was elevated, while expression of the neutrophil mobilizing/ growth factor granulocyte-colony stimulating factor (G-CSF) was reduced, in the *Csf2r*$^{-/-}$ homogenates compared with WT

homogenates (Fig. 2.10A). These results are consistent with the increased frequency of B cells and decreased frequency of granulocytes that we observed in the CNS of *Csf2r*$^{-/-}$ adoptive transfer recipients (Fig. 2.8). IL-1α was significantly elevated in WT spinal cord homogenates, while levels of macrophage-colony stimulating factor (M-CSF), CXCL9, and CCL5 were higher in *Csf2r*$^{-/-}$ homogenates (Fig. 2.10A). Levels of the other factors measured in our panel, including IFNγ, TNFα, IL-4, IL-10, CXCL1, CXCL2, and CCL2, were comparable in the homogenates from the two groups (data not shown).

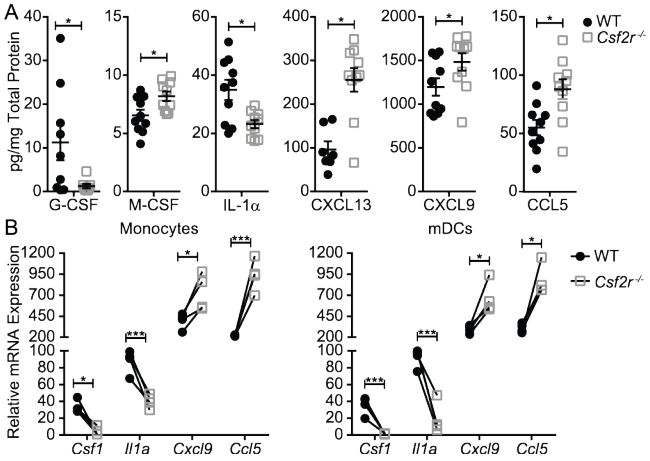

Figure 2.10 – CNS cytokine/ chemokine profiles differ between *Csf2r*$^{-/-}$ and WT mice with Th17-mediated EAE.
(A) Spinal cord homogenates obtained from WT and *Csf2r*$^{-/-}$ adoptive transfer recipients at peak EAE were analyzed via Luminex based multiplex analysis (G-CSF, M-CSF, IL-1α, CXCL9, CCL5) or ELISA (CXCL13). Data (± SEM) shown were combined from 2 independent experiments (n=5 per group per experiment). **(B)** RNA was extracted from monocytes and mDCs sorted from the CNS of WT:*Csf2r*$^{-/-}$ mixed bone marrow chimeras at peak disease and subjected to nanostring analysis. Each symbol represents CNS inflammatory cells that were pooled from 4 mice prior to sorting. Results were confirmed with independent samples by qPCR. * $p<0.05$, ** $p<0.01$, and *** $p<0.001$.

We next investigated expression of selected inflammatory factors on the transcript level in *Csf2r*$^{-/-}$ versus WT myeloid cells, that were flow sorted from the CNS of mixed bone marrow chimeric mice at peak EAE. *Il1a* mRNA levels were increased, while *Cxcl9* and *Ccl5* mRNA levels were decreased, in WT monocytes/ macrophages and mDCs compared with their *Csf2r*$^{-/-}$ counterparts (Fig. 2.10B), mirroring the pattern observed with the immunoassays. In contrast, M-

CSF (*Csf1*) mRNA levels were relatively low in the *Csf2r*$^{-/-}$ myeloid cells. We were unable to detect mRNA encoding CXCL13 or G-CSF (*Csf3*) in monocytes/ macrophages or mDCs isolated from the CNS of the mixed bone marrow chimeric mice, irrespective of genotype, suggesting that these factors are produced by alternative cell subsets. Published studies, and our own unpublished data, have implicated microglia as the primary source of CXCL13 in the inflamed CNS (73).

B cell depletion does not rescue chronic EAE in Csf2r$^{-/-}$ *transfer recipients*, *but granulocyte blockade ameliorates the course of EAE in WT recipients.* Given the significant enrichment of B cells in CNS infiltrates of *Csf2r*$^{-/-}$ transfer recipients, we questioned whether those cells were suppressing chronic EAE, either by playing an active regulatory role or by outcompeting more competent myeloid cells as APCs. However, administration of an αCD20 antibody, which depletes CNS infiltrating B cells by greater than 90% (data not shown), had no impact on the disease course compared to control mIgG2a (Fig. 2.11A).

We next questioned whether the increased number of neutrophils in the CNS of WT mice led to more severe CNS damage and chronic deficits. We previously showed that the prophylactic depletion of circulating neutrophils in adoptive transfer recipients, via administration of αCXCR2 antisera during the preclinical phase, prevents blood-brain-barrier breakdown and the onset of EAE (74). Therefore, we delayed starting αCXCR2 treatment until 2 days following adoptive transfer of WT CD4^{+} encephalitogenic T cells to naïve WT recipients. Compared to mice treated with normal rabbit sera, those receiving αCXCR2 developed a less severe disease course marked by delayed onset, reduced peak severity, and a decrease in incidence from 90% to 40% (Fig. 2.11B and data not shown). When evaluating only those αCXCR2 treated adoptive transfer recipients that developed clinical EAE, we observed a clinical course reminiscent of that of *Csf2r*$^{-/-}$ transfer recipients, with a reduction in peak severity and a lower degree of chronic disability (Fig. 2.11C).

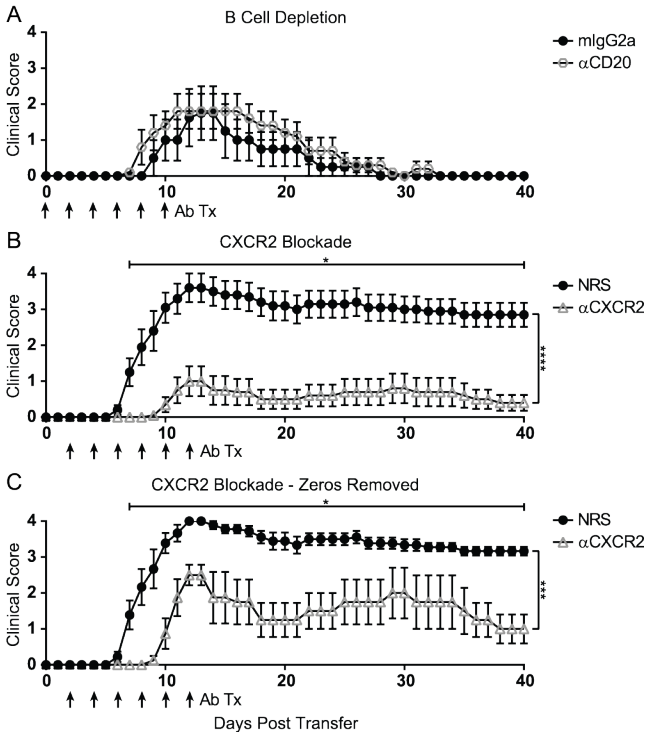

Figure 2.11 – B cell depletion does not exacerbate EAE in *Csf2r*$^{-/-}$ adoptive transfer recipients, but granulocyte blockade ameliorates chronic EAE in WT recipients.
(A) *Csf2r*$^{-/-}$ Th17 recipients were treated with either B cell-depleting αCD20 antibodies (n=5) or control mIgG2a (n=5) from the day of T cell transfer onward. **(B)** WT Th17 adoptive transfer recipients were treated with either polyclonal rabbit α-mouse CXCR2 (n=10) or control normal rabbit serum (NRS; n=10) between days 2 and 14 post-transfer. **(C)** The clinical courses of those mice in (B) that developed neurological signs (9 mice treated with NRS and 4 treated with αCXCR2). Data (± SEM) are representative of 2 (A) or 3 (B and C) experiments with 5-10 mice per group, per experiment. * $p<0.05$, ** $p<0.01$, *** $p<0.001$, and **** $p<0.0001$.

Discussion

Consistent with published data from our own and independent laboratories (42, 45, 70, 71), the current study demonstrates that T effector cell priming is compromised in the absence of GM-CSF. Specifically, we found that the expansion of MOG_{35-55}-specific T cells was reduced in the dLNs of immunized *Csf2*$^{-/-}$ mice when compared with WT mice. Although the differences in the immune response between WT and knock-out mice were modest, they were highly reproducible and statistically significant. We speculate that impaired priming contributes to the resistance of *Csf2*$^{-/-}$ and *Csf2r*$^{-/-}$ mice to induction of EAE by active immunization. However, our data indicate

that GM-CSF also plays an independent role in augmenting CNS damage and sustaining neurological disability during the effector phase of disease.

Other laboratories have reported that the clinical manifestation of EAE in otherwise immunocompetent C57BL/6 mice is dependent on GM-CSF expression during the effector phase (39, 44). In those studies, disease was induced either by active immunization with MOG_{35-55} peptide in CFA or by transfer of 2D2 T cells that were primed and polarized *in vitro*. In contrast, we found that GM-CSF signaling is not required for the induction of neurological deficits in naïve C57BL/6 mice following the injection of polyclonal MOG_{35-55}-specific Th1 or Th17 cells, nor does it influence the trajectory of the initial clinical course. Similarly, Pierson and Goverman recently reported that expression of GM-CSF is dispensable for the manifestation of conventional disease in an alternative model of adoptively transferred EAE in C3HeB/FeJ mice (71). Together, these observations indicate that the relative importance of GM-CSF signaling for the manifestation of EAE is model dependent.

Although we could readily induce EAE in C57BL/6 *Csf2r*$^{-/-}$ adoptive transfer recipients, or in C57BL/6 WT recipients treated with αGM-CSF antibodies, the spatial distribution and cellular composition of CNS infiltrates were altered in those mice compared with their respective controls, and they were more likely to undergo remission. Inflammatory infiltrates in WT adoptive transfer recipients were neutrophil rich and extended into the parenchymal tissue, while infiltrates in *Csf2r*$^{-/-}$ recipients were B cell rich and confined to the meningeal space and peripheral white matter of the spinal cord. These distinct spatial patterns were evident in individual mice matched for degree of clinical disability, including those with overt paraparesis, suggesting that the deficits that accrue during acute EAE are not dependent on deep parenchymal infiltration by inflammatory cells. Rather, it is likely that early neurological dysfunction is secondary to toxic and vasoactive factors

that are released by infiltrating immune cells and diffuse into the adjacent white matter to trigger edema and disrupt axonal transport and/ or signal transmission. The fact that mice deficient in GM-CSF receptor signaling undergo clinical remission suggests that those early events are, for the most part, reversible. The chronic deficits incurred by GM-CSF sufficient mice may reflect irreversible damage directly inflicted on axons and glial cells by pathogenic leukocytes via cell-to-cell contact.

The mechanism by which GM-CSF supports parenchymal invasion by immune cells remains to be elucidated. One possibility is that neutrophils (which constitute a significant percentage of the WT infiltrates) secrete proteases that digest the extracellular matrix. This hypothesis is consistent with our finding that blockade of neutrophil trafficking reduces disease incidence and induces remission in those WT transfer recipients that succumb to disease. The role of GM-CSF in EAE pathogenesis is likely multifocal. Hence, the milder clinical course of *Csf2r*$^{-/-}$ transfer recipients may also be attributable to the reduced frequency of donor T cells, and possibly of mDCs, in CNS infiltrates at peak EAE (Fig. 2.8). A relative paucity of autoreactive T cells in the CNS could result in a reduction in local chemoattractants and immunostimulatory molecules (produced by either the T cells themselves or bystander myeloid or glial cells) that enhance inflammatory infiltration of the deep white matter. Finally, lower IL-1α expression by mDCs and macrophages (Fig. 2.10B) may limit the extent of destructive inflammation. The mechanism of action of GM-CSF during EAE is further complicated by the possibility that it suppresses the expression of factors with potential neuroprotective or immunoregulatory properties, such as M-CSF and CCL5 (Fig. 2.10) (75–77).

The distinctive cellular composition of inflammatory infiltrates in *Csf2r*$^{-/-}$ versus WT transfer recipients was associated with differential expression of leukocyte mobilizing/ growth

factors. G-CSF was disproportionately elevated in spinal cord homogenates of WT mice, consistent with the predominance of neutrophils in their neuroinflammatory infiltrates (Figs 2.8B and 2.6A). We previously showed that G-CSF plays a critical role in EAE pathogenesis by driving mobilization and activation of neutrophils (78). Activated neutrophils can mediate blood-brain-barrier breakdown during EAE and facilitate the mobilization of monocytes from the bone marrow into the circulation, from where they can be recruited to the CNS (74, 78). The hypothesis that GM-CSF drives tissue damage during EAE, at least in part, via the direct modulation of neutrophils is challenged by the observation that *Csf2r*$^{flox/flox}$x*LysM-cre* conditional knock-out mice (in which neutrophils are devoid of GM-CSF receptor) remain susceptible to EAE (41). However, we have found that *LysM-cre* does not drive genetic recombination in a significant percent of CNS-infiltrating neutrophils (unpublished data). Furthermore, the data in Fig. 2.9 indicate that, in addition to direct effects, GM-CSF could activate neutrophils indirectly by stimulating other CNS myeloid cells to produce G-CSF.

The data presented in this paper illustrate the pleiotropic effects of GM-CSF during Th17 mediated EAE, which collectively increase susceptibility to active immunization and exacerbate the clinical course following adoptive transfer. Our results suggest that GM-CSF is not required for the initial influx of leukocytes to the CNS or development of neurological deficits in our model, but facilitates deep intraparenchymal infiltration and mediates long-lasting damage to myelin and axons. We believe that this study is the first to implicate a specific role of GM-CSF in the establishment of chronic, as opposed to acute, neurological disability. Interestingly, a growing body of literature indicates that myeloid cell dysregulation is more prominent in chronic progressive that in relapsing-remitting forms of MS (31, 79–82). Our results support the position than GM-CSF may be a viable therapeutic target for the treatment of progressive MS.

CHAPTER 3 – GM-CSF Drives Chronic EAE via Activation of the CCR1/ CCL6 Chemokine Pathway

****Portions of this chapter are being prepared for publication**
Duncker PC, Munie AN, Wilkinson NM, Washnock-Schmid JM, Segal BM. GM-CSF drives chronic EAE via activation of the CCR1/ CCL6 chemokine pathway.

Abstract

Granulocyte-macrophage colony-stimulating factor (GM-CSF), a myeloid cell mobilizing and growth factor, has been implicated in the pathogenesis of autoimmune demyelinating disease. It plays a critical role in experimental autoimmune encephalomyelitis, an animal model that simulates many of the clinical and pathological features of multiple sclerosis (MS). We recently showed that although GM-CSF receptor-deficient (*Csf2r*$^{-/-}$) mice initially succumb to EAE following the adoptive transfer of encephalitogenic CD4^{+} T cells, they undergo clinical remission while their WT counterparts develop chronic deficits. We found that the cellular composition and spatial distribution of central nervous system (CNS) infiltrates differ between *Csf2r*$^{-/-}$ and WT adoptive transfer recipients at peak EAE. The most striking finding was a relative dearth of neutrophils in the CNS of *Csf2r*$^{-/-}$ adoptive transfer recipients, and that inflammatory cells do not penetrate deeply into the parenchyma compared with WT transfer recipients. However, the pathways underlying these differences remain to be elucidated. In this study, we show that protein levels of the chemokine CCL6 are relatively low in CNS homogenates obtained from *Csf2r*$^{-/-}$ adoptive transfer recipients compared with WT recipients at peak EAE. We further found that GM-CSF receptor signaling into CNS-infiltrating monocytes, dendritic cells, and neutrophils directly drives production of CCR1 and its ligand, CCL6, by those cells. Our data support that a GM-CSF

dependent CCR1/ CCL6 pathway perpetuates the retention of CNS infiltrates in the later stages of EAE, resulting in permanent neurological deficits. In support of that hypothesis, treatment of WT adoptive transfer recipients with a small molecule CCR1 antagonist prevented clinical EAE when administered prophylactically and triggered clinical remission when administered starting at EAE onset. CCR1 antagonism led to alterations in CNS myeloid infiltrates that mimicked the effects of GM-CSF receptor deficiency. Our data indicate that GM-CSF drives chronic CNS damage and disability in EAE via activation of the CCR1/ CCL6 chemokine pathway, which supports prolonged infiltration of the CNS by pathogenic myeloid cells.

Introduction

Multiple sclerosis (MS) is an autoimmune demyelinating disease of the central nervous system (CNS) believed to be initiated by $CD4^+$ T cells expressing auto-reactive T cell receptors (TCRs) specific for CNS antigens (83). The specific antigen recognized by these TCRs are unknown. However, the efficacy of lymphocyte targeted DMTs in suppressing MS relapses supports a predominant role for those cells in lesion formation. Additionally, numerous studies in experimental autoimmune encephalomyelitis (EAE, an animal model of MS) demonstrate that myelin-reactive $CD4^+$ Th1 or Th17 cells are capable of driving CNS autoimmune disease with clinical and pathological features reminiscent of MS (31, 84, 85). When transferred into unmanipulated syngeneic hosts, the T cells enter the CNS where they are reactivated by resident antigen presenting cells (APCs) that bear endogenous myelin peptides bound to MHCII molecules. The interaction between myelin-reactive Th1/ 17 cells and CNS APCs lead to an inflammatory cascade which drives brain and spinal cord damage, resulting in neurological disability.

A principal step in the neuroinflammatory cascade is the production of granulocyte-macrophage colony-stimulating factor (GM-CSF) by reactivated $CD4^+$ T cells (40, 42, 44, 71, 86). Within the hematopoietic compartment, GM-CSF receptor (GM-CSFR) is exclusively expressed by cells of the myeloid lineage, including monocytes, macrophages, dendritic cells (DCs), and granulocytes, and its ligation promotes survival, activation, and differentiation (87). The primary target, and mechanism of action, of GM-CSF during the development of EAE is heavily debated. Microglia, $Ly6C^{hi}CCR2^+$ monocytes, myeloid-derived DCs (mDCs), and neutrophils have each been suggested to be impacted by GM-CSF signaling during EAE in a manner that is requisite for disease induction and/ or maintenance (41, 49, 71, 86). Not only does GM-CSF enhance phagocytosis by myeloid cells (potentially of myelin), but it can promote recruitment of leukocytes by induction of chemokines, including CCL2 (88, 89). CCL6 and its cognate receptor CCR1 have been found to be upregulated by GM-CSF signaling, but their role on myeloid cells during the effector phase of EAE has largely been overlooked, unlike CCL2/ CCR2 which are considered essential for disease development (90–96).

CCR1 is expressed by macrophages and microglia in active MS lesions (97). C57BL/6 CCR1 deficient (*Ccr1*$^{-/-}$) mice have a decreased incidence and severity of actively induced EAE compared with C57BL/6 WT mice (98). Blockade of CCR1 signaling using a small molecule antagonist reduced the clinical severity of EAE in rats (99). CCR1 can be ligated by a wide array of chemokines, however, CCL6 is specific for CCR1. High levels of CCL6 have been found in the CNS of mice with EAE (100–102). CCL6 is primarily a macrophage chemoattractant, although it has been shown to also attract B cells, $CD4^+$ T cells, and eosinophils under specific conditions.

The overall goal of the current study was to characterize the role of the CCR1/ CCL6 chemokine pathway in adoptive transfer EAE, particularly as it pertains to the function of GM-

CSF driven chronic disease. We found that GM-CSF signaling is critical for persistent CCL6 and CCR1 expression by myeloid cells in the CNS during later stages of EAE. CCR1 blockade starting immediately after T cell transfer resulted in complete resistance to EAE, while its administration following disease onset triggered clinical remission, mirroring the clinical course of GM-CSFR deficient adoptive transfer recipients.

Methods and Materials

Mice. Six- to eight-week-old CD45.1 congenic and WT C57BL/6 mice were obtained from Charles River Laboratories. *Csf2r*$^{-/-}$ mice (B6.129S1-Csf2rb^{1tm1Cgb}/J) mice were obtained from L. Robb (The Walter and Eliza Hall Institute), *Csf2*$^{-/-}$ mice were obtained from D. McGavern (National Institutes of Health), mT/mG (B6.129(Cg)-*Gt(ROSA)26Sor*$^{tm4(ACTB-tdTomato,-EGFP)Luo}$/J) mice were obtained from B. Moore (University of Michigan, Ann Arbor), and *Ccr1*$^{-/-}$ mice obtained from P. Murphy (National Institutes of Health) and bred in our facility. Mice were housed in micro-isolator cages under specific pathogen-free conditions. All animal studies were approved by the University Committee on Use and Care of Animals.

Induction and scoring of EAE. Mice were immunized s.c. with 100 μg of the MOG_{35-55} peptide (MEVGWYRSP-FSRVVHLYRNGK; Biosynthesis) in CFA (Difco) at four sites over the flanks. For active immunization, mice were also administered 300 ng inactivated Bordetella pertussis toxin i.p. on days 0 and 2. For adoptive transfer EAE, inguinal, axial, and brachial dLNs were harvested from donor mice 10-14 days post-immunization, pooled, homogenized, and passed through a 70 μm strainer (Fisher Scientific). Cells were cultured under Th17-polarizing conditions: MOG_{35-55} [50 μg/ml], rmIL-23 [8 ng/ml], rmIL-1α [10 ng/ml], and αIFNγ [10 μg/ml]. Following

96 hours of culture, $CD4^+$ T cells were purified by positive selection using L3T4 magnetic microbeads (Miltenyi Biotec). 3-6x10^6 $CD4^+$ T cells were injected i.p. to naïve recipients. The recipient mice were observed daily for signs of EAE, and rated for degree of disability using a 5 point scale, as previously described (68).

Flow cytometry. For surface staining, cells were resuspended in PBS with 2% FBS and Fc Block (αCD16/32) [100 ng/ml] before 1:2 dilution with fluorochrome-conjugated Abs. For intracellular staining, cells were stimulated either; overnight with MOG_{35-55} before brefeldin A (BFA) [5 µg/ml] was added for 4-6 hours, or with PMA [50 ng/ml], ionomycin [2 µg/ml], and BFA [5 µg/ml] for 4-6 hours. Cells were stained for surface markers, as above, fixed in 4% PFA, permeabilized with 0.5% saponin, and incubated with fluorochrome-conjugated anti-cytokine mAbs. Flow gating began with comparison of SSC-A vs. FSC-A to exclude events outside the normal parameters of leukocytes followed by doublet exclusion comparing FSC-A vs. FSC-H. Dead cells were gated out using fixable viability dyes. Microglia were identified as $CD45^{int}CD11b^+$. CNS-infiltrating immune cells were identified as $CD45^{hi}$. Data were collected with a FACSCanto II flow cytometer using FACSDiva software (v6.1.3 and v7.0, Becton Dickinson). A FACS Aria III cell sorter was used to purify immune cells from the CNS and spleen. Data were analyzed using FlowJo software (vX 10.0, Treestar).

Antibodies and reagents. The following antibodies were obtained from BD Biosciences: Allophycocyanin-Cy7-(αIFNγ [XMG1.2], αLy6G [1A8]). The following antibodies were obtained from BioLegend Allophycocyanin-(αCCR1 [S15040E], αCD26 [H194-112], αCD88 [20/70], Biotin-(αCD88 [20/70]), FITC-(αCCR1 [S15040E], αCD26 [H194-112]), PE-(αCD88 [20/70]).

The following antibodies were obtained from ThermoFisher: Allophycocyanin-(αB220 [RA3-6B2], αCD11c [N418]), eFluor 450-(αCD45 [30-F11], αCD45.1 [A20]), eFluor 506-Fixable Viability, eFluor 780-Fixable Viability, FITC-(αGM-CSF [MP1-22E9], αMHCII [M5/114.15.2]), PE-αCD4 [RM4-5], PE-Cy7-(αCD44 [IM7], αCD11b [M1/70], αCD4 [RM4-5]), and PerCP-Cy5.5-(αIL-17A [eBio17B7], αCD11c [N418]). rmIL-23 and rmIL-1α were obtained from R&D Systems. αGM-CSF (22E9.11) and αCD16/32 (2.4G2) were produced in house via hybridoma. 500μg of αGM-CSF or whole rat IgG (Sigma Aldrich) was administered i.p. every other day, beginning at time of immunization or T cell transfer, during blocking experiments. αIFNγ (XMG1.2) was obtained from Bio X Cell.

Isolation of inflammatory cells from the CNS, spleen, and blood. Tissue was harvested following intracardiac perfusion with 1X PBS. CNS was separated into whole brain or spinal cord, homogenized in 1 ml 1X PBS containing a protease inhibitor (Roche), and pelleted at 800 x g for 5-10 min. Supernatants were isolated and stored at -80°C. Pellets were resuspended in 3 ml collagenase A (1 mg/ml) and DNase I (1 mg/ml) in HBSS with calcium and magnesium and incubated in a 37°C water bath for 10 minutes. Samples were pelleted at 800 x g, resuspended in 27% Percoll, and centrifuged for 10 minutes at 800 x g. The myelin/ debris layer and Percoll were removed, and the cell pellet used for flow cytometric staining. Splenic immune cells were isolated by homogenization through a 70 μm strainer (BD Falcon). RBCs were lysed using ACK lysis buffer (Quality Biologicals). Blood was isolated into microtainers with EDTA (Becton Dickinson). Following centrifugation, plasma was isolated and stored at -80°C. Cells were resuspended in 6 ml 1X PBS with 2% FBS and underlayed with 3 ml pre-warmed Lympholyte-M (Cedarlane)

before centrifugation at 1750 x g for 20 min at room temperature. White blood cells were harvested from the interface, washed, and remaining RBCs were lysed using ACK lysis buffer.

Transwell assays. $Ly6G^+$ cells were purified by magnetic bead sorting (Miltenyi) as described by the manufacturer protocol. 3-µm-pore 65-mm-diamter transwells (Corning) were pre-coated with 2.5 µg/ml fibrinogen. Purified neutrophils were resuspended in 0.5% BSA in PBS at a concentration of $1x10^6$ cell/ml. 100 µl of cells ($5x10^5$ cells) were added to the top of the transwell. 600 µl CCL6 (R&D Systems) or CXCL2 (R&D Systems) were added to the bottom of the well at concentrations of 1 µg/ml and 20 ng/ml, respectively. Cells were allowed to incubate at 37°C for 2 hours before addition of 60 µl 0.5M EDTA to the bottom of the well. Cells were incubated for an additional 15 min at 4°C. The media in the bottom of the chamber was collected and analyzed for cell number by flow cytometry.

In vivo administration of CCR1 antagonist. Animals were administered 600 µg J113863 (Tocris) daily as described for each experiment. J113863 was first suspended in 100% DMSO, then brought to 5% DMSO by addition of 1X PBS. 5% DMSO in PBS was used as a vehicle control in all experiments in which J113863 was used.

Construction of mixed bone marrow chimeric mice. Mixed bone marrow chimeras were constructed by first ablating the endogenous hematopoietic cells of congenic (CD45.1) C57BL/6 WT mice with a lethal dose of 1300 Rads, delivered in two 650 Rad doses separated by 3 hours. For experiments comparing CNS immune cell infiltrates at peak EAE, irradiated mice were reconstituted with mT/mG and *Csf2r*$^{-/-}$ bone marrow mixed at a 1:2 ratio, respectively, to obtain

an approximate 50:50 composition of circulating leukocytes following reconstitution. Animals were kept on Baytril water for 2 weeks and allowed to reconstitute for an additional 6 weeks before induction of EAE.

qPCR. Cells were resuspended in either 300 µl RLT buffer or 1 ml Trizol (Life Technologies) before Qiagen RNeasy RNA purification. Purified RNA was converted into cDNA using the High Capacity cDNA Reverse Transcription Kit (Life Technologies). Relative RNA levels were quantified by SYBR Green qPCR performed on either a QuantStudio 3 or 6 (Applied Biosystems).

Multiplex cytokine analysis and ELISA. CNS cytokine levels in homogenate supernatants were measured using Luminex multiplex bead-based analysis (Millipore) using a Bio-Plex 200 system following the manufacturer's protocols. Data shown indicate levels within the linear portion of appropriate standard curves. CXCL13 Quantikine ELISA kit (R&D Systems) was used, according to manufacturer protocols, to determine the concentration of CXCL13 in CNS homogenate supernatants. Total protein was determined via Bradford assay (Thermo Scientific) and used to normalize analyte concentrations.

Immunofluorescence. Following intracardiac perfusion with Tyrode's and 4% paraformaldehyde (PFA), spinal columns were removed, post-fixed for 3 days in PFA, decalcified in 0.5 M EDTA for 4 days, cryoprotected in 30% sucrose, and embedded and frozen in OCT (Cellpath). 12 µm sections were blocked with Avidin B and biotin (Vector Labs) before staining with the following primary and secondary antibodies: goat αMBP (Santa Cruz Biotechnology), Alexa Fluor 488-conjugated donkey αgoat IgG (Life Technologies), rat αCD45 (eBiosciences), Alexa Fluor 647-

conjugated goat αrat (Life Technologies), mouse αSMI-32 (Covance), and Alexa Fluor 594 conjugated goat αmouse IgG. DAPI (Life Technologies) was used to label nuclei. Images were acquired on a Nikon Eclipse Ti, CoolSnap EZ camera, and NIS Elements: Basic Research v3.10. Appropriate image processing, including image merging and black level and brightness adjustments, was performed in Photoshop CC 2017 and applied equally to all samples.

Statistical analysis. Statistical analyses were performed using GraphPad Prism software (v6.05). Disease curves were compared by Two-way ANOVA and T-tests (day-by-day) without multiple comparisons. Immune parameters were compared using either unpaired two-tailed student's T-test with Welch's correction or two-way ANOVA with correction for multiple comparisons using Tukey's post-hoc test. Leukocyte numbers and mRNA from mixed bone marrow chimera mice were analyzed via paired, parametric T-test. Outliers were identified by ROUT analysis and removed as necessary. A p-value < 0.05 (*) was considered significant, with $p < 0.01$ (**), $p < 0.001$ (***), and $p < 0.0001$ (****).

Results

CCL6 is upregulated in the CNS during EAE; its expression during later stages of disease is GM-CSF dependent. We have previously shown GM-CSF receptor deficient (*Csf2r*$^{-/-}$) and WT recipients of encephalitogenic T cells develop EAE with comparable incidence and peak clinical scores (Fig. 2.2C). However, unlike WT adoptive transfer recipients, the *Csf2r*$^{-/-}$ recipients undergo spontaneous remissions and, therefore, do not develop chronic neurological deficits (86). This milder clinical course was associated with a decrease in the frequency of neutrophils in the CNS during the pre-clinical, onset, and peak phases of disease, as well as a reduction in myeloid-

derived DCs and donor CD4$^+$ T cells in the CNS at peak disease. To investigate the mechanism underlying these differences, we measured levels of an array of chemokines in the CNS of WT and *Csf2r*$^{-/-}$ recipients at serial time points during the course of EAE. Expression of the prototypic neutrophil chemokines, CXCL1 and CXCL2, and the monocyte chemokine, CCL2, were comparable in the CNS of WT and *Csf2r*$^{-/-}$ recipients during every stage of EAE (Fig. 3.1). CCL6 levels were also similar between the groups at disease onset. However, while CNS CCL6 levels continued to rise in WT recipients from onset through peak EAE, they fell to near baseline levels in *Csf2r*$^{-/-}$ mice during the peak and late stages of disease (Fig. 3.1).

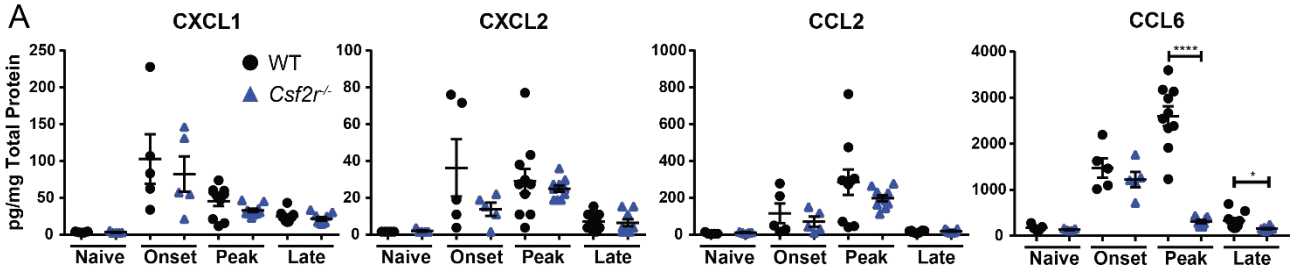

Figure 3.1 – CNS CCL6 expression is significantly reduced in *Csf2r*$^{-/-}$ adoptive transfer recipients during later stages of EAE compared with their WT counterparts.
EAE was induced in WT and *Csf2r*$^{-/-}$ mice by adoptive transfer of WT congenic Th17-polarized MOG-specific CD4$^+$ T cells. Spinal cord homogenates were collected at onset, peak, and late time points and analyzed for chemokine levels by Luminex based multiplex (CXCL1, CXCL2, and CCL2) or ELISA (CCL6) and normalized to total protein as determined by Bradford protein quantification. *p>0.05 and ****p>0.0001. Statistical significance was determined by two-tailed student's T-test.

CCL6 and CCR1 are expressed by CNS-infiltrating myeloid cells during EAE; CCL6 expression during later stages of disease is GM-CSF dependent. We next measured CCR1 and CCL6 expression by CNS-infiltrating cells during the course of EAE. Congenic (CD45.1$^+$) encephalitogenic CD4$^+$ T cells were adoptively transferred to CD45.2$^+$ WT recipients which were euthanized at onset, peak, and late time points. Flow cytometric analysis of the spinal cord infiltrates showed that CCR1 and CCL6 were expressed in infiltrating myeloid cells, but not lymphocytes, throughout the disease course. (Fig. 3.2A). The frequency of CCR1 expressing neutrophils monocyte/ macrophages, and myeloid-derived DCs rose steadily throughout the

disease course, peaking at late disease (Fig. 3.2B). Similarly, the frequency of CCL6^{+} cells within each myeloid cell subset was below 20% at disease onset, but rose steadily throughout the disease course, peaking at peak disease in monocytes/ macrophages and myeloid-derived DCs, and at late disease in neutrophils (Fig. 3.2B).

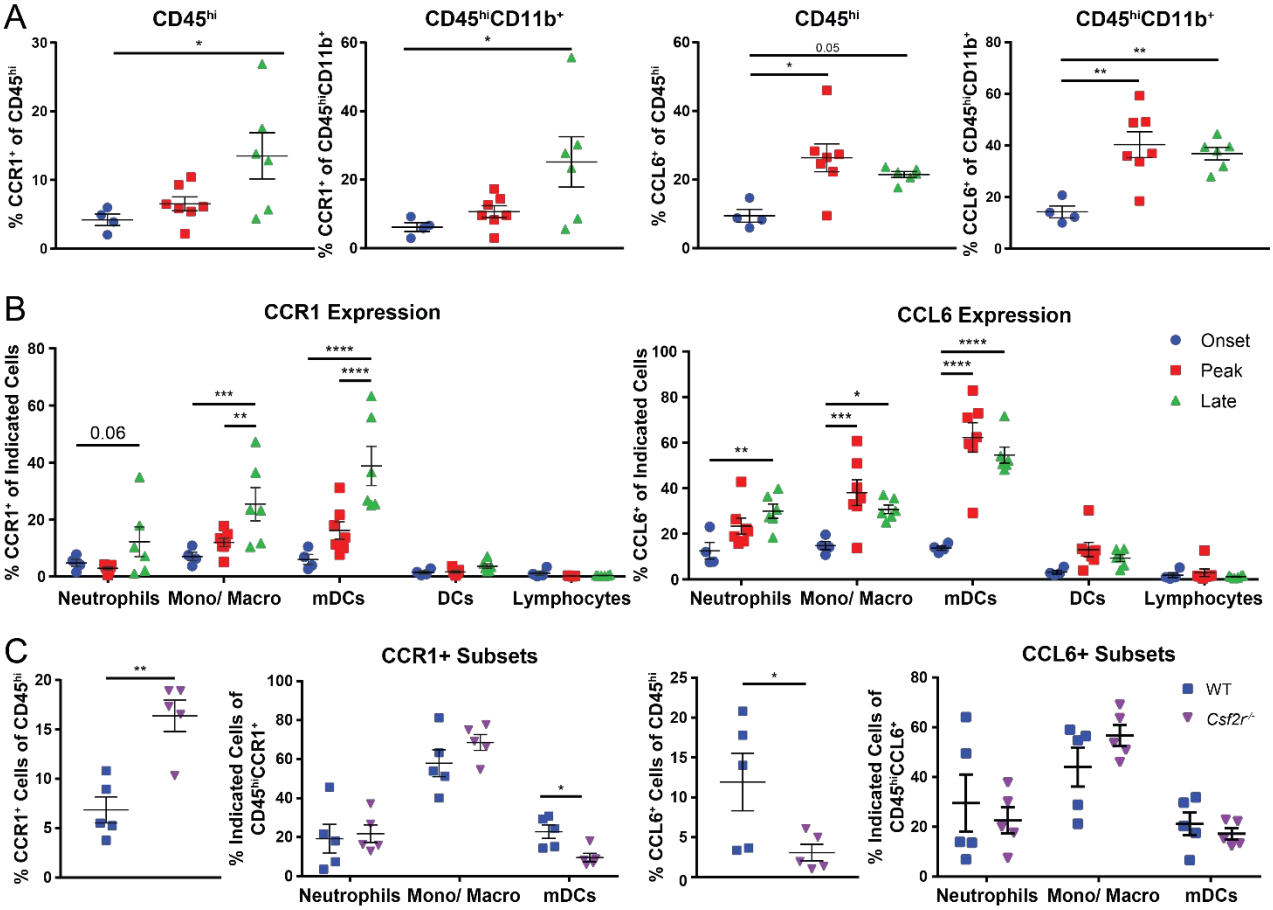

Figure 3.2 – CCR1 and CCL6 are detectable in CNS-infiltrating myeloid cells, expand throughout disease progression, and are GM-CSF dependent.
EAE was induced by adoptive transfer of congenic WT encephalitogenic Th17 CD4^{+} T cells to either (A, B, C) WT or (C) *Csf2r*$^{-/-}$ recipients. (A, B) Animals were euthanized at onset, peak, and late time points to analyze CCR1 and CCL6 expression by infiltrating myeloid cells. (A) shows the frequency of CCR1^{+} and CCL6^{+} cells in all CNS-infiltrating (CD45^{hi}) cells or in myeloid cells (CD45^{hi}CD11b^{+}). (B) Quantification of the frequency of CCR1 and CCL6 expressing cells within the identified cellular subsets. (C) Score matched WT and *Csf2r*$^{-/-}$ recipients were euthanized at peak EAE and CCR1 and CCL6 expression were determined as a frequency of all infiltrating cells, as well as the frequency of positive cells within each indicated myeloid cell subset. Error bars represent mean ± SEM. *p<0.05, **p<0.01, ***p<0.001, ****p<0.0001. Significance was determined by (A, B) two-way ANOVA with Tukey's post-hoc test or student's T-test.

Interrogation of these same markers in the spleen and blood revealed dynamic changes in those compartments as well (Fig. 3.3). In contrast to the CNS, which showed a progressive accumulation of CCR1^{+} neutrophils, monocytes/ macrophages, and mDCs throughout the disease course, the frequency of CCR1+ neutrophils and monocytes/ macrophages declined in the spleen between onset and peak disease (Fig. 3.3A left). However, the frequencies of CCR1^{+} monocytes/ macrophages, mDCs, and DCs rose in the blood throughout disease, more reminiscent of pattern observed in the CNS (Fig. 3.3 left). CCL6 expression increased in neutrophils in both the spleen and CNS following clinical onset but was stable in the blood (Fig. 3.3A and B right).

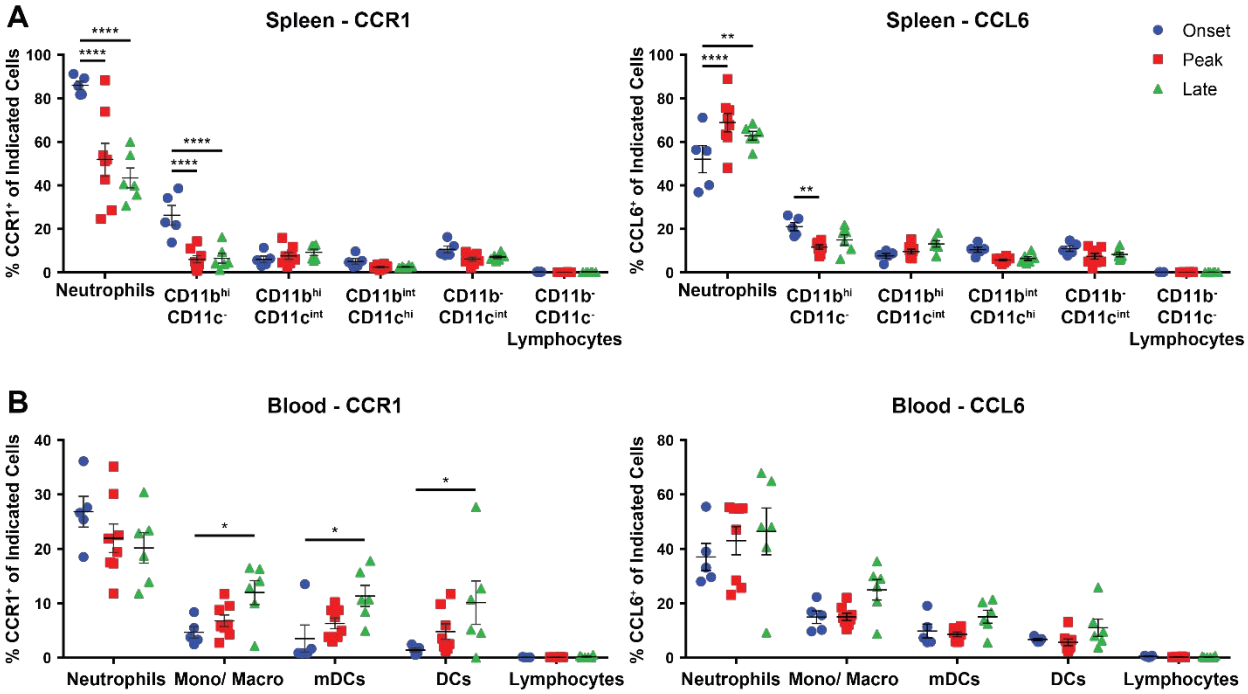

Figure 3.3 – CCR1 and CCL6 expression by circulating and splenic leukocytes evolves through the disease course.
EAE was induced by adoptive transfer of congenic WT encephalitogenic Th17 CD4^{+} T cells to WT recipients. Animals were euthanized at onset, peak, and late time points to analyze CCR1 and CCL6 expression by hematopoietic cells in the (A) spleen and (B) blood. Quantification of the frequency of CCR1 and CCL6 expressing cells within the identified cellular subsets for each tissue is shown. Error bars represent mean ± SEM. *p<0.05, **p<0.01, ****p<0.0001. Significance was determined by two-way ANOVA with Tukey's post-hoc test.

In order to determine whether expression of CCR1 and/ or CCL6 by the CNS myeloid cells is GM-CSF dependent, we repeated the flow cytometric analysis comparing WT and *Csf2r*$^{-/-}$

adoptive transfer mice at peak disease. The frequency of CCL6 expressing $CD45^{hi}$ CNS-infiltrating cells was significantly lower in *Csf2r*$^{-/-}$ versus WT recipients. However, the distribution of myeloid subsets within the $CCL6^{+}$ population was similar between the groups (Fig. 3.2C right). The percentage of CNS myeloid cells that were $CCR1^{+}$ cells was significantly elevated in the absence of GM-CSF signaling, possibly reflecting decreased CCL6 driven internalization of the receptor (Fig. 3.2C left).

Neutrophils isolated from the spleens of MOG/ CFA primed mice, or mice with adoptive transfer EAE, migrate toward CCL6. To determine if neutrophils would migrate in response to CCL6, and if this chemotaxis was activation dependent, spleen-derived neutrophils ($Ly6G^{+}$) were magnetically sorted from WT naïve or MOG_{35-55}-primed and analyzed in a transwell assay for chemotaxis towards CCL6, or CXCL2 as a positive control. In parallel experiments, neutrophils were derived from both the spleen and CNS of WT recipients of encephalitogenic $CD4^{+}$ T cells at peak disease and tested under the same conditions. Splenic neutrophils from primed, but not naïve, animals migrated across the transwell in response to CCL6 (Fig. 3.4A). The migration of the primed neutrophils towards CCL6 was completely blocked by the selective CCR1 antagonist J113863 (Fig. 3.4B). Splenic neutrophils from both primed and naïve mice migrated in response to CXCL2, however, the former did so more efficiently (Fig. 3.4A). Splenic, but not CNS, neutrophils isolated from mice with adoptively transferred EAE responded to both CCL6 and CXCL2 (Fig. 3.4C). Based on these results, we hypothesize that activation of neutrophils within the inflamed CNS may lead to internalization of CCR1 and/ or CXCR2 secondary to binding by their respective ligands (which are expressed at high levels in that microenvironment), making them less responsive to those chemoattractants *ex vivo*.

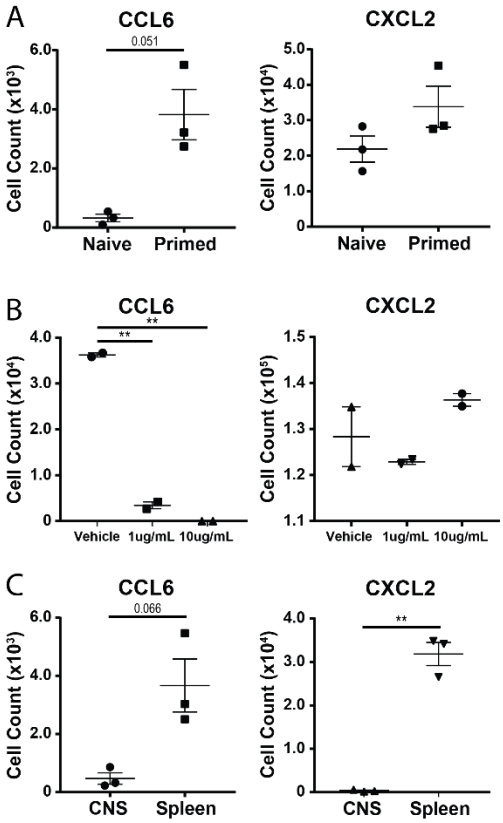

Figure 3.4 – Neutrophils isolated from the spleens of MOG$_{35-55}$ primed mice, or the CNS of mice with adoptively transferred EAE, exhibit enhanced chemotaxis towards CCL6.
(A-C) Ly6G$^+$ neutrophils were magnetically purified from the following tissues before being tested for CCL6 induced chemotaxis in a transwell assay. (A) Spleens of naïve and MOG$_{35-55}$-primed WT mice. (B) Spleen of MOG$_{35-55}$-primed which were then pretreated with the CCR1 antagonist J113863 at 1 and 10 μg/ml. (C) The spleen and CNS of mice WT mice at peak adoptive transfer EAE. *p<0.05, **p<0.01. Significance was determined by (A, B, C) student's T-test or (D) two-way ANOVA with Tukey's post-hoc test.

GM-CSF stimulates CCR1 and CCL6 expression by peripheral myeloid cells. Previous research has shown that GM-CSF stimulation can induce CCL6 expression by mouse bone marrow myeloid cells and CCR1 expression by human granulocytes (90, 91). To directly investigate the effects of GM-CSF signaling on CCR1 and CCL6 expression by mature murine myeloid cells, we cultured either Ly6G$^+$, or unsorted, splenic cells isolated from naïve GM-CSF deficient (*Csf2*$^{-/-}$) mice in the presence or absence or recombinant mouse GM-CSF (rmGM-CSF), for mRNA or protein analysis, respectively. Selected chemokines and their receptors were measured on the mRNA level at 4 hours via qPCR, and on the protein level at 6 and 24 hours by flow cytometry.

GM-CSF stimulation led to a robust upregulation of mRNA encoding CCL6, CCR1, CXCL2, and CXCR2 in both $Ly6G^{+}$ cells at 6 hours. CCL2, CCR2, and CXCL1 were universally detected at low levels at baseline and were not altered in response to GM-CSF stimulation (Fig. 3.5A). On the protein level, $Ly6G^{+}$ neutrophils, $Ly6G^{-}CD11b^{hi}CD11c^{-}$ monocytes/ macrophages, and $Ly6G^{-}CD11b^{hi}CD11c^{int}$ myeloid-derived DCs were the major sources of both CCR1 and CCL6 among splenic cells. Very few $Ly6G^{-}CD11b^{int}CD11c^{hi}$ or $Ly6G^{-}CD11b^{-}CD11c^{int}$ DCs, and essentially no $Ly6G^{-}CD11b^{-}CD11c^{-}$ lymphocytes, expressed either CCR1 or CCL6 (Fig 3.5D and 3.4E right, and data not shown). Within 6 hours of GM-CSF stimulation, CCR1 protein expression was elevated from baseline on neutrophils, monocytes/ macrophages, and $CD11b^{hi}CD11c^{int}$ DC. (Fig. 3.5D). CCR1 levels returned to baseline on all cell types by 24 hours (Fig. 3.5D right). Intracellular CCL6 protein expression was also enhanced in neutrophils, monocytes/ macrophages, and monocyte-derived DCs following a 6-hour culture with recombinant GM-CSF (Fig. 3.5E). In contrast to CCR1, CCL6 protein levels progressively rose in each of those GM-CSF stimulated subsets between 6 and 24 hours (Figs. 3.5D, E).

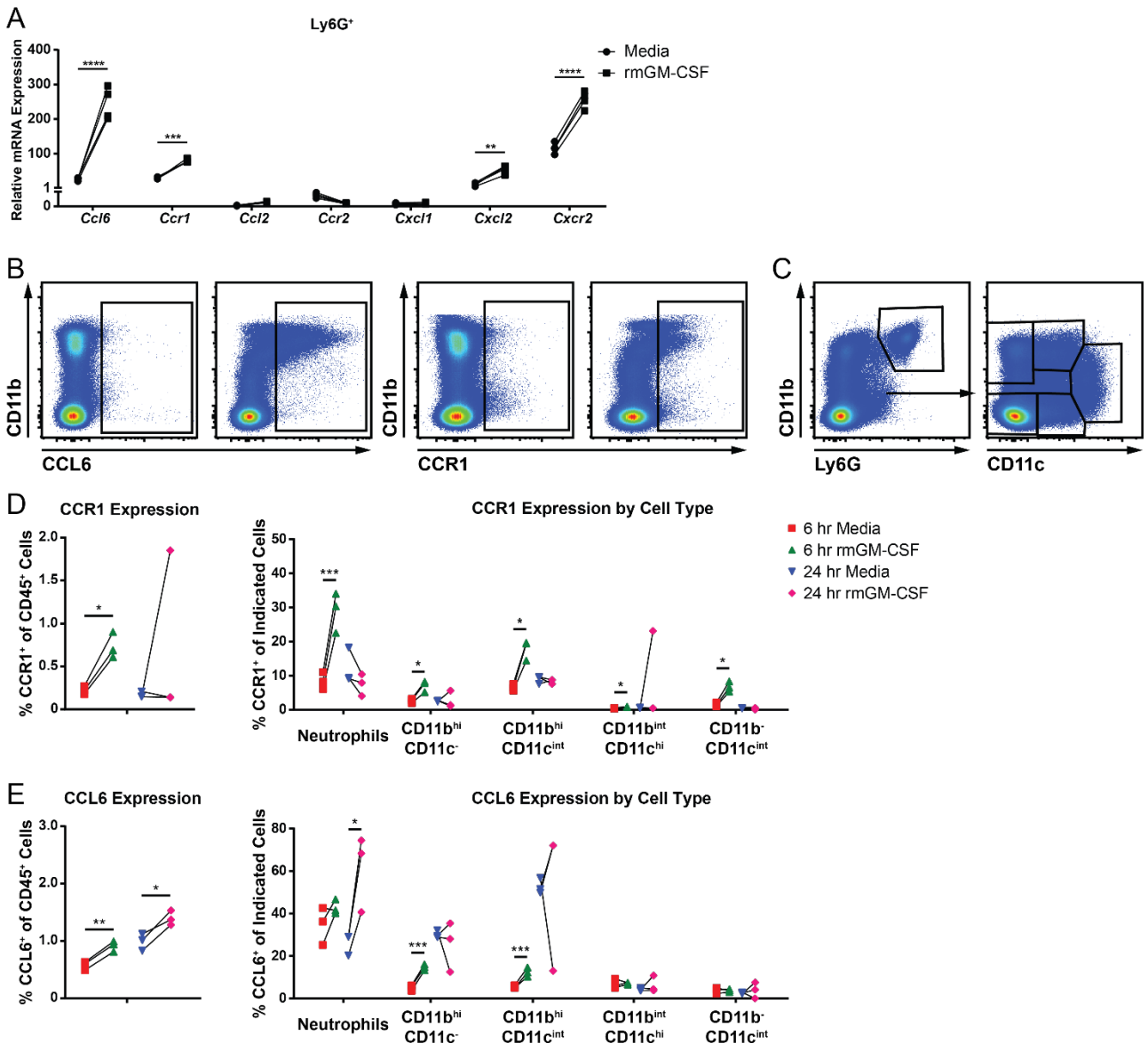

Figure 3.5 – GM-CSF stimulation drives CCL6 and CCR1 expression by splenic myeloid cell subsets.

(A) Ly6G^{+} neutrophils were magnetically sorted from the spleen of MOG$_{35-55}$-primed *Csf2*$^{-/-}$ mice and stimulated *in vitro* for 4 hours with rmGM-CSF, or control media, before purification of mRNA for qPCR analysis of gene expression changes. (B-E) Splenocytes were isolated from MOG$_{35-55}$-primed *Csf2*$^{-/-}$ mice and stimulated *in vitro* with rmGM-CSF, or control media, for 6 or 24 hours before analysis of CCR1 and CCL6 protein expression changes as determined by flow cytometry. (B) Shows isotype controls for CCL6 and CCR1 compared to 24-hour time points. (C) Shows gating used to identify neutrophils and subsets of myeloid cells for which (D) CCR1 and (E) CCL6 frequencies are quantified. *p<0.05, **p<0.01, ***p<0.001, ****p<0.0001. Significance was determined by two-way ANOVA with Tukey's post-hoc test or student's T-test.

Therapeutic treatment with CCR1 antagonist suppresses adoptive transfer EAE and curtails CNS-infiltration by monocytes and CNS-initiating cDCs. In order to determine whether

the development of chronic deficits in WT adoptive transfer recipients is dependent on CCR1, we compared the clinical courses of WT mice treated with a CCR1 small molecule antagonist versus vehicle beginning on the day following adoptive transfer of encephalitogenic T cells. CCR1 antagonism prevented the development of clinical signs (Fig. 3.6A). Following treatment cessation, animals rapidly developed EAE to an equivalent incidence as vehicle-treated mice, although they experienced milder disease (Fig. 3.6A, B). We analyzed the composition of CNS infiltrating cells isolated from both groups on the day before expected clinical onset in the control group.

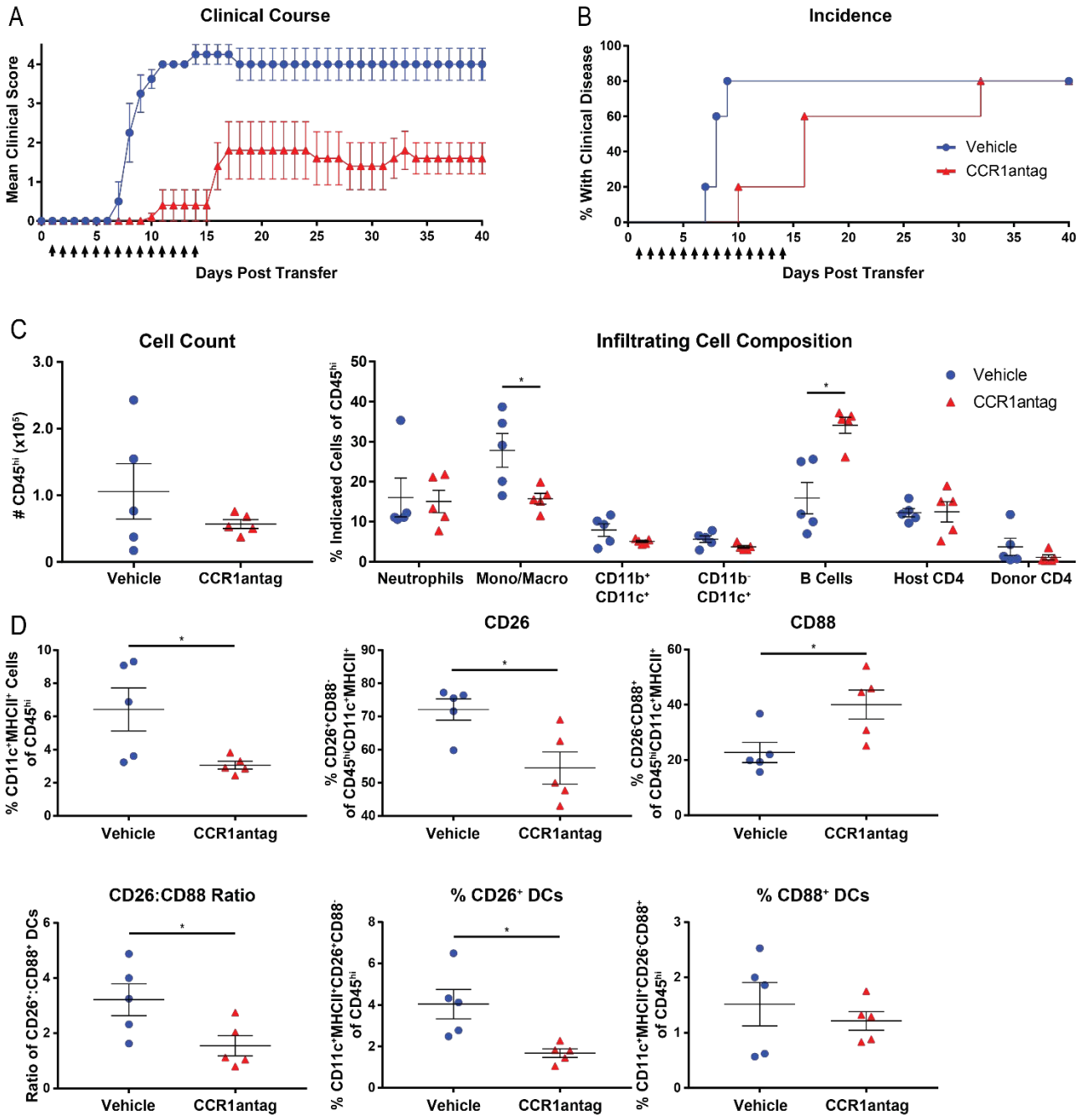

Figure 3.6 – Therapeutic treatment with a CCR1 antagonist blocked adoptive transfer EAE and was marked by a reduction in monocytes, macrophages, and CD26$^+$ cDCs.

EAE was induced in WT mice by adoptive transfer of congenic MOG_{35-55}-primed CD4$^+$ T cells. CCR1 antagonist, or vehicle control, was administered i.p. daily beginning the day after T cell transfer. (A, B) Animals were monitored daily for signs of disease. (C) Some animals were euthanized on day 6, before development of clinical symptoms, and changes in CNS infiltration were characterized by flow cytometry. (D) Changes in DC accumulation in the CNS were quantified by comparison of CD26 and CD88 expressing cells within the CD11c$^+$MHCII$^+$ population. *p<0.05. Statistical significance was determined by (C, D) student's T-test.

We observed no difference in the total number of infiltrating $CD45^{hi}$ cells per CNS specimen. However, there was a reduction in the frequency of monocytes/ macrophages ($CD45^{hi}CD11b^{+}Ly6G^{-}CD11c^{-}$) and an increase in the frequency of B cells in CNS infiltrates from mice treated with the CCR1 antagonist (Fig. 3.6C). We previously reported that mice which develop EAE in the absence of GM-CSF signaling have a significant reduction in the number of infiltrating neutrophils, and an increase in infiltrating, B cells early in disease development (86). Although others have reported CCR1 expression by B cells, we have not observed *Ccr1* mRNA or CCR1 protein expression by those cells (data not shown).

We recently reported that CNS-infiltrating $CD11c^{+}MHCII^{+}$ DCs are a heterogeneous population that encompasses $CD88^{+}CD26^{-}$ monocyte-derived DC (moDC) and $CD88^{-}CD26^{+}$ classical (cDCs) (103). We found that moDC isolated from the CNS of mice with EAE are inefficient APCs, while cDCs induce robust activation/ reactivation, proliferation, and differentiation of MOG_{35-55}-specific T cells. Furthermore, depletion of $CD26^{+}$ cDCs decreased the incidence of adoptively transferred EAE. Although prophylactic treatment with the CCR1 antagonist did not alter the frequency of total $CD45^{hi}CD11b^{+/-}CD11c^{+}$ DC in the CNS during the preclinical phase, it caused a selective depletion of $CD26^{+}$ cDC, resulting in a decreased cDC:moDC ratio (Fig. 3.6D).

Therapeutic CCR1 antagonism triggers clinical remission associated with a reduction in CNS-infiltrating neutrophils and B cells and restriction of infiltrates to the peripheral edges of the spinal cord. When WT recipients of encephalitogenic T cells were treated with a small molecule CCR1 antagonist on the day of clinical onset, they subsequently experienced clinical remission, while vehicle-treated mice developed chronic deficits (Fig. 3.67A, B). The former mimics the clinical course of $Csf2r^{-/-}$ adoptive transfer recipients (86). CCR1 antagonist induced clinical

remission was associated with a reduction in the total number of CD45^{hi} CNS infiltrating cells and a reduction in the frequencies of neutrophils and B cells (Fig. 3.7C). We did not observe any effect on the frequencies of CD26^{+} cDCs or CD88^{+} moDCs (data not shown).

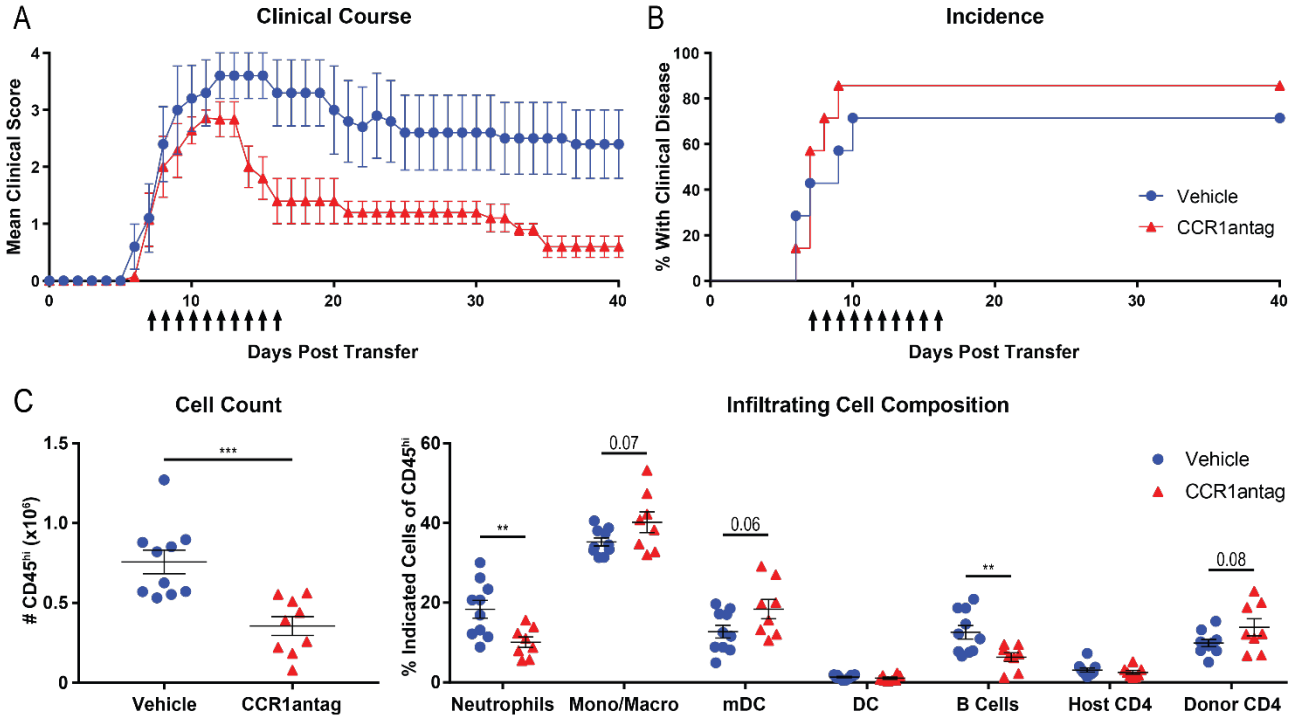

Figure 3.7 – Therapeutic treatment with a CCR1 antagonist leads to clinical remission marked by a significant reduction in CNS-infiltrating immune cells.
EAE was induced in WT mice by adoptive transfer of congenic MOG$_{35-55}$-primed CD4^{+} T cells. CCR1 antagonist, or vehicle control, was administered i.p. daily beginning the second day after disease symptoms were observed. (A, B) Animals were monitored daily for signs of disease. (C) Some animals were euthanized at peak disease and changes in CNS infiltration were characterized by flow cytometry. **p<0.01, ***p<0.001. Statistical significance was determined by (C) student's T-test.

At peak EAE, we obtained spinal cords from adoptive transfer recipients in which vehicle or CCR1 antagonist had been administered therapeutically and performed histological analyses. Specimens from the active treatment cohort demonstrated less demyelination (Fig. 3.8). The vast majority of inflammatory cells were restricted to the meningeal space surrounding the spinal cord, similar to what was observed in EAE induced in the absence of GM-CSF signaling (86). In contrast, inflammatory infiltrates penetrated into the parenchyma of spinal cords from vehicle-treated mice.

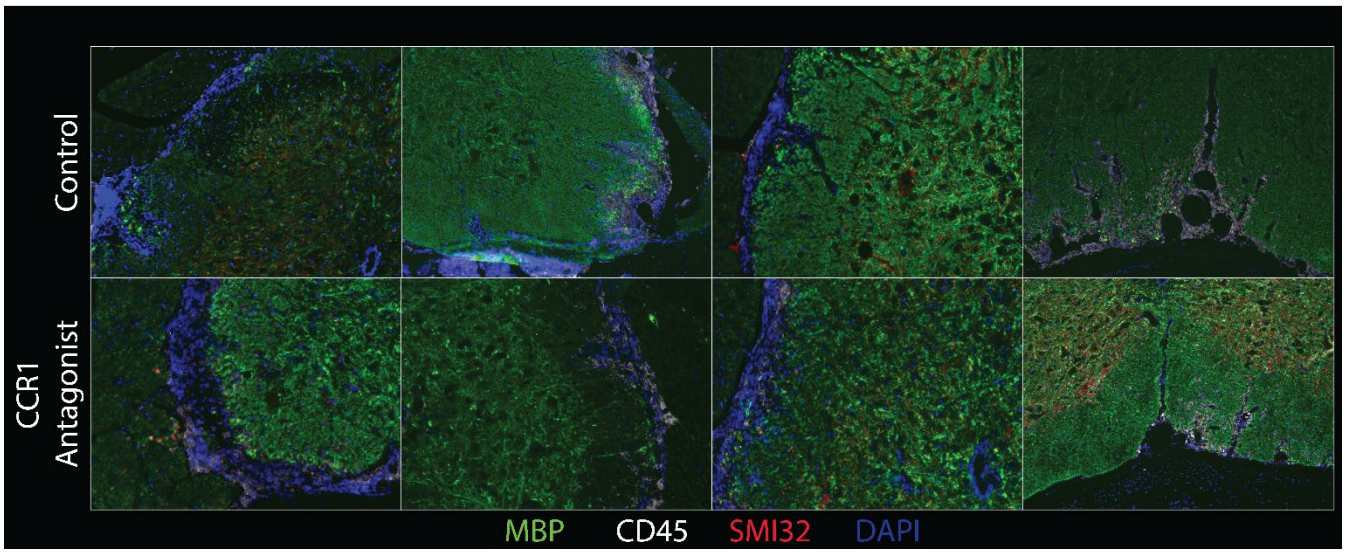

Figure 3.8 – Inflammatory infiltrates in CCR1 antagonist treated mice penetrate less deep in the spinal cord white matter and induce less demyelination compared to vehicle-treated mice.
EAE was induced in WT mice by adoptive transfer of congenic MOG_{35-55}-primed $CD4^+$ T cells. CCR1 antagonist, or vehicle control, was administered i.p. daily, beginning the day after neurological deficits were observed. Score matched mice were euthanized at peak disease for immunohistochemical analyses of CNS-inflammation and demyelination.

Discussion

The research presented in this chapter expands understanding of the role of GM-CSF in the development of autoimmune demyelinating diseases, particularly as it pertains to the interplay of the adaptive and innate immune systems. We show that, in our model, CCL6 is expressed at high levels in the CNS throughout the course of EAE. This not only affirms previous findings, but also mechanistically links sustained CCL6 expression by myeloid cells in EAE with GM-CSF signaling (Figs. 3.1 and 3.2) (90, 91, 97). Longitudinal studies of WT and *Csf2r*$^{-/-}$ adoptive transfer recipients revealed that CCL6 expression in the CNS is GM-CSF independent at clinical onset. However, in the absence of GM-CSF signaling, CCL6 levels fall precipitously in the CNS later in the course, in association with clinical remission (Figs. 3.1 and 3.2). Collectively, our data show that CCL6 expression is maintained and promoted by GM-CSF following disease onset. In contrast, CNS levels of CXCL2, CXCL1, and CCL2 were unaffected by GM-CSFR deficiency at any time point

following cell transfer (Fig. 3.1), despite our observation that GM-CSF stimulates the upregulation of CXCL2 mRNA expression in neutrophils *in vitro* (Fig. 3.5A). This paradox may be due to compensatory production of CXCL2 and CCL2 by alternative cell sources in the inflamed CNS that are not GM-CSF dependent.

Other laboratories have shown that GM-CSF signaling in human neutrophils can drive expression of CCR1 and that, under certain circumstances, neutrophils infiltrate peripheral tissues in response to a CCR1 chemokine gradient (91, 104, 105). Here we show that GM-CSF directly drives CCR1 expression by murine $CD11b^{hi}CD11c^{-}$ monocytes/ macrophages, DCs, and neutrophils (Fig. 3.5B-D). Additionally, GM-CSF stimulation drove robust expression of CCL6 in neutrophils, monocytes/ macrophages, and $CD11b^{hi}CD11c^{int}$ DCs (Fig. 3.5E). Neutrophils isolated from the periphery of mice actively immunized with MOG_{35-55} in CFA, or injected with encephalitogenic T cells, were highly responsive to CCL6 (Fig. 3.4A, B). In contrast, neutrophils isolated from the CNS of adoptive transfer recipients did not migrate toward CCL6 in transwell assays (Fig. 3.4). We speculate this to be a result of CCL6-mediated downregulation of CCR1 within the CNS, as has been described in other experimental systems (106).

The experiments in Figures 3.6 and 3.7 indicate dual roles for CCR1 in CNS inflammatory demyelinating disease. Interestingly, in a model of antibody-mediated arthritis, it was shown that CCR1 and CXCR2 act in a non-redundant manner to drive different stages of joint inflammation (107). In this model, initial joint infiltration by pathogenic neutrophils occurred via a CCR1 dependent pathway. Later in disease, joint-infiltrating neutrophils required CXCR2 to enter the synovium and induce damage. CXCR2 is crucial for the development of EAE, as *Cxcr2*$^{-/-}$, or WT mice treated with a CXCR2 blocking antibody, are resistant to disease (33, 74, 78, 108). To date, no studies have interrogated the relative contributions of CXCR2 and CCR1 on CNS infiltration

by neutrophils in EAE, although our data suggest CXCR2 is required for early infiltration of the CNS by damage-inducing neutrophils while CCR1 mediates neutrophil infiltration following disease onset.

In this study, we show that the CCR1 chemokine pathway is employed early in EAE to promote the infiltration of inflammatory myeloid cells into the CNS (Fig. 3.6A-C). Most notably, we observed that defective CCR1 signaling led to a significant reduction in the ratio of $CD88^{+}$ moDCs to $CD26^{+}$ cDCs in CNS infiltrates (Fig. 3.6D). Considering that $CD26^{+}$ cDCs are the most efficient CNS APCs for encephalitogenic T cell reactivation, their decline in mice treated prophylactically with CCR1 antagonists is a likely mechanism for the improvement of clinical EAE in these mice (103). However, our data suggest that CCL6/ CCR1 interactions play a distinct role later in the course. When we delayed the administration of CCR1 antagonists until mice developed clinical signs, we found that neutrophils were preferentially blocked from accumulating in the CNS, while the frequency of CNS DC subsets was unperturbed (Fig. 3.7C). Therapeutic treatment with CCR1 antagonists triggered clinical remissions, while control mice maintained a high level of neurological disability (Fig. 3.7A, B). WT adoptive transfer recipients treated therapeutically with CCR1 antagonists and untreated *Csf2r*$^{-/-}$ adoptive transfer recipients exhibit similar clinical and immunopathological changes when compared with their respective control groups (86). This suggests that one of the mechanisms by which GM-CSF promotes chronic EAE is to stimulate expression of CCL6 and CCR1 expression by CNS infiltrating myeloid cells beyond the time of clinical onset.

Flow cytometric analyses of CNS infiltrates does not address the spatial distribution of inflammatory cells within the spinal cord. Although there were no differences in the total number of $CD45^{hi}$ inflammatory cells in the CNS of WT and *Csf2r*$^{-/-}$ adoptive transfer recipients at peak

clinical EAE, infiltrates were largely confined to the meningeal space of the latter mice, while they penetrated into the white matter of the former mice (86). Here we found that in the spinal cord of mice treated therapeutically with the CCR1 antagonist, when compared to score matched control mice, immune cells were concentrated in the meningeal space, and penetrated less deeply into the parenchymal tissue. This was accompanied by a reduction in overall demyelination (Fig. 3.8). Considering these spatial differences, changes in the immune infiltrate, and the strong association with GM-CSF, we hypothesize that neutrophils initially enter the CNS meningeal space through CXCR2-mediated chemotaxis. Their subsequent migration from the meningeal space into the parenchymal white matter is mediated by GM-CSF dependent CCR1:CCL6 interactions. Further studies are underway to identify the spatial localization of CCL6 and CXCL2 within the inflamed spinal cord.

The results of these experiments indicate dual roles for the CCR1 pathway in EAE. First, during the preclinical and onset phases of disease, CCL6 is upregulated in the CNS by a GM-CSF independent mechanism and promotes infiltration of monocytes and classical DCs, thereby increasing T cell:APC interactions and allowing the initiation of clinical symptoms. Following disease onset, CCL6 plays a critical role in promoting the accumulation of neutrophils in the CNS, thus driving persistent damage and chronic EAE. MS is a complex disease which may be driven by distinct pathways in different populations of people who are affected. The effectiveness of current disease modifying therapies (DMTs) varies depending on individual patient responsiveness. Each of the current DMTs functions by either blockade or depletion of potentially pathogenic lymphocytes. None specifically target myeloid cells. Differences in responsiveness to DMTs may be reflective of differences in the underlying pathogenic mechanisms in individuals. CNS-infiltrating myeloid cells are a major driver of pathogenesis in EAE and, ostensibly, MS.

Targeting the myeloid compartment could lead to novel therapeutics which may be effective in patients who have been unresponsive to lymphocyte targeting DMTs. Our data support further investigation of GM-CSF, CCR1, and myeloid cell activation/ trafficking as therapeutic targets in the treatment of MS.

CHAPTER 4 – CNS-Resident Classical DCs Play a Critical Role in CNS Autoimmune Disease

Giles DA*, **Duncker PC***, Wilkinson NM, Washnock-Schmid JM, Segal BM. CNS-resident classical DCs play a critical role in CNS autoimmune disease. Accepted for publication September 2018 at Journal of Clinical Investigation.

*Co-first authors

Abstract

Experimental autoimmune encephalomyelitis (EAE) is an inflammatory demyelinating disease of the central nervous system (CNS), induced by the adoptive transfer of myelin-reactive $CD4^+$ T cells into naïve syngeneic mice. It is widely used as a rodent model of multiple sclerosis (MS). EAE lesion development is initiated when transferred $CD4^+$ T cells access the CNS and are reactivated by local antigen presenting cells (APCs) bearing endogenous myelin peptide/ MHC Class II complexes. The identity of the CNS-resident, lesion-initiating APC is widely debated. Here we demonstrate that classical dendritic cells (cDCs) normally reside in the meninges, brain, and spinal cord in the steady state. These cells are unique among candidate CNS APCs in their ability to stimulate naïve, as well as effector, myelin-specific T cells to proliferate and produce pro-inflammatory cytokines directly *ex vivo*. cDCs expanded in the meninges and CNS parenchyma in association with disease progression. Selective depletion of cDCs led to a decrease in the number of myelin-primed donor T cells in the CNS and reduced the incidence of clinical EAE by half. Based on our findings, we propose that cDCs, and the factors that regulate them, be further investigated as potential therapeutic targets in MS.

Introduction

Experimental autoimmune encephalomyelitis (EAE), an autoimmune demyelinating disease of the central nervous system (CNS), is widely used as an animal model of multiple sclerosis (MS). EAE can be induced by the adoptive transfer of highly purified, myelin-reactive $CD4^+$ T-helper (Th)1 or Th17 effector cells into otherwise unmanipulated, syngeneic hosts. Lesion formation in adoptively transferred EAE is triggered when myelin-specific $CD4^+$ T cells access the naïve CNS and are reactivated by local antigen presenting cells (APCs) bearing endogenous myelin peptide/ MHC Class II (MHCII) complexes (109). The identity of the CNS-resident, lesion-initiating APC is widely debated. By definition, the cell type in question must express MHCII and co-stimulatory molecules and possess the machinery necessary to process immunogenic peptides from larger myelin proteins. In order to mediate epitope spreading during clinical relapse and/ or progression, a candidate APC would also have to be capable of activating naïve $CD4^+$ T cells specific for secondary myelin epitopes and of polarizing them toward encephalitogenic Th1 or Th17 lineages (110).

Microglia have been posited as the critical resident APC of the CNS (111). It has become increasingly recognized that microglia are heterogeneous and that distinct subsets may play different roles during the evolution of disease (112). However, the ability of microglia, particularly when in a resting state, to efficiently activate T cells has been questioned by several laboratories (113, 114). Although astrocytes and cerebrovascular endothelium were reported to express MHCII in response to inflammatory stimuli (115, 116), they do not do so during homeostasis, nor do they express molecules necessary for antigenic processing and loading. Furthermore, experiments with reciprocal WT/ $MHCII^{-/-}$ bone marrow chimeric mice indicate that induction of EAE by adoptive

transfer requires MHCII expression on radiosensitive hematopoietic host cells, while expression on radioresistant non-hematopoietic host cells is dispensable (117).

Several subsets of bone marrow-derived $MHCII^+$ cells normally populate the CNS, including perivascular, meningeal, and choroid plexus macrophages (118). In addition, $MHCII^+$ cells with characteristics of dendritic cells (DCs), based on cell surface marker expression, morphology, and/ or ultrastructural characteristics, are normal constituents of the choroid plexus, meninges, and perivascular spaces in the uninjured CNS of both humans and rodents (117, 119–125). These CNS-resident DCs are optimally positioned to interact with infiltrating T cells since the choroid plexus and meninges, as well as CNS parenchymal blood vessels, are important portals of leukocyte entry during EAE and MS (126–129). The lineage(s) and biological properties of putative CNS DCs have yet to be delineated. Genetically engineered mice in which MHCII expression is restricted to $CD11c^+$ cells are susceptible to EAE, suggesting that DCs alone are sufficient to present antigen to encephalitogenic T cells *in vivo* and, thereby, promote their local expansion and effector functions (117). DCs are generally considered potent APCs, due to their ability to activate and polarize naïve T cells, which have an elevated threshold for T cell receptor (TCR) signaling compared to effector and/ or memory T cells. However, the potential role of DCs in EAE pathogenesis is complicated by the fact that DCs are heterogeneous with a range of functional phenotypes, and can even be tolerogenic under certain circumstances (130). It is also unclear whether CNS-resident $CD11c^-MHCII^+$ cells can independently activate encephalitogenic T cells *in situ*. Indeed, depletion of $CD11c^+$ cells in transgenic mice that express diphtheria toxin receptor (DTR) under control of the CD11c promotor has been variably reported to ameliorate or exacerbate the clinical course of EAE, or to have no impact whatsoever (131, 132).

$CD11c^+MHCII^+$ DCs include monocyte-derived DCs (moDCs) and classical DCs (cDCs) subsets. A third DC subset, plasmacytoid DCs (pDCs), express low levels of CD11c and MHCII, limiting their ability to present antigen to $CD4^+$ T cells. moDCs are not normally present in healthy parenchymal tissues but differentiate from infiltrating $Ly6C^{hi}$ monocytes in the setting of inflammation. We and others have previously shown that moDCs accumulate in the CNS during EAE and that their depletion or inactivation ameliorates clinical disability (41, 54, 93, 133). However, the fact that moDCs primarily emerge in the setting of active inflammation precludes their role in lesion initiation. Unlike moDCs, cDCs populate lymphoid, as well as some non-lymphoid, tissues in the steady state. They are derived from a common DC precursor, called the pre-DC, in the bone marrow and expand in response to the hematopoietin FMS-like receptor tyrosine kinase 3 (FLT3) ligand. DCs that have been detected in the murine CNS under physiological conditions are FLT3 dependent, differentiate from transferred pre-DC, and express a transcriptome consistent with cDCs (134). FLT3 ligand antagonists suppress, while FLT3 ligand agonists exacerbate, clinical EAE, suggesting that cDCs can modulate disease severity (117, 135). However, the ability of CNS-resident cDCs to directly stimulate and polarize myelin-reactive T cells *in vivo*, and their relative importance in EAE pathogenesis by comparison to infiltrating moDCs or other APC subsets, has yet to be elucidated.

Detailed *in vivo* studies of moDCs and cDCs have been undermined by a dearth of distinguishing cell surface markers. It was recently reported that CD88 (complement 5a receptor 1; C5ar1) and CD26 (dipeptidyl peptidase; DPP4), an enzyme involved in peptide hydrolysis, are reciprocally expressed by moDCs and cDCs (62). The transcription factor ZBTB46 has also been identified as a singular marker of cDCs in mice and humans (64, 65). These molecules are not exclusive to DCs but are useful in delineating $CD11c^+$ DC lineages. In the present study, we

employ the above markers to investigate the heterogeneity of DCs during EAE. We detect both moDCs and cDCs in the inflamed target organ but demonstrate that CNS cDCs are uniquely capable of processing immunogenic peptides from larger myelin fragments and activating myelin-specific naïve, as well as effector, $CD4^+$ T cells. We found that cDCs are present in the naïve CNS and that selective depletion of that subset reduces the incidence of EAE. Hence, cDCs play an important role in disease initiation. Collectively, our data suggest that cDCs, and the factors that regulate them, be investigated as potential therapeutic targets in patients with MS, particularly in those individuals who are not responsive to currently available DMTs.

Methods and Materials

Mice. C57BL/6 and B6.Ly5.1 mice were from Charles River Laboratories. *Zbtb46-gfp*, *Zbtb46-dtr*, *CD11c-dtr*, and 2D2 TCR transgenic mice were from the Jackson Laboratory. Both male and female mice, age 6-12 weeks, were used in experiments. All mice were bred and maintained under specific pathogen-free conditions at the University of Michigan.

Induction and assessment of EAE. For adoptive transfer, C57BL/6 mice were subcutaneously immunized over the flanks with 100 µg MOG_{35-55} (Biosynthesis) in complete Freund's adjuvant (Difco). At 10-14 days post-immunization (p.i.), the draining lymph nodes (inguinal, brachial, and axillary) were collected and cultured for 96 hours in the presence of 50 µg/mL MOG_{35-55}, 8 ng/ml IL-23 (R&D Systems), 10 ng/ml IL-1α (Peprotech), and 10 µg/mL anti-IFNγ (Clone XMG1.2, BioXcell). At the end of culture, $CD4^+$ T cells were purified with CD4 positive selection magnetic beads (Miltenyi), and 3-5x10^6 $CD4^+$ T cells were transferred intraperitoneally into naïve recipients. For active EAE, mice were immunized as above and injected with 300 ng of pertussis toxin (List

Biological) on days 0 and 2 p.i. EAE was assessed by a clinical score of disability: 1, limp tail; 2, hind-limb weakness; 3, partial hind-limb paralysis; 4, complete hind-limb paralysis; and 5, moribund state.

Cell Isolation. Mice were anesthetized with isoflurane and perfused with PBS. Meninges were isolated by removing the calvarium, placing the calvarium in a dish with PBS, and stripping the meninges from the inner surface. The meninges tissue and loosely adherent cells released in the PBS were collected, pelleted, and incubated in a solution of HBSS with 1 mg/ml collagenase A (Roche) and 1 mg/ml DNase 1 (Sigma-Aldrich) for 20 minutes at 37°C. The meninges were then passed through a 70-µm mesh filter to remove debris and generate a single cell suspension. The brain was removed from the skull, and the spinal cord was flushed from the spinal column with PBS. The brain and spinal cord were homogenized with an 18G needle in the collagenase solution and incubated at 37°C for 20 minutes. Mononuclear cells were separated from myelin with a 27% Percoll solution (GE Healthcare). Spleens were isolated and passed through a 70-µm mesh filter to generate a single cell suspension. Red blood cells from the spleen were lysed by a brief incubation in ACK lysis buffer (Quality Biological) followed by a wash in PBS.

Cytokine production by DC subsets. Mononuclear cells were isolated as above and cultured with Brefeldin A (BFA) (10 µg/mL) or BFA + LPS (1 µg/ml) for 4 hours. At the end of culture, cells were collected and stained for cytokines by intracellular flow cytometry.

Ex vivo cultures. Mononuclear cells were isolated as above, and DC subsets, microglia, and B cells were FAC sorted from the CNS and spleen according to the indicated surface markers. For

purification of naïve $CD4^+$ T cells, lymph nodes and spleen were collected from naïve 2D2 TCR transgenic mice. $CD4^+$ T cells were enriched by positive selection with magnetic beads (Miltenyi), and naïve T cells were further purified by flow sorting for live $CD4^+CD44^-CD62L^+$ T cells. For purification of effector T cells, mononuclear cells from the CNS were flow sorted for live $CD45^+CD11b^-CD3^+CD4^+MHCII^-$ T cells. T cells were labeled with CFSE according to the manufacturer's instructions (ThermoFisher). APC and T cells were co-cultured for 96 hours at a ratio of 1:20 (typically 5,000 myeloid cells with 95,000 T cells) with media, myelin peptide (MOG_{35-55} peptide [Biosynthesis]), or myelin protein (MOG_{1-125} [Anaspec]). At the end of culture, cells were cultured with PMA (50 ng/ml), ionomycin (2 µg/ml), and BFA (10 µg/ml) for 4 hours to stimulate cytokine production. Cells were collected and stained for activation by surface markers and cytokine production by intracellular staining.

Multiplex cytokine analysis. Cytokine levels were measured using Luminex multiplex bead-based analysis (Millipore) used the Bio-Plex 200 system (BD Biosciences) according to the manufacturer's protocols. Total protein was measured via Bradford assay (ThermoFisher) and used to normalize analyte concentrations to total protein.

Phagocytosis. Myelin was purified from the naïve mouse brain by ultracentrifugation as previously described (136). Purified myelin was conjugated to the pH-sensitive dye pHrodo Red, succinimidyl ester (ThermoFisher) per the manufacturer protocol. Mononuclear cells were isolated from the CNS at the peak of adoptive EAE and cultured overnight with the unlabeled or pHrodo-labeled myelin (1 µg/200 µl). Cells were collected, washed, and stained for flow cytometry. Phagocytosis was determined by pHrodo Red fluorescence.

Flow cytometry. Cells were labeled with fixable viability dye (eFluor506, eBioscience), blocked with anti-CD16/32 (Clone 2.4G2, hybridoma), and stained with fluorescent antibodies. For intracellular staining of cytokines and enzymes, cells were fixed with 4% paraformaldehyde, permeabilized with 0.5% saponin, and stained with fluorescent antibodies. For intracellular staining of ZBTB46, cells were fixed and permeabilized with the Transcription Factor Buffer Set (BD Pharmingen). Data were acquired using a FACSCanto II flow cytometer or FACSAria III flow sorter (BD Biosciences) and analyzed with FlowJo software (Treestar). Cells were sorted with a FACSAria III flow sorter (BD Biosciences).

Antibodies. The following antibodies were obtained from BD Biosciences: αH2M [2E5A], APC-Cy7-(αIFNγ [XMG1.2], αLy6G [1A8]), Biotin-(αRat IgG1 [RG11/39.4]), FITC-(αCD40 [HM40-3], αCD62L [MEL-14], αRat IgG1 [RG11/39.4]), PE-(αCD4 [GK1.5 and RM4-5], α ZBTB46 [U4-1374]). The following antibodies were obtained from Biolegend: APC-(αCD26 [H194-112], αCD88 [20/70]), FITC-(αCD26 [H194-112]), Biotin-(αCD88 [20/70]), PE-(αCD88 [20/70], αPD-L1 [10F.9G2]), PE-DAZZLE-(αCD11c [N418]). The following antibodies and reagents were obtained from ThermoFisher: APC-(αCD19 [MB19-1], αCD44 [IM7], αIL-23p19 [fc23cpg], Streptavidin), APC-Cy7/ APC-eF780-(αCD11b [M1/70], αCD45.2 [104], αMHCII [M5/114.15.2], Biotin-(αI-Ab [AF6-120.1]), BV510-(αCD45 [30F11], αCD45.1 [A20]), eF450-(αCD4 [RM4-5]), eF700-(Streptavidin), FITC-(αCD45.2 [104], αCD317 [eBio927], αMHCII [M5/114.15.2], Streptavidin), PE-(αCD86 [GL1], αIL-10 [JES5-16E3], αGM-CSF [MP1-22E9]), PE-Cy7-(αCD11b [N418], Streptavidin), PE-eF610-(αiNOS [CXNFT]), PerCP-Cy5.5-(αCD11c [N418], αIL-12p40 [C17.8], αMHCII [M5/114.15.2]), PerCP-eF710-(αI-Ab [AF6-120.1]), V506

Fixable Viability Dye). The following antibodies were obtained from R&D Systems: αArg1 [sheep IgG], FITC-(αArg1 [sheep IgG]). Alexa-488-Donkey-αSheep was obtained from Life Technologies.

Nanostring gene expression analysis and qPCR. Sorted cells were resuspended in RLT buffer, and cell lysates were directly analyzed for expression of 750 immune-related genes with the nCounter PanCancer Immune Panel (Nanostring Technologies). Data were processed using the nSolver Analysis Software by normalization to the geometric mean of positive controls and housekeeping genes. R was used to perform paired Student's t-tests and calculate Benjamini & Hochberg's false discovery rate (FDR), comparing the gene expression of the $CD26^+$ and $CD88^+$ populations. Cells used to confirm the Nanostring results via qPCR were resuspended in RLT buffer before Qiagen RNeasy RNA purification. Relative mRNA levels were quantified by SYBR Green qPCR performed on an iQ Thermocycler (Bio-Rad).

Bone marrow chimeras. B6.Ly5.1 ($CD45.1^+$) congenic hosts were lethally irradiated with 1300 Rad split into two doses and reconstituted by tail vein injection of $4x10^6$ $CD45.2^+$ bone marrow cells from WT, *CD11c*-dtr, or *Zbtb46-dtr* donors. Mice were allowed to reconstitute for 6 weeks prior to use.

DT Ablation. Diphtheria toxin (Sigma) was administered in two stages. Three daily doses of 1 µg/20 g mouse (50 µg/kg) in 200 µl of PBS were given i.p. prior to the assessment of DC depletion or to the induction of EAE. Daily doses of 100 ng/20 g mouse (500 ng/kg) in 200 µl of PBS were given i.p. starting on the day of adoptive transfer and continued until the end of the experiment.

Histology. Spinal columns were harvested from mice perfused intracardially with 1X PBS and 4% PFA, post-fixed with 4% PFA, decalcified with 0.5 M EDTA, cryopreserved with sucrose, and embedded in OCT for cryosectioning. 12 μm sections were stained with the following primary antibodies; rat αMBP$_{82\text{-}87}$ (Millipore) and biotinylated rat αMHCII (ThermoFisher). Avidin/biotin block (ThermoFisher) was used to prevent streptavidin binding to endogenous biotin. Normal goat serum (Sigma) was used to block non-specific binding of secondary goat α-rat IgG Alexa Fluor 488 (ThermoFisher). Steptavidin-APC (ThermoFisher) was used to visualize bound biotinylated αMHCII. Confocal images were acquired using an Olympus IX83 with Fluoview 31 software.

Statistics. Statistical analysis was performed in GraphPad Prism (v7) using paired or unpaired 2-tailed Student's t-test, or 1-way or 2-way ANOVA with correction for multiple comparisons with Tukey's posthoc test, as indicated in the legends. Disease curves were compared by 2-way ANOVA. Outliers were identified by ROUT analysis and removed when indicated. A p-value < 0.05 (*) was considered significant. $p < 0.01$ (**), $p < 0.001$ (***), and $p < 0.0001$ (****).

Results

cDCs, as well as moDCs, are present in EAE infiltrates. In order to characterize APC subsets that accumulate in the CNS during EAE, we performed flow cytometric analysis on brain and spinal cord mononuclear cells isolated at the time of peak clinical severity. MHCII$^+$ cells in the brain included CD45^{int}CD11b^{int} microglia, CD45^{hi}CD11b$^+$CD11c$^-$ monocytes/ macrophages, CD19$^+$ B cells, and CD45^{hi}CD11c$^+$ DCs (Fig. 4.1A and data not shown). Spinal cord infiltrates had a similar cellular composition (data not shown). The CNS DC population was comprised of

both $CD88^{-}CD26^{+}$ cells, consistent with cDCs, and $CD88^{+}CD26^{-}$ cells, consistent with moDCs (Fig. 4.1A, upper right panel). Microglia and macrophage/ monocytes expressed CD88 but not CD26 (Fig. 4.1A, lower panels). We also detected $CD26^{+}$ pDCs; however, the majority of pDCs were $MHCII^{-}$ and constituted <5% of the $MHCII^{+}CD26^{+}$ population in the inflamed CNS (Fig. 4.2). In order to confirm the lineages of the $CD26^{+}$ versus $CD88^{+}$ CNS DC subsets, we performed transcriptional profiling. The $CD26^{+}$ DC cohort expressed high levels of genes identified by the Immunological Genome Project (ImmGen) (137) as core cDC transcripts, including *Amica1*, *Ccr7*, and *Kit*, while the $CD88^{+}$ DC cohort expressed markers associated with monocyte-derived cells, including *Slc11a1* (138), *CD84* (139), and *Bst1* (140) (Fig. 4.1B). CNS $CD26^{+}$ DCs expressed elevated levels of *Flt3* and *Tlr3*, while $CD88^{+}$ DCs expressed high levels of *Tlr4*, which mirrors the expression of those stimulatory molecules by peripheral cDCs and moDCs, respectively (Fig. 4.1B, right panel) (141). The designation of CNS $CD11c^{+}CD26^{+}$ cells as cDCs was corroborated by their selective expression of the transcription factor, ZBTB46, as demonstrated via intracellular staining and flow cytometry (Fig. 4.1C). Similarly, $CD11c^{+}CD26^{+}$, but not $CD11c^{+}CD88^{+}$, cells isolated from *Zbtb46-gfp* reporter mice at peak EAE were GFP^{+} (Fig. 4.1D).

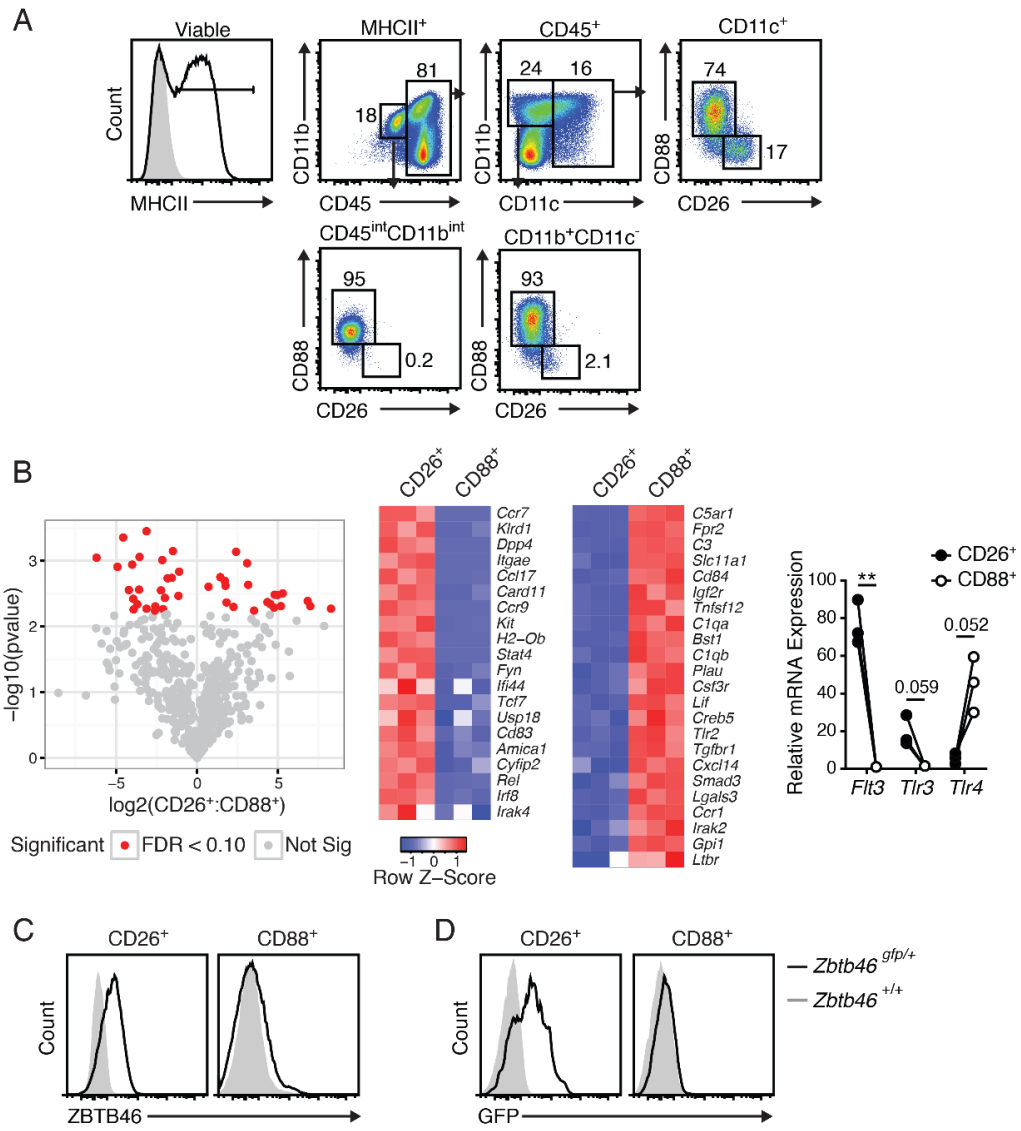

Figure 4.1 – CD26$^+$ZBTB46$^+$ cDCs accumulate in the CNS during adoptively transferred EAE.

EAE was induced by adoptive transfer of WT myelin-primed CD4$^+$ Th17 cells into naïve syngeneic hosts. (A) Brain mononuclear cells were harvested at peak EAE and analyzed by flow cytometry. Dot plots are gated on the population indicated directly above each plot. The numbers indicate the percent of the gated population. The data are representative of 3 experiments. (B) MHCII$^+$CD11c$^+$ CD88$^+$ or CD26$^+$ cells were purified from the CNS (N=3 per group) by flow sorting, and gene expression was measured by Nanostring nCounter analysis. Genes with a false discovery rate (FDR) < 0.10 are identified in the heatmaps. The right panel shows *Flt3*, *Tlr3*, and *Tlr4* mRNA levels in paired DC subsets from individual mice. P values were determined by paired, 2-tailed Student's t-test. **p<0.01. (C, D) Expression of ZBTB46 was measured in MHCII$^+$CD11c$^+$ CD26$^+$ or CD88$^+$ brain mononuclear cells, harvested at peak EAE, by flow cytometry. The open histograms reflect intracellular staining with anti-ZBTB46 antibodies (C) or GFP expression in cells from *Zbtb46*$^{gfp/+}$ reporter mice (D). The shaded grey histograms reflect the (C) isotype or (D) non-reporter control.

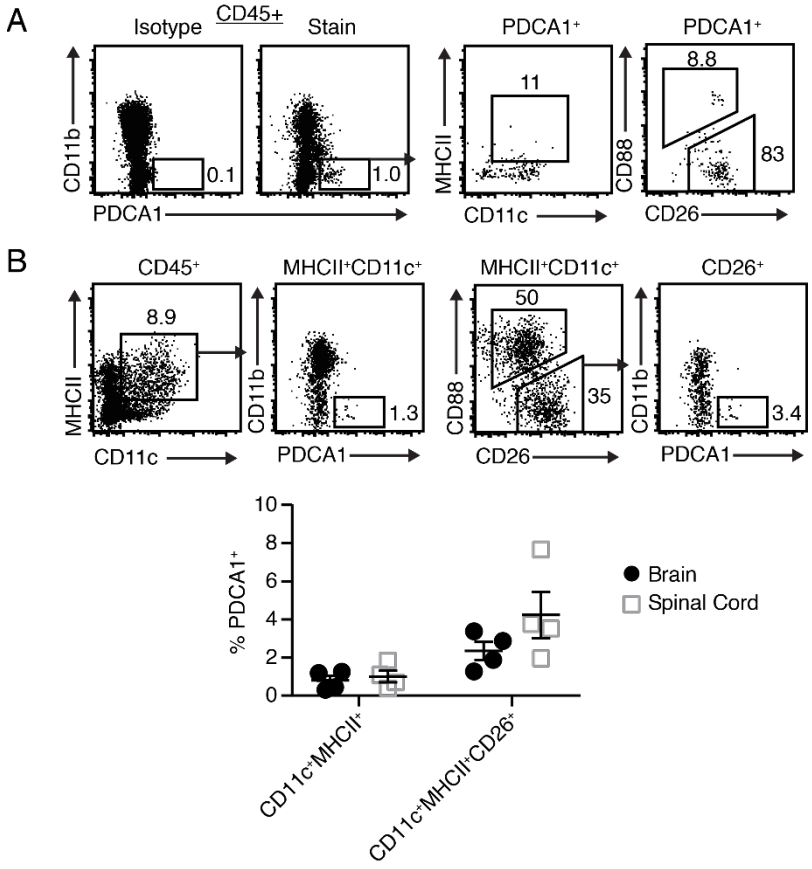

Figure 4.2 – pDCs are present in the CNS during EAE but express low levels of MHCII. EAE was induced by adoptive transfer of WT myelin-primed Th17 cells into naïve syngeneic hosts. Mononuclear cells were isolated from the brain and spinal cord at peak clinical disease and analyzed by flow cytometry. (A) pDCs were identified by expression of PDCA1. Expression of MHCII and CD11c (middle panel) and CD88 and CD26 (right panel) was assessed gating on PDCA1$^+$ cells. (B) Quantification of pDCs as a percentage of total CD11c$^+$MHCII$^+$ DCs or CD11c$^+$MHCII$^+$CD26$^+$ DCs. The dot plots show representative results obtained with brain mononuclear cells. Gating is indicated above each plot. Error bars represented as mean ± SEM.

CNS cDCs are highly efficient antigen presenting cells. We next compared the ability of CNS cDCs and moDCs to present antigen to myelin-specific CD4$^+$ T cells *ex vivo*. MHCII$^+$CD11c$^+$ CD88$^+$ moDCs and CD26$^+$ cDCs were FAC sorted from the CNS at peak EAE and co-cultured with naïve CD4$^+$ T cells that express a transgenic T cell receptor specific for the myelin oligodendrocyte glycoprotein $(MOG)_{35-55}$ peptide (2D2 cells) (142). 2D2 cells underwent multiple rounds of proliferation, upregulated the activation marker CD44, and expressed intracellular IFNγ

and/ or GM-CSF upon co-culture with MOG_{35-55} peptide and CNS cDCs (Fig. 4.3A, B). In contrast, 2D2 cells neither proliferated, upregulated CD44, nor expressed effector cytokines when co-cultured with MOG_{35-55} and CNS moDCs. Similar results were obtained with cDCs and moDCs sorted from the spleens of the same mice (data not shown). 2D2 cells did not express FoxP3 under any of the culture conditions. In order to determine whether CNS cDCs could process immunogenic epitopes from larger myelin proteins, we repeated the APC assays using a longer fragment of MOG (MOG_{1-125}) as antigen. CNS cDCs were able to process MOG protein and activate 2D2 cells, whereas their moDCs counterparts were incompetent (Fig. 4.3A, B). The superior APC properties of CNS cDCs over moDCs are not antigen-specific since only the former were able to activate OVA-specific TCR transgenic OT-II cells upon co-culture in the presence of either OVA peptide or whole ovalbumin protein (143) (data not shown).

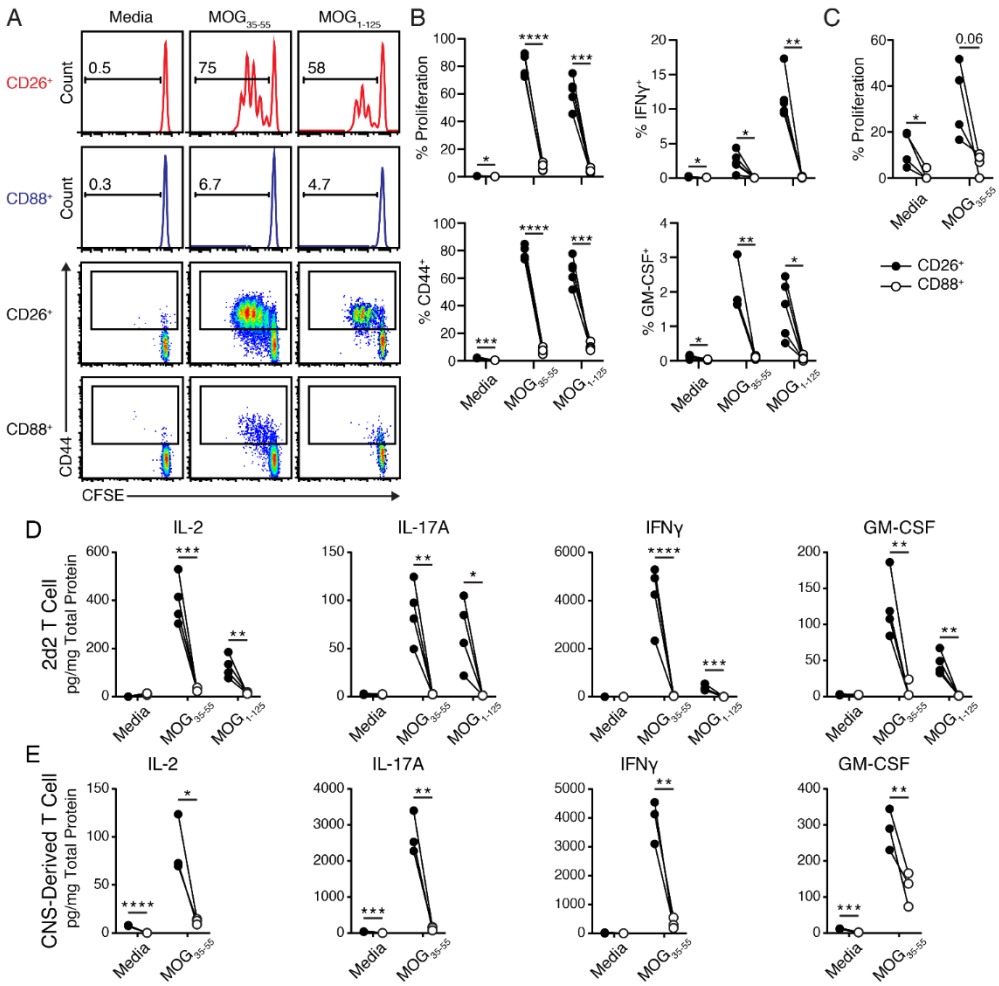

Figure 4.3 – CNS cDCs stimulate naïve and effector myelin-specific T cells to proliferate and produce pro-inflammatory cytokines, while CNS moDCs are incompetent APCs.
EAE was induced by active immunization with MOG_{35-55} peptide in CFA. CNS mononuclear cells were harvested at peak disease. $CD26^+$ or $CD88^+$ DC subsets ($CD45^+MHCII^+CD11c^+$) were purified by FAC sorting and co-cultured with MOG-reactive T cells in the presence or absence of myelin peptide (MOG_{35-55}) or myelin protein (MOG_{1-125}). (A, B, D) The CNS DC subsets were co-cultured with $CD44^-CD62L^+$ $CD4^+$ T cells that had been isolated from the spleens and lymph nodes of naïve 2D2 TCR transgenic mice. (A, B) T cell proliferation was measured by CFSE dilution. The percent of $CD4^+$ T cells that underwent 1 or more division, or that expressed the activation marker CD44, is shown for each group. (B) Cytokine production was measured by intracellular flow cytometry. The percent of cytokine producers among total $CD4^+$ T cells is shown. (D) Cytokine levels were measured in culture supernatants via a multiplex Luminex bead-based assay. (C, E) CNS DC subsets were co-cultured with $CD4^+$ T cells isolated from the CNS at the peak of EAE. (C) T cell proliferation was measured as in (A). (E) Cytokine levels were measured in culture supernatants via Luminex. (B-E) Each circle represents a data point generated with CNS DC subsets isolated from a single mouse. Connected circles indicate paired samples from the same mouse. *p<0.05, **p<0.01, ***p<0.001, ****p<0.0001 by paired, 2-tailed Student's t-test. Data in A, B, and D, and in C and E, are from individual experiments, that are representative of 2-4 independent experiments with similar results. N=3-5 mice per group per experiment.

The majority of $CD4^+$ T cells that infiltrate the CNS during EAE or MS are $CD44^{hi}$ effector cells. As a transgenic T cell line, 2D2 cells do not reflect the heterogeneity of encephalitogenic T cells that infiltrate the CNS during EAE, both in terms of TCR affinity and biological properties. To more accurately simulate the local T cell-APC interactions that occur during autoimmune demyelinating disease, we isolated $CD4^+$ T cells from the CNS of mice at peak EAE and reconstituted them with purified DC subsets obtained from the same tissues. Notably, CNS cDCs spontaneously induced the proliferation of the CNS-infiltrating effector $CD4^+$ T cells in the absence of exogenous antigen, ostensibly due to the presence of endogenous myelin peptide/ MHCII complexes on their cell surface (Fig. 4.3C). Proliferation of the effector T cells was enhanced by pulsing the CNS cDCs with MOG_{35-55}. moDCs failed to induce a significant effector T cell response, even when the co-cultures were supplemented with MOG_{35-55} (Fig. 4.3C). Taken together, these data demonstrate that cDCs, but not moDCs, are proficient at activating both naïve and antigen-experienced myelin-specific T cells.

We next measured a panel of selected cytokines in supernatants from the APC assays. Co-culturing 2D2 cells with CNS cDCs, in the presence of either MOG_{35-55} or MOG_{1-125}, resulted in the production of IL-2, IL-17A, IFNγ and GM-CSF (Fig. 4.3D). Similar results were obtained when $CD4^+$ effector T cells, isolated from the inflamed CNS, were co-cultured with MOG_{35-55} and CNS cDCs (Fig. 4.3E). In contrast, we did not detect any cytokines in supernatants from co-cultures of 2D2 cells and moDCs with MOG peptides (Fig. 4.3D). moDCs did elicit production of GM-CSF (but none of the other cytokines in the panel) when co-cultured with CNS-infiltrating effector T cells and MOG_{35-55} (Fig. 4.3E). The amount of GM-CSF produced was significantly lower than the amount elicited by CNS cDCs.

We performed APC assays with resident microglia, and splenic and CNS-infiltrating B cells, as a foil to the CNS DC subsets. B cells, isolated from either the CNS or spleen at peak EAE, induced 2D2 cell proliferation in response to exogenous MOG_{35-55} peptide (Fig. 4.4A). Conversely, they were inefficient at processing and presenting the larger MOG_{1-125} protein to the naïve myelin-reactive T cells. CNS-infiltrating B cells induced the spontaneous proliferation of myelin-primed effector T cells, but this was not enhanced by the addition of exogenous antigen (Fig. 4.4B). $MHCII^{+}CD45^{int}CD11b^{int}$ microglia did not stimulate the proliferation of either naïve or effector T cells, even when cultured with MOG_{35-55} (Fig. 4.4C, D).

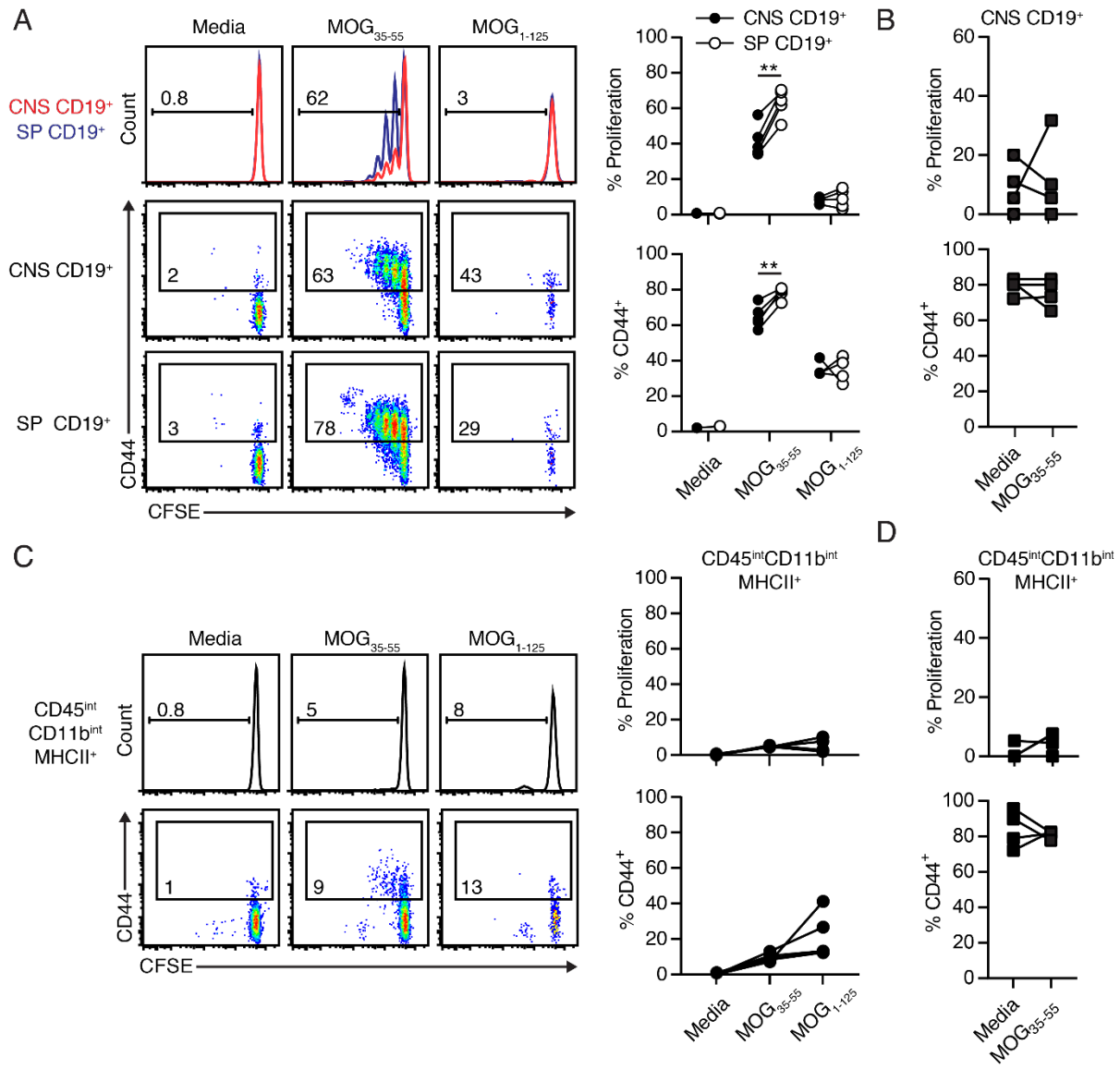

Figure 4.4 – B cells are able to present MOG$_{35-55}$ peptide, but not MOG$_{1-125}$ protein, to MOG-reactive CD4$^+$ T cells; microglia are incompetent as antigen presenting cells.
EAE was induced by active immunization with MOG peptide, and immune cells were isolated from the CNS and spleen (SP) at peak disease. B cells (MHCII$^+$CD45$^+$CD11b$^-$CD11c$^-$CD19$^+$) and microglia (MHCII$^+$CD45^{int}CD11b^{int}) were FAC sorted and co-cultured with MOG-reactive T cells in the presence of myelin peptide (MOG$_{35-55}$) or myelin protein (MOG$_{1-125}$). B cells (A) or microglia (C) were co-cultured with CD44$^-$CD62L$^+$CD4$^+$ T cells from naïve 2D2 TCR transgenic mice. B cells (B) or microglia (D) were co-cultured with CD4$^+$ T cells isolated from the CNS of actively immunized WT mice at the peak of EAE. T cell proliferation was measured by CFSE dilution. Activation was measured as the percentage of CD44$^+$ cells among total CD4$^+$ T cells. Each circle represents a data point generated from a single mouse. Connected circles indicate paired samples from the same mouse. *p<0.05, **p<0.01 by paired, 2-tailed Student's t-test. Data are representative of at least 2 experiments. N=3-5 mice per group.

cDCs express high levels of H2M molecules. We next investigated the mechanism underlying the disparate APC capacities of CNS cDCs versus moDCs. First, we measured the cell surface density of MHCII molecules on each subset via mean fluorescence intensity (MFI). This analysis revealed the presence of two populations within the CNS $CD26^+$ cDC subset, that were distinguished by expression of either high ($CD11c^{int}MHCII^{++}$) or comparable ($CD11^{hi}MHCII^+$) levels of MHCII in comparison to their $CD88^+$ counterparts (Fig. 4.5A). The $CD26^+MHCII^{++}$ subpopulation also expressed elevated levels of the co-stimulatory markers, CD40, CD80, and CD86 (Fig. 4.5B). In order to determine whether these disparities in MHCII and co-stimulatory molecule expression translated into functional differences, we performed APC assays with the CNS DC subsets side by side. There was no significant difference in the proliferation of 2D2 cells co-cultured with the $CD26^+MHCII^+$ versus $CD26^+MHCII^{++}$ cDC subpopulations. Both of the $CD26^+$ cDC subpopulations promoted more 2D2 cell activation than $CD88^+$ moDCs sorted from the same CNS mononuclear suspension (Fig. 4.6). We also measured expression of the inhibitory ligand, PDL1, and found that it was expressed on all three subsets. Blockade of PDL1 did not rescue myelin-specific T cell activation by CNS moDCs (data not shown). Based on these results, we concluded that heightened MHCII and/ or co-stimulatory molecule expression was not responsible for the superior antigen-presenting capacity of CNS cDCs.

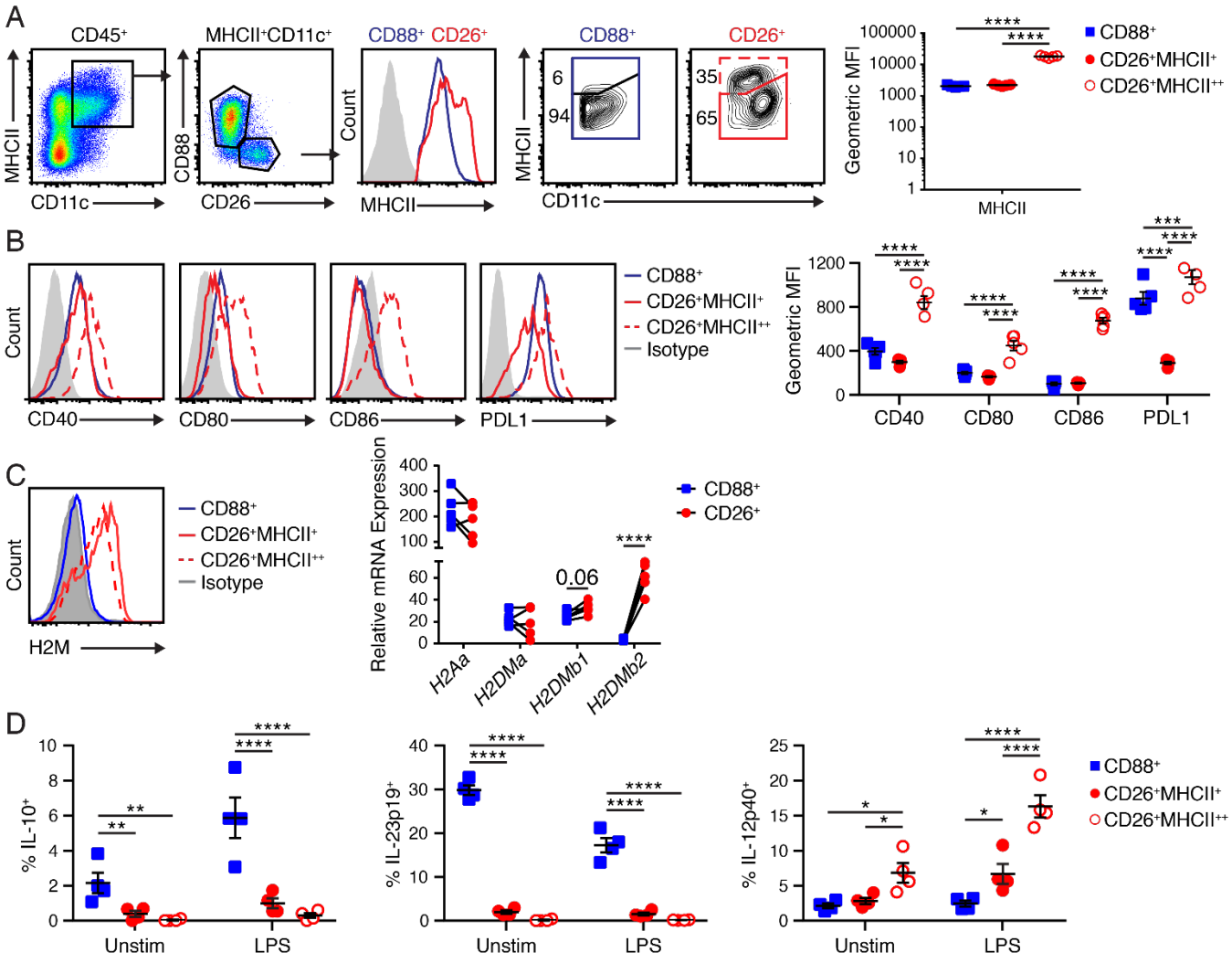

Figure 4.5 – CNS moDCs are deficient in expression of H2M and have a distinct cytokine profile in comparison to CNS cDCs.

EAE was induced by adoptive transfer of WT myelin-primed Th17 cells into naïve syngeneic hosts. (A, B) CNS mononuclear cells were isolated at peak clinical severity and subjected to flow cytometric analysis. The geometric mean fluorescence intensity (MFI) of MHCII (A) and costimulatory molecules (B) was measured on gated DC subsets. (C) H2M expression was assessed in CNS DC subsets by flow cytometry (left). The levels of transcripts encoding MHCII and H2M subunits were quantified in FAC sorted $CD88^+$ and $CD26^+$ CNS DCs via qPCR (right). (D) CNS mononuclear cells, isolated from individual mice with EAE, were cultured for 4hr with Brefeldin A (BFA), with or without LPS. Cytokine production was assessed by intracellular staining and flow cytometry. The data are shown as the percentage of cytokine-positive cells within the indicated DC population. Each symbol represents a data point generated from a single mouse. Connected symbols indicate paired samples from the same mouse. *p<0.05, **p<0.01, ***p<0.001, ****p<0.0001. Statistical significance was determined using 1-way (D) or 2-way (A, B) ANOVA with Tukey's post-hoc test or (C) paired 2-tailed Student's t-test. N=3-5 mice per group or condition. All data are representative of at least 2 experiments. All error bars indicate mean ± SEM.

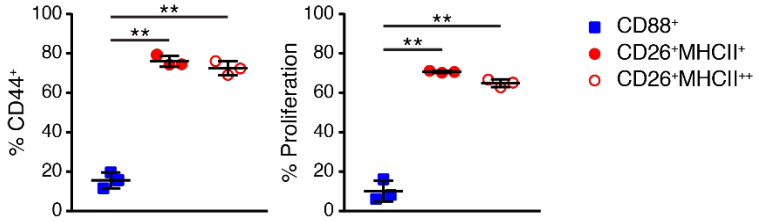

Figure 4.6 – MHCII^{+} and MHCII^{++} CNS cDCs demonstrate comparable efficacy as APCs when activating MOG-specific CD4^{+} T cells.
EAE was induced by adoptive transfer of WT myelin-primed Th17 cells into naïve syngeneic hosts. CNS mononuclear cells were isolated at peak clinical severity and FAC sorted to isolate CD88^{+}, CD26^{+}MHCII^{+}, and CD26^{+}MHCII^{++}, DC subsets. Each DC subset was co-cultured with MOG-reactive, CD44^{-}CD62L^{+} CD4^{+} T cells that were isolated from pooled spleens and lymph nodes of naïve 2D2 TCR transgenic mice. T cell proliferation was measured by CFSE dilution. The percent of CD4^{+} T cells that expressed the activation marker CD44 or that underwent 1 or more division is shown for each group. **p<0.01 P values were determined using 1-way ANOVA with Tukey's post-hoc test. N=3 mice. Data are representative of 3 experiments. Error bars indicate mean ± SEM.

H2M (HLA-DM in humans) is a non-classical MHC molecule that facilitates antigen loading into the binding groove of MHCII. It functions by catalyzing the exchange of class II-associated invariant chain peptide (CLIP, a space holding peptide that is inserted into the binding groove during the assembly of MHCII to stabilize its structure), and endosomal peptides (144). H2M-deficient mice are defective in the processing of native MOG for presentation to encephalitogenic T cells and are resistant to EAE, induced either by active immunization or adoptive transfer (145). Therefore, we questioned whether CNS moDCs are incompetent APCs due to reduced expression of H2M. We found that CNS cDCs expressed high levels of H2M protein (Fig. 4.5C, left panel). Conversely, we did not detect H2M protein in CNS moDCs. In addition, CNS cDCs expressed much higher levels of the transcripts encoding H2M subunits than CNS moDCs (Fig. 4.5C, right panel). Hence, insufficient processing and binding of immunogenic myelin peptides to MHCII may underlie the relative inability of CNS moDCs to activate encephalitogenic T cells.

cDCs and moDCs have distinct cytokine profiles. In order to further characterize the immunological properties of the CNS DC subsets, we measured intracellular expression of candidate polarizing factors. We observed distinctive cytokine profiles among the DC subsets, in that $CD26^+$ cDCs expressed IL-12p40 following short-term incubation with Brefeldin A, while $CD88^+$ moDCs expressed IL-23p19 and IL-10 (Fig. 4.5D). IL-12p40 is a subunit of both IL-12 and IL-23. Production of IL-12p40 by CNS $CD26^+$ cDCs is consistent with their induction of IFNγ in myelin-reactive T cells (Fig. 4.3B, D, and E). Measurement of IL-12p35, the second subunit of bioactive IL-12 heterodimer, was limited by available methods. IL-23 is a heterodimer of IL-12p40 and IL-23p19 (146) and polarizes T cells toward IL-17 production and the Th17 phenotype (147). Although CNS $CD88^+$ moDCs express IL-23p19, they would be unable to synthesize bioactive IL-23 in the absence of IL-12p40. This might explain the failure of CNS moDCs to induce IL-17 production upon co-culture with myelin-specific T cells (Fig. 4.3D, E). Instead, $CD88^+$ moDCs production of IL-10 may exert a regulatory influence on the inflammatory process. Stimulation of the CNS DC subsets with LPS altered the level, but not the pattern, of cytokine production (Fig. 4.5D).

moDCs efficiently phagocytose myelin. Having established CNS-derived cDCs as superior APCs, we questioned the role of moDCs in neuroinflammatory disease. We recently reported that $CD11b^+CD11c^+$ DCs evolve during the course of EAE, and shift from a proinflammatory phenotype (denoted by expression of the enzyme, inducible nitric oxide synthase (iNOS)) at clinical onset, to a non-inflammatory or immunosuppressive state (denoted by expression of the alternative enzyme, arginase-1 (Arg1)), in anticipation of clinical remission/ stabilization (112). During this transition, some of the CNS DCs acquire an $iNOS^+Arg1^+$ intermediary phenotype. Our published study did not address the lineage of the CNS DC populations. Upon revisiting this issue,

we found that that iNOS and/ or Arg1 expression is restricted to moDCs throughout the disease course (Fig. 4.7A).

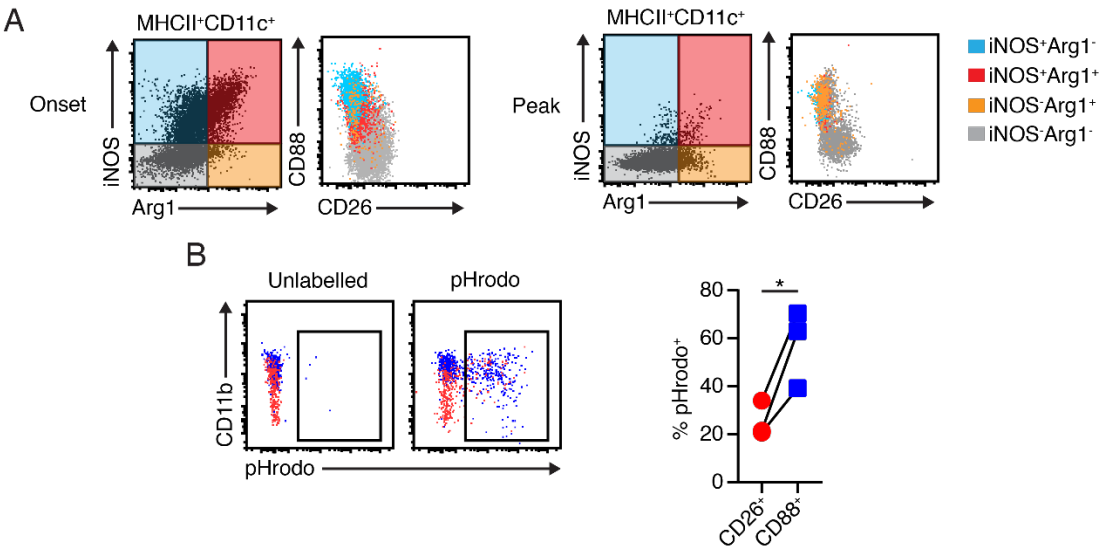

Figure 4.7 – CNS moDCs express iNOS and Arg1 and efficiently phagocytose myelin. (A) EAE was induced by active immunization with myelin peptide, and CNS mononuclear cells were isolated at clinical onset (left panels) or peak disease (right panels). Expression of iNOS and ARG1 in $CD88^+$ or $CD26^+$ CNS DCs was assessed by intracellular flow cytometry. All of the dot plots are gated on $MHCII^+CD11c^+$ cells. Cells in the CD88 versus CD26 dot plots are color-coded based on patterns of iNOS and ARG1 expression. (B) EAE was induced by adoptive transfer of WT myelin-primed Th17 cells. Mononuclear cells were isolated from the CNS at the peak of EAE and cultured overnight with unlabeled or pHrodo-labeled purified myelin. Phagocytosis was measured as the percentage of $pHrodo^+$ cells within gated $CD26^+$ or $CD88^+$ DC populations. Each symbol represents a data point generated from a single mouse. Connected symbols indicate paired samples from the same mouse. Data are representative of 2 experiments. *$p<0.05$ by paired, 2-tailed Student's t-test. N=3-5 mice per group or condition.

Since the monocyte/ macrophage lineage is specialized in phagocytosis, we also compared the capacity of CNS moDCs and cDCs to internalize extracellular myelin. We isolated total CNS mononuclear cells from mice with EAE and cultured them overnight with purified myelin that had been obtained from a naïve mouse and labeled with the pH-sensitive dye, pHrodo. In a representative experiment, we detected myelin in the cytoplasm of approximately 55% of $CD88^+$ moDCs compared with ~25% of cDCs (Fig. 4.7B). Similar results were obtained when FAC sorted moDCs and cDCs were cultured independently (data not shown). Myelin phagocytosis by both DC subsets was inhibited by the addition of cytochalasin D, demonstrating dependence on actin

polymerization (148) (data not shown). These data indicate that the inability of CNS moDCs to present antigen to myelin-specific T cells is not secondary to a defect in myelin phagocytosis. Moreover, our results suggest potential roles for $CD88^+$ moDCs in modulation of the inflammatory milieu and clearance of myelin debris.

cDCs are present in the naïve CNS and expand during autoimmune demyelinating disease. We hypothesized that resident cDCs are the primary APCs encountered by encephalitogenic T cells as they enter the uninflamed CNS and that cDCs drive T cell activation at the inception of neuroinflammation, and possibly during epitope spreading. In support of this theory, FLT3-dependent, radiosensitive DCs were recently discovered in the meninges under steady-state conditions (124, 134, 149). Similarly, we detected $MHCII^+CD11c^+CD26^+$ DCs in the naïve meninges and brain and, to a lesser extent, in the naïve spinal cord, by flow cytometric analysis (Fig. 4.8A). The CNS DC population in naïve C57BL/6 mice was predominantly $CD88^-CD26^+$ (Fig. 4.8A). $CD26^+$, but not $CD88^+$, $CD11c^+$ DCs isolated from the CNS of unmanipulated *Zbtb46-gfp* reporter mice expressed GFP (Fig. 4.8B). $MHCII^+CD11c^+CD26^+$ cDCs isolated from uninflamed CNS tissues readily activated naïve, myelin-specific $CD4^+$ T cells directly *ex vivo* and enhanced T cell survival during short-term culture (Fig. 4.8C).

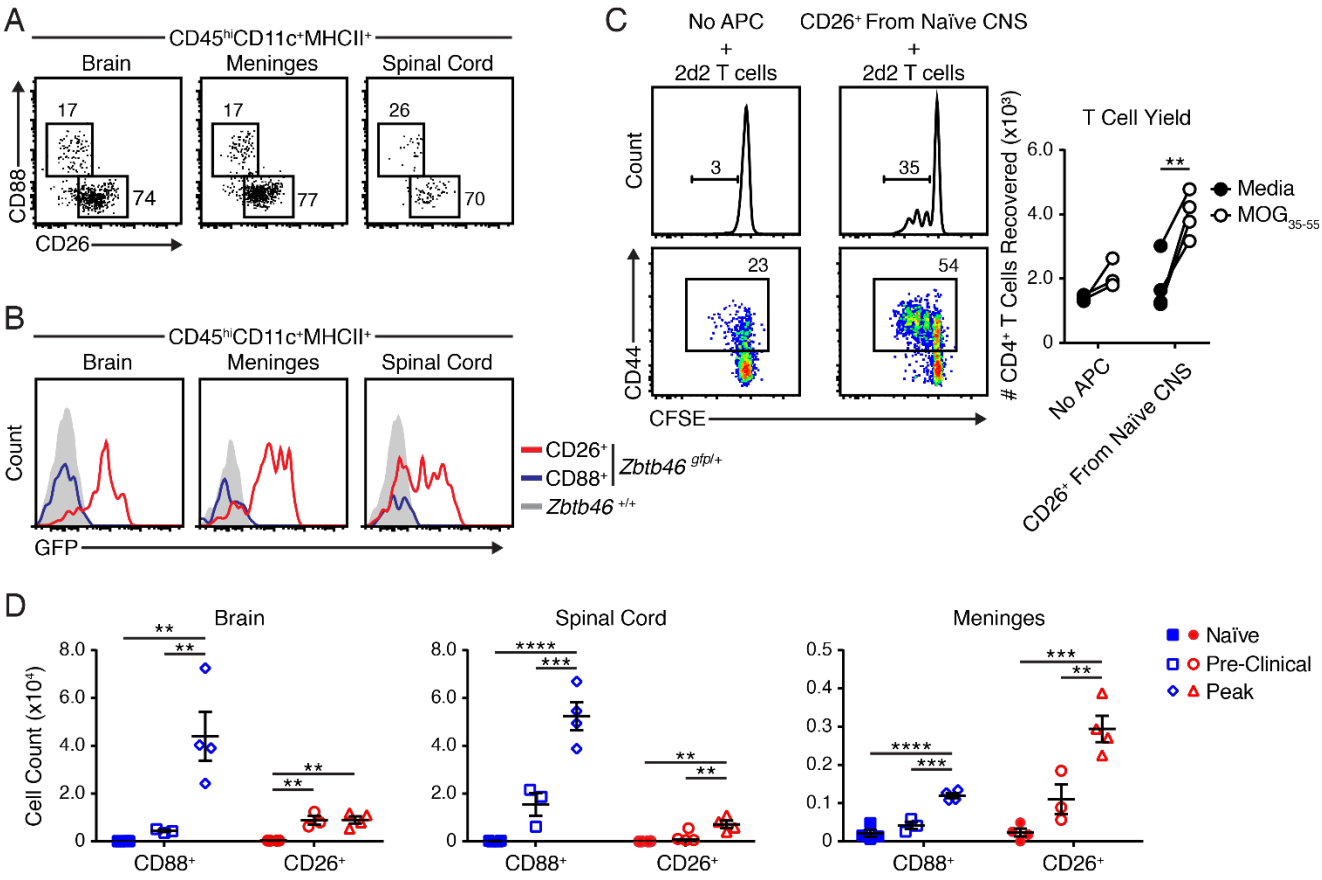

Figure 4.8 – cDCs reside in the naïve CNS and expand during EAE.
(A) Mononuclear cells were isolated from the naïve brain, meninges, and spinal cord, and analyzed by flow cytometry. The dot plots are gated on MHCII$^+$CD45^{hi}CD11c$^+$ cells. (B) CNS mononuclear cells harvested from naive *Zbtb46*$^{gfp/+}$ reporter mice or *Zbtb46*$^{+/+}$ controls were analyzed for GFP expression, gating on MHCII$^+$CD11c$^+$ DC subsets. (C) MHCII$^+$CD11c$^+$CD26$^+$ cDCs were isolated from the naïve CNS and co-cultured with naïve 2D2 transgenic T cells in the presence or absence of MOG peptide. 2D2 cells were also cultured in the absence of APCs as a negative control. 2D2 proliferation was measured by CFSE dilution, and activation by upregulation of CD44 (left). The numbers in the histograms and dot plots represent the percent of 2D2 T cells that divided or expressed CD44, respectively. Live 2D2 cells were counted at the beginning and completion of culture (right). Connected symbols indicate paired samples from the same mouse. (D) Cells were isolated from the naïve CNS or from the CNS during the pre-clinical or peak stages of adoptively transferred EAE. CNS DC subsets were quantified by flow cytometry. Each symbol represents a data point generated from a single mouse. *p<0.05, **p<0.01, ***p<0.001, ****p<0.0001. Statistical significance was determined using (C) paired, 2-tailed Student's t-test or (D) 1-way ANOVA with Tukey's post-hoc test. N=3-5 mice per group or condition. All data are representative of at least 2 experiments. Error bars indicate mean ± SEM.

Time course studies revealed that cDCs and moDCs progressively expand from baseline through the onset and peak of EAE in every CNS compartment that we examined (Fig. 4.8D).

Although cDCs consistently accumulated in the brain and spinal cord in association with increasing neurological disability, their expansion was overshadowed by a dramatic rise in the frequency of moDCs. Consequently, moDCs were the predominant DC subset in the brain and spinal cord by peak disease. In contrast, the frequency of meningeal cDCs exceeded that of moDCs at both the pre-clinical and peak stages of EAE. We and others have found the choroid plexus and meninges to be the initial portal of entry of CNS-infiltrating T cells during EAE (unpublished data and 17, 19, 20). Meningeal inflammation is widespread in the early stage, as well as progressive forms, of MS, and is spatially associated with cortical pathology (122, 150). In a survey of postmortem brain and spinal cord tissues from 11 patients with MS, cells expressing mature DC markers were consistently detected in meningeal infiltrates and were often in close proximity to, or in contact with, proliferating lymphocytes (122). Therefore, the presence of cDCs in the meninges might facilitate the development of nascent demyelinating lesions in the subpial grey matter in addition to the white matter.

cDCs are critical for initiation of experimental autoimmune encephalomyelitis. To definitively investigate the role of cDCs in EAE, we employed transgenic mice with diphtheria toxin receptor (DTR) expressed under control of the ZBTB46 promoter (*Zbtb46-dtr* mice) (64). ZBTB46 is expressed by endothelial cells as well as DCs (65). Consequently, we generated *Zbtb46-dtr*→WT bone marrow chimeric mice to restrict diphtheria toxin (DT) to the cDC population. In parallel, we generated *CD11c-dtr*→WT bone marrow chimeric mice, which target both cDCs and moDCs (151), as a positive control, and WT→WT bone marrow chimeric mice as a negative control. We optimized the DT dosing strategy to deplete DCs in the CNS prior to disease induction and to maintain depletion through the clinical course. Following three doses of DT, $CD26^+$ cDCs counts were reduced by over 50% in the brain, spinal cord, and meninges of both

sets of DTR bone marrow chimeras (Fig. 4.9A). As expected, CD88$^+$ moDCs were also diminished in the brain and spinal cords of DT treated *CD11c-dtr*, but not *Zbtb46-dtr*, chimeras.

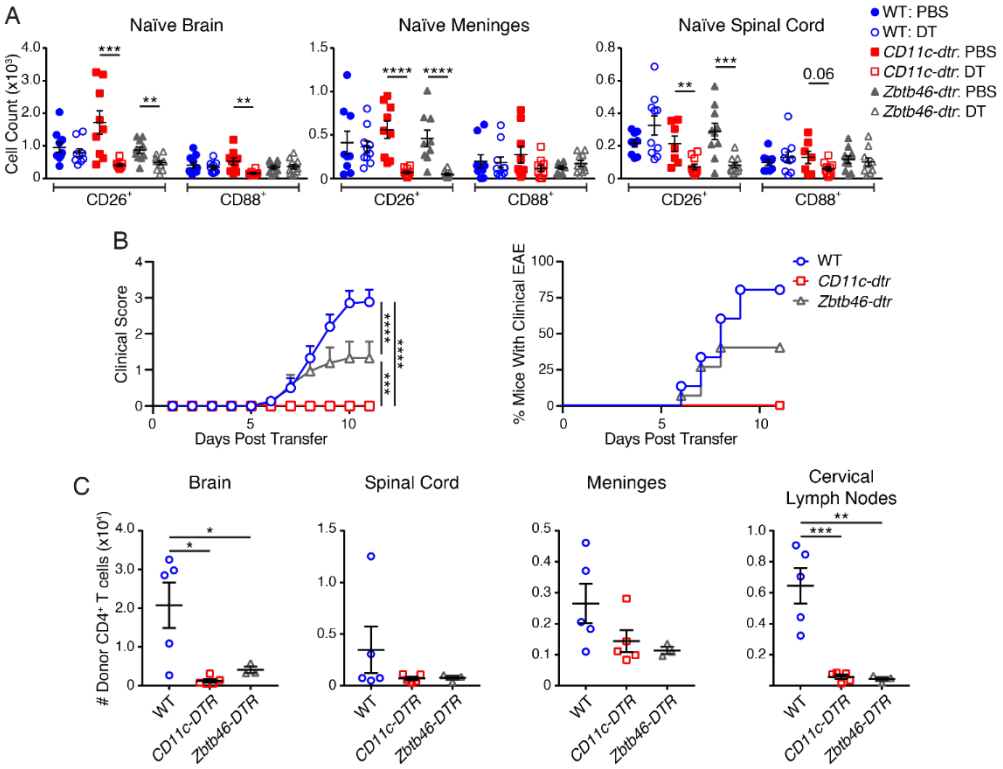

Figure 4.9 – Depletion of cDCs in adoptive transfer recipients results in a decreased number of myelin primed donor T cells in the CNS and reduces the incidence of clinical EAE.

Bone marrow chimeric mice were generated by reconstituting lethally irradiated CD45.1$^+$ hosts with CD45.2$^+$ WT, *CD11c-dtr*, or *Zbtb46-dtr* bone marrow cells. (A) Naïve chimeric mice in each group were treated with DT or PBS for 3 consecutive days. CNS cDC and moDC subsets were quantified by flow cytometric analysis. (B, C) Chimeric mice were treated with DT as in panel A, and EAE was induced by the adoptive transfer of WT myelin-primed Th17 cells. Daily DT injections were continued throughout the clinical course. (B) Mice were monitored on a daily basis and rated for degree of neurological disability by an examiner blinded to the identity of the experimental groups. Clinical scores and incidence are shown for each group. (C) Total number of donor (CD45.1+) CD4+ T cells were enumerated in DT treated adoptive transfer recipients 1-2 days prior to expected clinical onset. Each symbol in A and C represents a data point generated from a single mouse. *p<0.05, **p<0.01, ***p<0.001, ****p<0.0001. Statistical significance was determined by (A) unpaired 2-tailed Student's t-test, (B) 2-way ANOVA, or (C) 1-way ANOVA with Tukey's post-hoc test. Data are combined from (A), or representative of (B, C), at least 2 experiments with N=3-15 mice per group or condition. All error bars indicate mean ± SEM.

All of the chimeric mice were treated with 3 daily doses of DT before injection with highly purified myelin-primed Th17 cells. Daily DT injections were continued through the experimental

time course. Global depletion of DCs completely prevented clinical EAE in *CD11c-dtr*→WT bone marrow chimeras (Fig. 4.9B). Strikingly, selective depletion of cDCs in *Zbtb46-dtr*→WT chimeras reduced the incidence of clinical EAE by half in comparison to the WT→WT chimeras (40% versus 80%). Histological findings reflected the clinical scores in that there was no evidence of CNS parenchymal inflammation or tissue damage in spinal cord sections from *Zbtb46-dtr*→WT mice that remained free of neurological deficits (Fig. 4.10). In fact, we did not detect any $MHCII^+$ APCs in those sections. The susceptibility of some of the DT treated *Zbtb46-dtr*→WT mice to EAE may reflect incomplete cDCs depletion, as a small number of $CD11c^+CD26^+$ cells persisted in the CNS of DT treated mice (Fig. 4.9A). DT treatment resulted in decreased numbers of donor $CD4^+$ T cells in the brain, spinal cord, meninges, and the CNS draining cervical lymph nodes of *Zbtb46-dtr*→WT, as well as *CD11c-dtr*→WT, adoptive transfer recipients (Fig. 4.9C). Collectively, our data indicate that cDCs promote the accumulation/ expansion of myelin-reactive T cells in the CNS during the effector stage of EAE, thereby increasing susceptibility to clinical disability. The *Zbtb46-dtr*→WT mice that did develop disease had a similar day of onset, maximum score, and degree of weight loss compared with symptomatic WT→WT adoptive transfer recipients (Fig. 4.11 and data not shown). This suggests that cDCs play a pivotal role in the inception of the neuroinflammatory response, but that other APC subsets, such as infiltrating B cells, might be able to perpetuate disease activity thereafter.

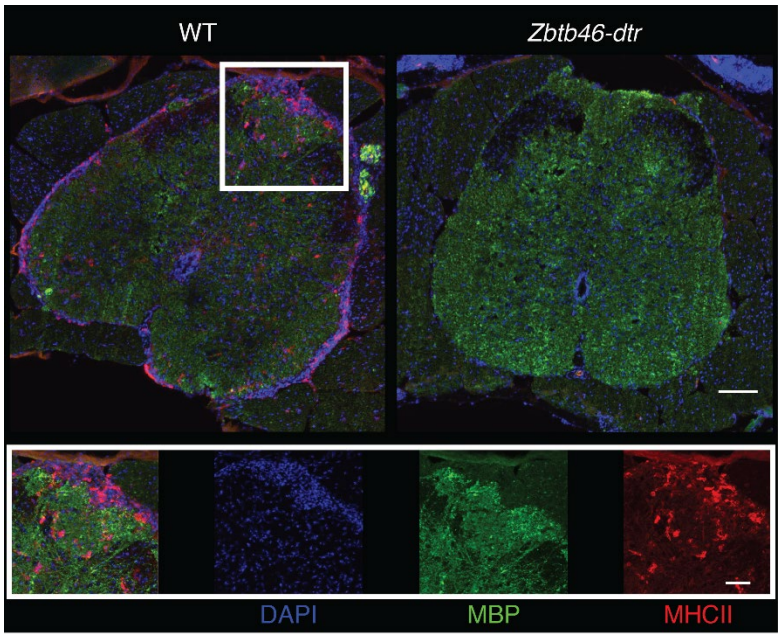

Figure 4.10 – cDCs depleted *Zbtb46-dtr*→WT adoptive transfer recipients with a clinical score of 0 show no signs of CNS inflammation or tissue damage on histological examination. Bone marrow chimeric mice were generated by reconstituting lethally irradiated CD45.1$^+$ hosts with CD45.2$^+$ WT or *Zbtb46-dtr* bone marrow cells. EAE was induced by the adoptive transfer of WT myelin-primed Th17 cells into fully reconstituted chimeric mice. DT was administered on a daily basis beginning 3 days prior to adoptive transfer. Mice in all groups were euthanized at the time of peak disease in the WT→WT cohort. CNS samples were subjected to immunohistological analysis. Spinal cord sections from a representative WT→WT mouse (top left panel, score 3) and a *Zbtb46-dtr*→WT (top right panel, score 0) mouse are shown. The inset shows an inflammatory lesion in the WT spinal cord higher magnification of. Scale bars are 100 µm (top) and 50 µm (bottom).

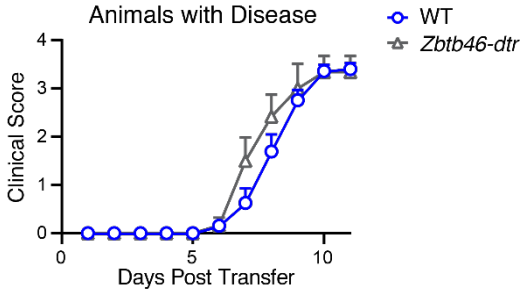

Figure 4.11 – DT treated *Zbtb46-dtr*→WT adoptive transfer recipients that succumbed to EAE followed a similar clinical course to their WT→WT counterparts.
Bone marrow chimeric mice were generated by reconstituting lethally irradiated CD45.1$^+$ hosts with CD45.2$^+$ WT or *Zbtb46-dtr* bone marrow cells. EAE was induced by the adoptive transfer of WT myelin-primed Th17 cells into fully reconstituted chimeric mice. DT was administered daily, beginning 3 days prior to adoptive transfer. Mice were monitored on a daily basis and rated for degree of neurological disability by an examiner blinded to the identity of the experimental groups. Shown are average disease scores only for animals which developed neurological deficits; WT→WT (13 of 15), and *Zbtb46-dtr*→WT (6 of 15).

Discussion

The current study adds to a growing body of literature that challenges the traditional portrayal of the uninjured CNS as an immune privileged site. Numerous laboratories have documented the presence of a network of $MHCII^+$ innate immune cells, many of which have DC characteristics, in human, as well as rodent, brain and spinal cord under steady-state conditions (119, 123–125). These cells are concentrated in the meninges, choroid plexus, and perivascular space, regions that interface with the periphery, where they are optimally positioned to serve as sentinels and first responders to foreign threats. The possibility that the same leukocytes could be subverted to support autoimmune neuroinflammation is supported by the fact that DCs are enriched in perivascular infiltrates within MS white matter lesions as well as in the meninges overlying cortical lesions (121–123).

Two recent studies suggested that a population of DCs normally present in the healthy mouse meninges and choroid plexus is of the cDCs lineage (124, 134). Parabiont experiments indicate that CNS-resident DCs originate from a pre-DC bone marrow precursor and have a half-life of 5-7 days (134). However, the role of those cells in autoimmune demyelination was not addressed. The current study corroborates these earlier findings by demonstrating that the dominant DC population in the uninflamed CNS expresses markers and transcripts typical of cDCs (Figs. 4.1 and 4.8). Our data indicate that $CD26^+ZBTB46^+$ DCs are unique among CNS APC subsets in their ability to process immunogenic peptides from larger myelin fragments and activate myelin-specific naïve, as well as effector, $CD4^+$ T cells to proliferate and produce pro-inflammatory cytokines (Fig. 4.3). Most importantly, selective depletion of cDCs led to a reduction in the frequency of transferred myelin-primed $CD4^+$ T cells in the meninges, brain, spinal cord, and cervical lymph nodes, and significantly lowered the incidence of clinical EAE (Fig. 4.9).

DT treatment of *Zbtb46-dtr*→WT adoptive transfer recipients targets cDCs in the periphery as well as in the CNS. However, we believe that cDCs depletion in the CNS is most likely responsible for the results shown in Fig. 4.9B. This is supported by prior evidence that MOG-specific donor T cells, analyzed via flow cytometry at serial time points following adoptive transfer, first upregulate activation markers and proliferate within the CNS, as opposed to peripheral lymphoid tissues, 1-2 days prior to expected clinical onset (unpublished data). Our current data demonstrate that cDCs support the expansion/ survival of encephalitogenic T cells within the CNS and play an important role in disease initiation (Fig. 4.9B, C). An analogous role of CNS DCs as APCs in the pathogenesis of human autoimmune demyelinating disease is suggested by the presence of myelin-laden cells expressing mature DC markers in close proximity to, or in contact with, proliferating lymphocytes within active MS lesions, as well as in the overlying meninges (123). The choroid plexus and meninges have been increasingly recognized as portals of entry for the infiltration of encephalitogenic T cells into the CNS (126–129). Furthermore, physical interactions between acutely activated myelin-reactive T cells and perivascular phagocytes have been directly visualized within the meningeal space at EAE onset using 2 photon microscopy (129, 152). We found that cDCs accumulate rapidly in the meninges during EAE (Fig. 4.8D). We are currently investigating whether activated encephalitogenic T cells drive the proliferation and maturation of CNS cDCs, possibly via production of FLT3 ligand and/ or GM-CSF (153).

Deficiency in H2M impedes endocytic processing and the loading of MHCII molecules with native peptides (154). Hence, low H2M expression may be, in part, responsible for the inability of MOG_{1-125}-pulsed CNS moDCs to activate MOG-reactive T cells (Fig. 4.3). In support of that hypothesis, it was previously shown that APCs isolated from H2M-deficient mice are

unable to process whole recombinant MOG protein into immunogenic epitopes (145, 155). We found that MOG_{35-55}-pulsed CNS moDCs are also poor APCs. This observation is consistent with published studies that show APCs from H2M-deficient C57BL/6 mice to be impaired in the presentation of short peptides (including MOG_{35-55}), as well as whole proteins, to $CD4^+$ T cells (145, 154, 156). The inefficient presentation of exogenous peptides by H2M-deficient APCs may reflect the need for those peptides to displace high-affinity CLIP peptides, which are bound to cell surface MHCII at an elevated density in the absence of H2M (154). H2M-independent pathways undoubtedly also contribute to APC dysfunction of CNS moDCs. Based on the data in Fig. 4.7, moDCs production of immunosuppressive cytokines might represent one such pathway.

The success of anti-CD20 B cell depleting monoclonal antibodies in suppressing MS lesion development and clinical exacerbations underscores the importance of B cells in MS pathogenesis (157). These reagents spare plasma cells, and therapeutic responsiveness does not correlate with a reduction in circulating or cerebrospinal fluid antibody levels, indicating an antibody-independent mechanism of action (158). A leading hypothesis is that B cell depletion ameliorates relapsing MS by limiting antigen presentation to encephalitogenic T cells. Meningeal B cell follicles have been discovered adjacent to large subcortical lesions in some patients with secondary progressive MS (159). $CD3^+$ T cells are a regular component of the meningeal follicles, raising the possibility that B cells also serve as APCs in that context (160). Our data are consistent with a potential role of B cells as APCs in EAE. B cells isolated from the CNS during EAE were able to present exogenous MOG_{35-55} peptide to autoreactive T cells and stimulate their proliferation *ex vivo* (Fig. 4.4). However, in contrast to CNS cDCs, they were inefficient at processing larger MOG proteins for presentation of immunogenic epitopes. This may be explained by the different pathways employed by B cells to acquire peptide versus protein antigen. Protein antigen uptake by B cells is primarily

mediated through the B cell receptor (BCR) (161), such that larger myelin fragments might only be efficiently internalized by myelin-specific B cells. However, the frequency of myelin-specific B cells is highly variable in MS and appears to be low at early time points in EAE (162). In fact, we found that B cells, isolated from the CNS at EAE onset or peak, failed to phagocytose pHrodo-labeled myelin *ex vivo* (data not shown). Based on these collective data, we speculate that infiltrating B cells can promulgate neuroinflammation in the setting of established autoimmune demyelinating disease, once myelin peptides are released into the CNS microenvironment via proteolysis. Conversely, the ability of CNS cDCs to process large myelin peptides/ proteins for presentation to naïve T cells may make them uniquely qualified to serve as APCs when antigen load is low. In support of that theory, encephalitogenic donor T cells are incapable of initiating neuroinflammation in naïve adoptive transfer recipients when polyclonal B cells are the sole APCs, unless the precursory frequency of MOG-specific B cells is artificially heightened (163). We have previously shown that CNS-infiltrating myeloid cells, including $CD11c^+$ DCs, shift from a pro-inflammatory phenotype during early EAE to an alternatively activated phenotype immediately prior to clinical remissions, which correlates with changes in APC function (112). In future studies, we plan to investigate how APCs evolve, on the cellular subset as well as the population level, across successive stages of EAE.

Despite the significant advances that have been made in MS therapeutics over the past 15 years, none of the medications approved for the management of MS, including anti-CD20 monoclonal antibodies, are cures, and none are effective in all patients. Up to the present, pharmaceutical development has focused on lymphocytes, and myeloid cells have largely been ignored. We and others have shown that the pathological mechanisms that drive CNS injury in MS are diverse and that the relative contribution of specific cytokine pathways and immune effector

cell subsets can vary from one patient to another (31, 85). Such differences may translate into different patterns of therapeutic responsiveness to individual DMTs. For example, B cell targeting approaches may be particularly effective in MS patients who harbor a high frequency of anti-myelin antibody expressors in their B cell repertoire, which would favor the uptake and presentation of myelin antigens by B cells (164). Conversely, cDCs modulating agents might be effective in individuals who are early in the disease course, when there is a lower lesion burden and less myelin breakdown, thereby limiting the accessibility of immunogenic peptides to B cells and lending a competitive advantage to CNS-resident cDCs as APCs. We would argue that inactivation of cDCs in some individuals with MS might abort the escalation of neuroinflammation and have long-lasting benefits. Furthermore, the discovery of myelin-laden DCs in MS lesions in chronic progressive, as well as recently diagnosed, patients raises the possibility that cDCs targeting might be therapeutically beneficial over a broad range of MS clinical subsets and disease stages (123, 150, 159).

CHAPTER 5 – Discussion

Since the initial observation that GM-CSF-deficient animals are protected from autoimmune demyelination (45), numerous laboratories have attempted to elucidate the mechanism of action of GM-CSF in the pathogenesis of EAE (36, 39, 44, 49, 165, 166). Since GM-CSF drives macrophage, DC, and granulocyte development, it had been speculated that GM-CSF-deficient mice would have a dearth of mature monocytes and granulocytes, as well as tissue-resident DCs. Surprisingly, those mice display only minor aberrations in myeloid cell populations, the most notable being a lack of alveolar macrophages and certain DC subsets (47, 167). Our laboratory previously showed that GM-CSF-deficient mice lack subsets of dermal DCs which normally facilitate the activation, polarization, and expansion of encephalitogenic $CD4^+$ T cells following immunization with myelin antigens (42). As discussed in Chapter 2, it is likely that GM-CSF promotes T cell priming via additional pathways, since treatment of WT mice with an anti-GM-CSF neutralizing antibody beginning at the time of immunization also reduces the frequency of myelin-reactive T cells.

GM-CSF appears to be even more critical during the effector phase of EAE. Several groups showed that myelin-reactive GM-CSF-deficient T cells could be polarized *in vitro,* but fail to induce EAE in naïve adoptive transfer recipients (39, 44). It was hypothesized that GM-CSF, secreted by infiltrating myelin-reactive T cells, directly stimulates myeloid cells within the CNS to produce IL-23. IL-23 then induces the T cells to produce more GM-CSF, thereby creating a pro-inflammatory feed-forward loop (38). Microglia, which express GM-CSFR, were initially posited as the CNS-resident APC population required for reactivation of CNS-infiltrating T cells.

However, their expression of GM-CSFR is not required for EAE (41, 49). The cellular target of GM-CSF during EAE has been a subject of heated debate.

In the work presented above, we interrogated the role of GM-CSF during the induction and maintenance of CNS autoimmunity in detail. We found that, contrary to contemporary dogma, GM-CSF is not required for the initiation of clinical deficits but is necessary for the development of chronic disability. We identified a previously unappreciated role of GM-CSF in activating the CCR1 chemokine pathway. Our data show that, during and after the peak of clinical EAE, GM-CSF induces infiltrating monocytes/ macrophages, neutrophils and monocyte-derived DC to produce CCR1 chemokines that support the persistent infiltration of pathogenic myeloid cell populations, particularly neutrophils, into the CNS. The fact that GM-CSF deficiency, or neutralization, does not abrogate EAE initiation suggests the presence of a GM-CSF independent population of CNS-resident APCs. In parallel studies, we identify such a CNS APC population, composed of $CD26^{+}CD88^{-}$ classical DCs. Collectively, the results of these studies illustrate the evolving role of leukocyte subsets and cytokine/ chemokine pathways during the course of EAE and provide insight into several novel therapeutic targets that may be prominent during distinct stages of MS.

Downstream Functions of GM-CSF in CNS Inflammation

GM-CSF signaling into myeloid cells drives a pro-inflammatory signature which serves to orchestrate immune responses (168, 169). Although often overlooked, some of these effector functions include the regulation of chemokine production which modulates leukocyte infiltration into inflamed tissue. Roberg et al. showed that GM-CSF stimulates the production of CCL3, a CCR1-binding chemokine, by human neutrophils (170). It was later shown that GM-CSF also

induces CCR1 expression by human neutrophils *in vitro* (91). Immunopathological analysis demonstrated the presence of $CCR1^{+}$ macrophages and CCL3 in MS lesions, but not in normal appearing white matter (97). Experiments with WT:*Csfr2*$^{-/-}$ mixed bone marrow chimeric mice showed that GM-CSF signaling into CNS monocytes directly modulates their expression of numerous chemokines, particularly the CCR4 ligands CCL17 and CCL22 and the CCR1 ligands CCL6 and CCL9 (41). We corroborate these findings in Chapter 3.

Prior to the current thesis, the specific role of the CCR1 chemokine pathway in EAE pathogenesis had yet to be elucidated. In fact, we found that its mechanism of action shifts during EAE progression. Hence, CCR1 antagonists primarily blocked monocyte accumulation in the CNS when administered early, and neutrophil accumulation when administered following clinical disease onset. In addition, we observed a reduction in the frequency of classical DC in the CNS of mice treated prophylactically with CCR1 antagonists. Interestingly, the importance of GM-CSF signaling in driving CNS expression of CCR1 ligands also varied during the evolution of EAE. CNS levels of CCL6 were similar between WT and *Csf2r*$^{-/-}$ adoptive transfer recipients at disease onset. However, while CNS CCL6 levels continued to rise in WT recipients from onset through peak EAE, they fell in *Csf2r*$^{-/-}$ mice during the peak and late stages of disease (Fig. 1). The critical CNS targets of GM-CSF signaling and cellular sources of CCR1 ligands at peak EAE included monocytes/ macrophages, mDCs, and neutrophils. Based on our histopathological studies, CCR1 interactions appear to be particularly critical for drawing myeloid cells from the meningeal space, which is the first site they occupy, deep into the white matter parenchyma. Whereas meningeal inflammation appears sufficient to induce the early development of clinical signs (ostensibly due to diffusion of soluble factors into the parenchyma that disrupts axonal transport), chronic disability and demyelination in EAE correlate strongly with leukocyte invasion into the white

matter parenchyma. The disruption of the glial limitans and breakdown of the basement membrane that deeper CNS penetration entails may be largely dependent on neutrophils. Taken together, these observations explain why GM-CSF signaling is required for long-term, but not immediate, neurological disability in adoptive transfer recipients. We previously reported that the CXCR2 chemokine pathway is critical for early neutrophil accumulation in the CNS and for the initiation of clinical EAE in both the adoptive transfer recipients of encephalitogenic T cells and in actively immunized mice (33, 74, 78). Consequently, the relative importance of specific chemokine pathways shifts from one stage of EAE to another. Similarly, in a mouse model of arthritis, neutrophils initially infiltrate the inflamed joint via CCR1-mediated chemotaxis but employ a CXCR2-dependent pathway later in disease evolution (107, 171).

Dendritic Cells in the Naïve and Inflamed CNS

$MHCII^{+}$ myeloid cells are required for the initiation and progression of EAE; however, the specific identity of the critical APC population, and its spatiotemporal kinetics, are debated. Although microglia were initially hypothesized to be the CNS-resident APC population which reactivates encephalitogenic T cells, this has since been disproven (41, 172). Several reports have concluded that $CCR2^{+}Ly6C^{hi}$ circulating monocytes, activated by GM-CSF, are required for the induction of EAE (41, 54, 95, 96, 133, 173). However, those studies do not distinguish between the role of monocytes as APC versus other functions. Our findings that *Csf2r*$^{-/-}$ mice are susceptible to EAE induced by the adoptive transfer of WT encephalitogenic T cells suggests the presence of a GM-CSF-independent APC population within the naïve CNS which is capable of reactivating myelin-specific T cells and driving EAE induction.

Recent studies indicate that the meninges and perivascular spaces are the sites where myelin-specific T cells are first reactivated within the CNS to drive autoimmune CNS disease

(174). Although the CNS parenchyma was long considered to be "immune-privileged", it is now appreciated that such a characterization does not extend to the barriers that serve as an interface between CNS tissue and the periphery. Both the meninges and perivascular spaces are constitutively populated by tissue-resident macrophages and DCs (61). Those cells act as sentinels, optimally positioned to respond to pathogens and prevent their invasion into the CNS proper (134). Our research has revealed meningeal DCs to be the initiating APCs that drive CNS autoimmune responses.

A lack of markers which could distinguish between DC subsets during homeostasis and inflammation has obfuscated understanding their relative functions in vivo. Recently, it was discovered that the reciprocal markers CD88 and CD26/ Zbtb46 could distinguish DC lineages derived from a monocyte or DC progenitor, respectively (62). GM-CSF primarily drives the development of $CD88^{+}$ moDCs while FLT3L drives the development of $CD26^{+}$, ZBTB46-dependent, cDCs. The relative contribution of these DC subsets in EAE was previously unexplored. We found that DCs within the naïve meninges primarily fall within the cDC subset. Via subset specific depletion we demonstrated the importance of cDCs for clinical EAE onset. The role of GM-CSF dependent mDCs becomes prominent during the later stages when they act as a source of CCR1 chemokines which mold the cellular composition of CNS myeloid cells and foster their penetration into the white matter in association with demyelination.

Shifting Myeloid Cell and APC Populations in the Progression of EAE

It has been held that CNS-inflammation in EAE follows a well-orchestrated pattern of cellular infiltration and activation. Surveilling myelin-reactive T cells enter the CNS and are reactivated by APCs. Production of pro-inflammatory mediators, such as GM-CSF, and

chemokines, like CXCL2 and CCL2, induce monocyte and neutrophil mobilization and entry into the CNS. T cell-derived GM-CSF acts on monocytes to induce monocyte differentiation into moDCs. These moDCs present myelin peptides to myelin-reactive T cells and produce IL-23 which drives more production of GM-CSF, propagating the cycle of CNS inflammation. Although the cellular composition kinetics have been broadly described, careful interrogation and characterization of early vs late myeloid cells has not been performed.

Our lab recently published a study exploring the plasticity and kinetics of macrophage and dendritic cell populations during the progression of EAE (112). By using the "pro-" or "anti-inflammatory" markers, iNOS and Arginase (Arg1), respectively, we showed that not only do the overall cellular populations shift, but the phenotype of individual cells changes *in situ*. Although we have yet to prove functional differences between $iNOS^+$ and $Arg1^+$ myeloid cells in our model, the observation that the same cell can be $iNOS^+Arg1^-$ early in disease and $iNOS^-Arg1^+$ later in disease suggests that a single cell may carry out distinct, and opposing, effector functions at different timepoints in EAE.

Our findings in Chapter 2 support previous data which suggests that GM-CSF promotes the differentiation of monocytes into moDCs *in situ*. However, we also showed that GM-CSF signaling has much broader effects. By controlling the expression of CCL6 and CCR1 by myeloid cells, GM-CSF regulates which cells enter the CNS, and when they do. Our data support the idea that a subset of early infiltrating/ accumulating monocytes and cDCs enter the CNS using CCR1, while later monocytes and cDCs employ alternative chemokine receptors. Conversely, early neutrophils enter the CNS independent of CCR1 while a subset of neutrophils requires CCR1 mediated chemotaxis to enter the CNS following disease onset. Isolation and transcriptional profiling of $CCR1^+$ and $CCR1^-$ monocytes and cDCs early in disease, and $CCR1^+$ and $CCR1^-$

neutrophils later in disease, will provide valuable insight into the heterogeneity of these populations and may shed light on the pathogenic subsets of each of these cell populations.

Beyond the GM-CSF pathway, we have also provided evidence that the dominant APC populations in EAE are dynamic. In the naïve CNS, $CD26^{+}$ cDCs are the dominant $MHCII^{+}$ APC population. Following induction of EAE, microglia upregulate MHCII and $MHCII^{+}$ moDCs and B cells accumulate in the inflamed CNS. Initially, a CNS-infiltrating T cell is most likely to encounter a cDC, which is a highly effective APC. By disease onset, a T cell in the CNS has a greater chance of interacting with an infiltrating B cell, or resident microglial cell, which also could present myelin antigens that are released as a consequence of demyelination and thereby perpetuate neuroinflammation. moDCs are more efficient phagocytes than cDCs but produce more anti-inflammatory IL-10. IL-10 inhibits T cell, and myeloid cell, proliferation and activation, and may induce T cell anergy (175). The emergence of moDCs as a dominant phagocyte and $MHCII^{+}$ cell following disease onset, might lead to a dampened immune response and facilitate debris clearance, paving the way for remission.

Monocytes and neutrophils are likely the primary phagocytes in EAE and MS. Consequently, they are also the primary drivers of persistent CNS damage. Although IL-10 producing moDCs may curtail T cell activation and expansion in the CNS, they also likely cause damage by phagocytosing healthy myelin, in addition to damaged myelin. Our data suggest that in the absence of GM-CSF signaling, there is a reduction in the number of moDCs which accumulate in the CNS by peak disease. GM-CSF is also known to enhance phagocytosis by monocytes and neutrophils, and thus may promote chronic damage if this leads to the engulfment of healthy myelin directly off of axons (176, 177). Unfortunately, if used therapeutically in patients with MS, GM-CSF blockade may leave patients immunocompromised and unable to mount

effective $CD4^+$ T cell responses to infections. Luckily, our data suggest that CCR1 may mark a more restricted pathogenic subset of myeloid cells which are selectively targetable in disease. This pathway is under active investigation in our laboratory and should provide further insight, and therapeutic targets, for the treatment of MS.

Translating Research Studies to Clinical Treatment

MS is a complex disease of unknown etiology. There is no known initiating antigen, and genetic and environmental risk factors vary widely between individuals. The clinical manifestation of MS is also heterogeneous. EAE is induced in genetically susceptible inbred strains of mice with defined antigens and can be reproducibly impacted by changing the environment. EAE follows a stereotypic clinical course. Despite these important distinctions, EAE has proven to be a valuable tool in studying MS pathogenesis and treatment. MS is a lifelong condition that evolves over decades. Practical, and ethical, challenges make clinical trials in MS time consuming, labor intensive, and very costly.

Despite a relatively high degree of genetic homology, and the conservation of immunological pathways between mice and humans, there are substantial differences in transcriptional regulation, chromatin state, and chromatin structure which influence gene expression (178). Ultimately, humans and mice will respond to some stimuli similarly and others differently. Experiments in mouse models of MS allow for much more rapid validation or rejection or potential therapeutics but has significant downsides. Treatments which may be effective in MS may not be effective in EAE, and vice versa. There is no way to assess the number of drugs which would be effective in treating MS but were excluded in experimental conditions. Similarly, it is

impossible to quantify the time, money, and patient-dissatisfaction which have gone into testing drugs which were effective in animal models but ultimately ineffective in people with MS.

GM-CSF, the CCR1 chemokine pathway, neutrophils, and DCs are all clinically targeted in a number of immunological disorders. Anti-GM-CSF blocking antibodies have concluded phase 1b trials in MS and were found to be safe (179). Assessment of its efficacy will have to await larger trials. Antagonists highly selective for human CCR1 are being tested in rheumatoid arthritis, COPD, and MS (180). Numerous drugs directly targeting neutrophil migration are being tested in phase 2 trials for COPD, asthma, and bronchiectasis (181). Dendritic cells are being targeted to better fight cancer and also produce more effective vaccines (182, 183). While the results of those clinical trials, and approval of these drugs as therapies, are likely several years away, without animal models they would have never been developed.

Conclusions

The data presented above aim to further the understanding of the function GM-CSF production by encephalitogenic $CD4^+$ T cells in the induction and evolution of CNS autoimmunity. To this end, we studied the effects of GM-CSF on myeloid cell maturation in, and recruitment to, the inflamed CNS. It is our hope that this work will encourage further investigation of GM-CSF, the CCR1 chemokine network, neutrophils, and classical DCs as therapeutic targets in MS.

BIBLIOGRAPHY

1. Brownlee WJ, Hardy TA, Fazekas F, Miller DH. Diagnosis of multiple sclerosis: progress and challenges. *Lancet*. 2017;389(10076):1336-1346.

2. GBD 2015 Neurological Disorders Collaborator Group. Global, regional, and national burden of neurological disorders during 1990-2015: a systematic analysis for the Global Burden of Disease Study 2015. *Lancet Neurol*. 2017;16(11):877-897.

3. Zhang T, Shirani A, Zhao Y, Karim ME, Gustafson P, Petkau J, Evans C, Kingwell E, van der Kop M, Zhu F, Oger J, Tremlett H, BC MS Clinic Neurologists. Beta-interferon exposure and onset of secondary progressive multiple sclerosis. *Eur J Neurol*. 2015;22(6):990-1000.

4. Signori A, Gallo F, Bovis F, Di Tullio N, Maietta I, Sormani MP. Long-term impact of interferon or Glatiramer acetate in multiple sclerosis: A systematic review and meta-analysis. *Mult Scler Relat Disord*. 2016;6:57-63.

5. University of California SFM-ET, Cree BAC, Gourraud P-A, Oksenberg JR, Bevan C, Crabtree-Hartman E, Gelfand JM, Goodin DS, Graves J, Green AJ, Mowry E, Okuda DT, Pelletier D, von Büdingen H-C, Zamvil SS, Agrawal A, Caillier S, Ciocca C, Gomez R, Kanner R, Lincoln R, Lizee A, Qualley P, Santaniello A, Suleiman L, Bucci M, Panara V, Papinutto N, Stern WA, Zhu AH, Cutter GR, Baranzini S, Henry RG, Hauser SL. Long-term evolution of multiple sclerosis disability in the treatment era. *Ann Neurol*. 2016;80(4):499-510.

6. Rae-Grant A, Day GS, Marrie RA, Rabinstein A, Cree BAC, Gronseth GS, Haboubi M, Halper J, Hosey JP, Jones DE, Lisak R, Pelletier D, Potrebic S, Sitcov C, Sommers R, Stachowiak J, Getchius TSD, Merillat SA, Pringsheim T. Practice guideline recommendations summary: Disease-modifying therapies for adults with multiple sclerosis: Report of the Guideline Development, Dissemination, and Implementation Subcommittee of the American Academy of Neurology. *Neurology*. 2018;90(17):777-788.

7. Lublin F. History of modern multiple sclerosis therapy. *J Neurol*. 2005;252 Suppl:iii3-iii9.

8. Absinta M, Sati P, Schindler M, Leibovitch EC, Ohayon J, Wu T, Meani A, Filippi M, Jacobson S, Cortese ICM, Reich DS. Persistent 7-tesla phase rim predicts poor outcome in new multiple sclerosis patient lesions. *J Clin Invest*. 2016;126(7):2597-2609.

9. Engell T. A clinico-pathoanatomical study of multiple sclerosis diagnosis. *Acta Neurol Scand*. 1988;78(1):39-44.

10. Reich DS, Lucchinetti CF, Calabresi PA. Multiple Sclerosis. *N Engl J Med*.

2018;378(2):169-180.

11. Kuhlmann T, Lassmann H, Brück W. Diagnosis of inflammatory demyelination in biopsy specimens: a practical approach. *Acta Neuropathol*. 2008;115(3):275-287.

12. Markowitz CE. Interferon-beta: mechanism of action and dosing issues. *Neurology*. 2007;68(24 Suppl 4):S8-11.

13. Mathias A, Perriot S, Canales M, Blatti C, Gaubicher C, Schluep M, Engelhardt B, Du Pasquier R. Impaired T-cell migration to the CNS under fingolimod and dimethyl fumarate. *Neurol Neuroimmunol neuroinflammation*. 2017;4(6):e401.

14. Baranzini SE, Oksenberg JR. The Genetics of Multiple Sclerosis: From 0 to 200 in 50 Years. *Trends Genet*. 2017;33(12):960-970.

15. Haines JL, Ter-Minassian M, Bazyk A, Gusella JF, Kim DJ, Terwedow H, Pericak-Vance MA, Rimmler JB, Haynes CS, Roses AD, Lee A, Shaner B, Menold M, Seboun E, Fitoussi RP, Gartioux C, Reyes C, Ribierre F, Gyapay G, Weissenbach J, Hauser SL, Goodkin DE, Lincoln R, Usuku K, Oksenberg JR. A complete genomic screen for multiple sclerosis underscores a role for the major histocompatability complex. The Multiple Sclerosis Genetics Group. *Nat Genet*. 1996;13(4):469-471.

16. Sawcer S, Jones HB, Feakes R, Gray J, Smaldon N, Chataway J, Robertson N, Clayton D, Goodfellow PN, Compston A. A genome screen in multiple sclerosis reveals susceptibility loci on chromosome 6p21 and 17q22. *Nat Genet*. 1996;13(4):464-468.

17. International Multiple Sclerosis Genetics Consortium, Wellcome Trust Case Control Consortium 2, Sawcer S, Hellenthal G, Pirinen M, Spencer CCA, Patsopoulos NA, Moutsianas L, Dilthey A, Su Z, Freeman C, Hunt SE, Edkins S, Gray E, Booth DR, Potter SC, Goris A, Band G, Oturai AB, Strange A, Saarela J, Bellenguez C, Fontaine B, Gillman M, Hemmer B, Gwilliam R, Zipp F, Jayakumar A, Martin R, Leslie S, Hawkins S, Giannoulatou E, D'alfonso S, Blackburn H, Martinelli Boneschi F, Liddle J, Harbo HF, Perez ML, Spurkland A, Waller MJ, Mycko MP, Ricketts M, Comabella M, Hammond N, Kockum I, McCann OT, Ban M, Whittaker P, Kemppinen A, Weston P, Hawkins C, Widaa S, Zajicek J, Dronov S, Robertson N, Bumpstead SJ, Barcellos LF, Ravindrarajah R, Abraham R, Alfredsson L, Ardlie K, Aubin C, Baker A, Baker K, Baranzini SE, Bergamaschi L, Bergamaschi R, Bernstein A, Berthele A, Boggild M, Bradfield JP, Brassat D, Broadley SA, Buck D, Butzkueven H, Capra R, Carroll WM, Cavalla P, Celius EG, Cepok S, Chiavacci R, Clerget-Darpoux F, Clysters K, Comi G, Cossburn M, Cournu-Rebeix I, Cox MB, Cozen W, Cree BAC, Cross AH, Cusi D, Daly MJ, Davis E, de Bakker PIW, Debouverie M, D'hooghe MB, Dixon K, Dobosi R, Dubois B, Ellinghaus D, Elovaara I, Esposito F, Fontenille C, Foote S, Franke A, Galimberti D, Ghezzi A, Glessner J, Gomez R, Gout O, Graham C, Grant SFA, Guerini FR, Hakonarson H, Hall P, Hamsten A, Hartung H-P, Heard RN, Heath S, Hobart J, Hoshi M, Infante-Duarte C, Ingram G, Ingram W, Islam T, Jagodic M, Kabesch M, Kermode AG, Kilpatrick TJ, Kim C, Klopp N, Koivisto K, Larsson M, Lathrop M, Lechner-Scott JS, Leone MA, Leppä V, Liljedahl U, Bomfim IL, Lincoln RR, Link J, Liu J, Lorentzen AR, Lupoli S, Macciardi F, Mack T, Marriott M,

Martinelli V, Mason D, McCauley JL, Mentch F, Mero I-L, Mihalova T, Montalban X, Mottershead J, Myhr K-M, Naldi P, Ollier W, Page A, Palotie A, Pelletier J, Piccio L, Pickersgill T, Piehl F, Pobywajlo S, Quach HL, Ramsay PP, Reunanen M, Reynolds R, Rioux JD, Rodegher M, Roesner S, Rubio JP, Rückert I-M, Salvetti M, Salvi E, Santaniello A, Schaefer CA, Schreiber S, Schulze C, Scott RJ, Sellebjerg F, Selmaj KW, Sexton D, Shen L, Simms-Acuna B, Skidmore S, Sleiman PMA, Smestad C, Sørensen PS, Søndergaard HB, Stankovich J, Strange RC, Sulonen A-M, Sundqvist E, Syvänen A-C, Taddeo F, Taylor B, Blackwell JM, Tienari P, Bramon E, Tourbah A, Brown MA, Tronczynska E, Casas JP, Tubridy N, Corvin A, Vickery J, Jankowski J, Villoslada P, Markus HS, Wang K, Mathew CG, Wason J, Palmer CNA, Wichmann H-E, Plomin R, Willoughby E, Rautanen A, Winkelmann J, Wittig M, Trembath RC, Yaouanq J, Viswanathan AC, Zhang H, Wood NW, Zuvich R, Deloukas P, Langford C, Duncanson A, Oksenberg JR, Pericak-Vance MA, Haines JL, Olsson T, Hillert J, Ivinson AJ, De Jager PL, Peltonen L, Stewart GJ, Hafler DA, Hauser SL, McVean G, Donnelly P, Compston A. Genetic risk and a primary role for cell-mediated immune mechanisms in multiple sclerosis. *Nature*. 2011;476(7359):214-219.

18. Willer CJ, Dyment DA, Risch NJ, Sadovnick AD, Ebers GC, Canadian Collaborative Study Group. Twin concordance and sibling recurrence rates in multiple sclerosis. *Proc Natl Acad Sci U S A*. 2003;100(22):12877-12882.

19. Kuusisto H, Kaprio J, Kinnunen E, Luukkaala T, Koskenvuo M, Elovaara I. Concordance and heritability of multiple sclerosis in Finland: study on a nationwide series of twins. *Eur J Neurol*. 2008;15(10):1106-1110.

20. Hansen T, Skytthe A, Stenager E, Petersen HC, Brønnum-Hansen H, Kyvik KO. Concordance for multiple sclerosis in Danish twins: an update of a nationwide study. *Mult Scler*. 2005;11(5):504-510.

21. Ota K, Matsui M, Milford EL, Mackin GA, Weiner HL, Hafler DA. T-cell recognition of an immunodominant myelin basic protein epitope in multiple sclerosis. *Nature*. 1990;346(6280):183-187.

22. Martin R, Howell MD, Jaraquemada D, Flerlage M, Richert J, Brostoff S, Long EO, McFarlin DE, McFarland HF. A myelin basic protein peptide is recognized by cytotoxic T cells in the context of four HLA-DR types associated with multiple sclerosis. *J Exp Med*. 1991;173(1):19-24.

23. Raddassi K, Kent SC, Yang J, Bourcier K, Bradshaw EM, Seyfert-Margolis V, Nepom GT, Kwok WW, Hafler DA. Increased frequencies of myelin oligodendrocyte glycoprotein/MHC class II-binding CD4 cells in patients with multiple sclerosis. *J Immunol*. 2011;187(2):1039-1046.

24. Rivers TM, Schwentker FF. Encephalomyelitis accompanied by myelin destruction experimentally produced in monkeys. *J Exp Med*. 1935;61(5):689-702.

25. Pérez O, Paolazzi CC. Production methods for rabies vaccine. *J Ind Microbiol Biotechnol*. 1997;18(5):340-347.

26. Stuart G, Krilkorian KS. The neuro-paralytic accidents of anti-rabies treatment. *Ann Trop Med Parasitol*. 1928;22:327.

27. Kabat EA, Wolf A, Bezer AE, Murray JP. Studies on acute disseminated encephalomyelitis produced experimentally in rhesus monkeys. *J Exp Med*. 1951;93(6):615-633.

28. Ando DG, Clayton J, Kono D, Urban JL, Sercarz EE. Encephalitogenic T cells in the B10.PL model of experimental allergic encephalomyelitis (EAE) are of the Th-1 lymphokine subtype. *Cell Immunol*. 1989;124(1):132-143.

29. Miller SD, Karpus WJ, Davidson TS. Experimental autoimmune encephalomyelitis in the mouse. *Curr Protoc Immunol*. 2010;Chapter 15(SUPPL. 88):Unit 15.1.

30. Nikolich-Zugich J, Slifka MK, Messaoudi I. The many important facets of T-cell repertoire diversity. *Nat Rev Immunol*. 2004;4(2):123-132.

31. Huber AK, Wang L, Han P, Zhang X, Ekholm S, Srinivasan A, Irani DN, Segal BM. Dysregulation of the IL-23/IL-17 axis and myeloid factors in secondary progressive MS. *Neurology*. 2014;83(17):1500-1507.

32. Segal BM, Constantinescu CS, Raychaudhuri A, Kim L, Fidelus-Gort R, Kasper LH. Repeated subcutaneous injections of IL12/23 p40 neutralising antibody, ustekinumab, in patients with relapsing-remitting multiple sclerosis: a phase II, double-blind, placebo-controlled, randomised, dose-ranging study. *Lancet Neurol*. 2008;7(9):796-804.

33. Kroenke MA, Chensue SW, Segal BM. EAE mediated by a non-IFN-γ/non-IL-17 pathway. *Eur J Immunol*. 2010;40(8):2340-2348.

34. Grifka-Walk HM, Lalor SJ, Segal BM. Highly polarized Th17 cells induce EAE via a T-bet independent mechanism. *Eur J Immunol*. 2013;43(11):2824-2831.

35. Grifka-Walk HM, Giles DA, Segal BM. IL-12-polarized Th1 cells produce GM-CSF and induce EAE independent of IL-23. *Eur J Immunol*. 2015;45(10):2780-2786.

36. Spath S, Becher B. T-bet or not T-bet: Taking the last bow on the autoimmunity stage. *Eur J Immunol*. 2013;43(11):2810-2813.

37. Segal BM. The unwavering commitment of regulatory T cells in the suppression of autoimmune encephalomyelitis: Another aspect of immune privilege in the CNS. *Eur J Immunol*. 2012;42(5):1102-1105.

38. McGeachy MJ. GM-CSF: the secret weapon in the TH17 arsenal. *Nat Immunol*. 2011;12(6):521-522.

39. El-Behi M, Ciric B, Dai H, Yan Y, Cullimore M, Safavi F, Zhang G-X, Dittel BN, Rostami A. The encephalitogenicity of TH17 cells is dependent on IL-1- and IL-23-induced production of the cytokine GM-CSF. *Nat Immunol*. 2011;12(6):568-575.

40. Spath S, Komuczki J, Hermann M, Pelczar P, Mair F, Schreiner B, Becher B. Dysregulation of the Cytokine GM-CSF Induces Spontaneous Phagocyte Invasion and Immunopathology in the Central Nervous System. *Immunity*. 2017;46(2):245-260.

41. Croxford AL, Lanzinger M, Hartmann FJ, Schreiner B, Mair F, Pelczar P, Clausen BE, Jung S, Greter M, Becher B. The Cytokine GM-CSF Drives the Inflammatory Signature of CCR2+ Monocytes and Licenses Autoimmunity. *Immunity*. 2015;43(3):502-514.

42. King IL, Kroenke MA, Segal BM. GM-CSF-dependent, CD103+ dermal dendritic cells play a critical role in Th effector cell differentiation after subcutaneous immunization. *J Exp Med*. 2010;207(5):953-961.

43. Becher B, Tugues S, Greter M. GM-CSF: From Growth Factor to Central Mediator of Tissue Inflammation. *Immunity*. 2016;45(5):963-973.

44. Codarri L, Gyülvészi G, Tosevski V, Hesske L, Fontana A, Magnenat L, Suter T, Becher B. RORγt drives production of the cytokine GM-CSF in helper T cells, which is essential for the effector phase of autoimmune neuroinflammation. *Nat Immunol*. 2011;12(6):560-567.

45. McQualter JL, Darwiche R, Ewing C, Onuki M, Kay TW, Hamilton JA, Reid HH, Bernard CCA. Granulocyte macrophage colony-stimulating factor: a new putative therapeutic target in multiple sclerosis. *J Exp Med*. 2001;194(7):873-882.

46. Burgess AW, Camakaris J, Metcalf D. Purification and properties of colony-stimulating factor from mouse lung-conditioned medium. *J Biol Chem*. 1977;252(6):1998-2003.

47. Robb L, Drinkwater CC, Metcalf D, Li R, Köntgen F, Nicola NA, Begley CG. Hematopoietic and lung abnormalities in mice with a null mutation of the common beta subunit of the receptors for granulocyte-macrophage colony-stimulating factor and interleukins 3 and 5. *Proc Natl Acad Sci U S A*. 1995;92(21):9565-9569.

48. Vremec D, Lieschke GJ, Dunn AR, Robb L, Metcalf D, Shortman K. The influence of granulocyte/macrophage colony-stimulating factor on dendritic cell levels in mouse lymphoid organs. *Eur J Immunol*. 1997;27(1):40-44.

49. Ponomarev ED, Shriver LP, Maresz K, Pedras-Vasconcelos J, Verthelyi D, Dittel BN. GM-CSF Production by Autoreactive T Cells Is Required for the Activation of Microglial Cells and the Onset of Experimental Autoimmune Encephalomyelitis. *J Immunol*. 2007;178(1):39-48.

50. Chastain EML, Duncan DS, Rodgers JM, Miller SD. The role of antigen presenting cells in multiple sclerosis. *Biochim Biophys Acta*. 2011;1812(2):265-274.

51. Arango Duque G, Descoteaux A. Macrophage cytokines: involvement in immunity and infectious diseases. *Front Immunol*. 2014;5:491.

52. Segal BM. CNS chemokines, cytokines, and dendritic cells in autoimmune demyelination.

J Neurol Sci. 2005;228(2):210-214.

53. Issazadeh S, Ljungdahl A, Höjeberg B, Mustafa M, Olsson T. Cytokine production in the central nervous system of Lewis rats with experimental autoimmune encephalomyelitis: dynamics of mRNA expression for interleukin-10, interleukin-12, cytolysin, tumor necrosis factor alpha and tumor necrosis factor beta. *J Neuroimmunol*. 1995;61(2):205-212.

54. King IL, Dickendesher TL, Segal BM. Circulating Ly-6C+ myeloid precursors migrate to the CNS and play a pathogenic role during autoimmune demyelinating disease. *Blood*. 2009;113(14):3190-3197.

55. Steinman RM, Cohn ZA. Identification of a novel cell type in peripheral lymphoid organs of mice. I. Morphology, quantitation, tissue distribution. *J Exp Med*. 1973;137(5):1142-1162.

56. Geissmann F, Manz MG, Jung S, Sieweke MH, Merad M, Ley K. Development of Monocytes, Macrophages, and Dendritic Cells. *Science (80-)*. 2010;327(5966):656-661.

57. Hjelmström P, Juedes AE, Fjell J, Ruddle NH. B-cell-deficient mice develop experimental allergic encephalomyelitis with demyelination after myelin oligodendrocyte glycoprotein sensitization. *J Immunol*. 1998;161(9):4480-4483.

58. Lyons JA, San M, Happ MP, Cross AH. B cells are critical to induction of experimental allergic encephalomyelitis by protein but not by a short encephalitogenic peptide. *Eur J Immunol*. 1999;29(11):3432-3439.

59. Mizutani M, Pino PA, Saederup N, Charo IF, Ransohoff RM, Cardona AE. The Fractalkine Receptor but Not CCR2 Is Present on Microglia from Embryonic Development throughout Adulthood. *J Immunol*. 2012;188(1):29-36.

60. Becher B, Schlitzer A, Chen J, Mair F, Sumatoh HR, Teng KWW, Low D, Ruedl C, Riccardi-castagnoli P, Poidinger M, Greter M, Ginhoux F, Newell EW, Wei K, Teng W, Low D, Ruedl C, Riccardi-castagnoli P, Poidinger M, Greter M, Ginhoux F, Newell EW. High-dimensional analysis of the murine myeloid cell system. *Nat Immunol*. 2014;15(12):1181-1189.

61. Goldmann T, Wieghofer P, Jordão MJC, Prutek F, Hagemeyer N, Frenzel K, Amann L, Staszewski O, Kierdorf K, Krueger M, Locatelli G, Hochgerner H, Zeiser R, Epelman S, Geissmann F, Priller J, Rossi FM V, Bechmann I, Kerschensteiner M, Linnarsson S, Jung S, Prinz M. Origin, fate and dynamics of macrophages at central nervous system interfaces. *Nat Immunol*. 2016;17(7):797-805.

62. Nakano H, Moran TP, Nakano K, Gerrish KE, Bortner CD, Cook DN. Complement Receptor C5aR1/CD88 and Dipeptidyl Peptidase-4/CD26 Define Distinct Hematopoietic Lineages of Dendritic Cells. *J Immunol*. 2015;194(8):3808-3819.

63. Schlitzer A, McGovern N, Teo P, Zelante T, Atarashi K, Low D, Ho AWS, See P, Shin A, Wasan PS, Hoeffel G, Malleret B, Heiseke A, Chew S, Jardine L, Purvis HA, Hilkens CMU,

Tam J, Poidinger M, Stanley ER, Krug AB, Renia L, Sivasankar B, Ng LG, Collin M, Ricciardi-Castagnoli P, Honda K, Haniffa M, Ginhoux F. IRF4 Transcription Factor-Dependent CD11b+Dendritic Cells in Human and Mouse Control Mucosal IL-17 Cytokine Responses. *Immunity*. 2013;38(5):970-983.

64. Meredith MM, Liu K, Darrasse-Jeze G, Kamphorst AO, Schreiber HA, Guermonprez P, Idoyaga J, Cheong C, Yao K-H, Niec RE, Nussenzweig MC. Expression of the zinc finger transcription factor zDC (Zbtb46, Btbd4) defines the classical dendritic cell lineage. *J Exp Med*. 2012;209(6):1153-1165.

65. Satpathy AT, KC W, Albring JC, Edelson BT, Kretzer NM, Bhattacharya D, Murphy TL, Murphy KM. Zbtb46 expression distinguishes classical dendritic cells and their committed progenitors from other immune lineages. *J Exp Med*. 2012;209(6):1135-1152.

66. Hollenbach JA, Oksenberg JR. The immunogenetics of multiple sclerosis: A comprehensive review. *J Autoimmun*. 2015;64(1):13-25.

67. Comi G, Radaelli M, Soelberg Sørensen P. Evolving concepts in the treatment of relapsing multiple sclerosis. *Lancet*. 2017;389(10076):1347-1356.

68. Stoolman JS, Duncker PC, Huber AK, Segal BM. Site-Specific Chemokine Expression Regulates Central Nervous System Inflammation and Determines Clinical Phenotype in Autoimmune Encephalomyelitis. *J Immunol*. 2014;193(2):564-570.

69. Haak S, Croxford AL, Kreymborg K, Heppner FL, Pouly S, Becher B, Waisman A. IL-17A and IL-17F do not contribute vitally to autoimmune neuro-inflammation in mice. *J Clin Invest*. 2009;119(1):61-69.

70. Sonderegger I, Iezzi G, Maier R, Schmitz N, Kurrer M, Kopf M. GM-CSF mediates autoimmunity by enhancing IL-6–dependent Th17 cell development and survival. *J Exp Med*. 2008;205(10):2281-2294.

71. Pierson ER, Goverman JM. GM-CSF is not essential for experimental autoimmune encephalomyelitis but promotes brain-targeted disease. *JCI insight*. 2017;2(7):e92362.

72. Datta SC, Opp MR. Lipopolysaccharide-induced increases in cytokines in discrete mouse brain regions are detectable using Luminex xMAP technology. *J Neurosci Methods*. 2008;175(1):119-124.

73. Rainey-Barger EK, Rumble JM, Lalor SJ, Esen N, Segal BM, Irani DN. The lymphoid chemokine, CXCL13, is dispensable for the initial recruitment of B cells to the acutely inflamed central nervous system. *Brain Behav Immun*. 2011;25(5):922-931.

74. Carlson T, Kroenke M, Rao P, Lane TE, Segal B. The Th17–ELR $^{+}$ CXC chemokine pathway is essential for the development of central nervous system autoimmune disease. *J Exp Med*. 2008;205(4):811-823.

75. Dilek N, Poirier N, Usal C, Martinet B, Blancho G, Vanhove B. Control of Transplant

Tolerance and Intragraft Regulatory T Cell Localization by Myeloid-Derived Suppressor Cells and CCL5. *J Immunol*. 2012;188(9):4209-4216.

76. Tan MCB, Goedegebuure PS, Belt BA, Flaherty B, Sankpal N, Gillanders WE, Eberlein TJ, Hsieh C-SC-S, Linehan DC. Disruption of CCR5-Dependent Homing of Regulatory T Cells Inhibits Tumor Growth in a Murine Model of Pancreatic Cancer. *J Immunol*. 2009;182(3):1746-1755.

77. He H, Xu J, Warren CM, Duan D, Li X, Wu L, Iruela-Arispe ML. Endothelial cells provide an instructive niche for the differentiation and functional polarization of M2-like macrophages. *Blood*. 2012;120(15):3152-3162.

78. Rumble JM, Huber AK, Krishnamoorthy G, Srinivasan A, Giles DA, Zhang X, Wang L, Segal BM. Neutrophil-related factors as biomarkers in EAE and MS. *J Exp Med*. 2015;212(1):23-35.

79. Filion LG, Matusevicius D, Graziani-Bowering GM, Kumar A, Freedman MS. Monocyte-derived IL12, CD86 (B7-2) and CD40L expression in relapsing and progressive multiple sclerosis. *Clin Immunol*. 2003;106(2):127-138.

80. Karni A, Abraham M, Monsonego A, Cai G, Freeman GJ, Hafler D, Khoury SJ, Weiner HL. Innate Immunity in Multiple Sclerosis: Myeloid Dendritic Cells in Secondary Progressive Multiple Sclerosis Are Activated and Drive a Proinflammatory Immune Response. *J Immunol*. 2006;177(6):4196-4202.

81. Weiner HL. A shift from adaptive to innate immunity: a potential mechanism of disease progression in multiple sclerosis. *J Neurol*. 2008;255 Suppl(SUPPL. 1):3-11.

82. Segal BM. Stage-Specific Immune Dysregulation in Multiple Sclerosis. *J Interf Cytokine Res*. 2014;34(8):633-640.

83. Goverman J. Autoimmune T cell responses in the central nervous system. *Nat Rev Immunol*. 2009;9(6):393-407.

84. Rao P, Segal BM. Experimental autoimmune encephalomyelitis. *Methods Mol Biol*. 2012;900(January 2003):363-380.

85. Carbajal KS, Mironova Y, Ulrich-Lewis JT, Kulkarni D, Grifka-Walk HM, Huber AK, Shrager P, Giger RJ, Segal BM. Th Cell Diversity in Experimental Autoimmune Encephalomyelitis and Multiple Sclerosis. *J Immunol*. 2015;195(6):2552-2559.

86. Duncker PC, Stoolman JS, Huber AK, Segal BM. GM-CSF Promotes Chronic Disability in Experimental Autoimmune Encephalomyelitis by Altering the Composition of Central Nervous System–Infiltrating Cells, but Is Dispensable for Disease Induction. *J Immunol*. 2017;200(3):ji1701484.

87. Hamilton JA, Anderson GP. GM-CSF Biology. *Growth Factors*. 2004;22(4):225-231.

88. Shinohara H, Yano S, Bucana CD, Fidler IJ. Induction of chemokine secretion and enhancement of contact-dependent macrophage cytotoxicity by engineered expression of granulocyte-macrophage colony-stimulating factor in human colon cancer cells. *J Immunol*. 2000;164(5):2728-2737.

89. Kedzierska K, Vardaxis NJ, Jaworowski A, Crowe SM. FcgammaR-mediated phagocytosis by human macrophages involves Hck, Syk, and Pyk2 and is augmented by GM-CSF. *J Leukoc Biol*. 2001;70(2):322-328.

90. Orlofsky A, Berger MS, Prystowsky MB. Novel expression pattern of a new member of the MIP-1 family of cytokine-like genes. *Cell Regul*. 1991;2(5):403-412.

91. Cheng SS, Lai JJ, Lukacs NW, Kunkel SL. Granulocyte-Macrophage Colony Stimulating Factor Up-Regulates CCR1 in Human Neutrophils. *J Immunol*. 2001;166(2):1178-1184.

92. Izikson L, Klein RS, Charo IF, Weiner HL, Luster AD. Resistance to Experimental Autoimmune Encephalomyelitis in Mice Lacking the CC Chemokine Receptor (CCR)2. *J Exp Med*. 2000;192(7):1075-1080.

93. Mildner A, Mack M, Schmidt H, Brück W, Djukic M, Zabel MD, Hille A, Priller J, Prinz M. CCR2+Ly-6Chi monocytes are crucial for the effector phase of autoimmunity in the central nervous system. *Brain*. 2009;132(Pt 9):2487-2500.

94. Gaupp S, Pitt D, Kuziel WA, Cannella B, Raine CS. Experimental autoimmune encephalomyelitis (EAE) in CCR2(-/-) mice: susceptibility in multiple strains. *Am J Pathol*. 2003;162(1):139-150.

95. Clarkson BD, Walker A, Harris MG, Rayasam A, Sandor M, Fabry Z. CCR2-Dependent Dendritic Cell Accumulation in the Central Nervous System during Early Effector Experimental Autoimmune Encephalomyelitis Is Essential for Effector T Cell Restimulation In Situ and Disease Progression. *J Immunol*. 2015;194(2):531-541.

96. Fife BT, Huffnagle GB, Kuziel WA, Karpus WJ. CC chemokine receptor 2 is critical for induction of experimental autoimmune encephalomyelitis. *J Exp Med*. 2000;192(6):899-905.

97. Balashov KE, Rottman JB, Weiner HL, Hancock WW. CCR5(+) and CXCR3(+) T cells are increased in multiple sclerosis and their ligands MIP-1alpha and IP-10 are expressed in demyelinating brain lesions. *Proc Natl Acad Sci U S A*. 1999;96(12):6873-6878.

98. Rottman JB, Slavin AJ, Silva R, Weiner HL, Gerard CG, Hancock WW. Leukocyte recruitment during onset of experimental allergic encephalomyelitis is CCR1 dependent. *Eur J Immunol*. 2000;30(8):2372-2377.

99. Liang M. Identification and Characterization of a Potent, Selective, and Orally Active Antagonist of the CC Chemokine Receptor-1. *J Biol Chem*. 2000;275(25):19000-19008.

100. Orlofsky A, Lin EY, Prystowsky MB. Selective induction of the beta chemokine C10 by

IL-4 in mouse macrophages. *J Immunol*. 1994;152(10):5084-5091.

101. Berger MS, Taub DD, Orlofsky A, Kleyman TR, Coupaye-Gerard B, Eisner D, Cohen SA. The chemokine C10: immunological and functional analysis of the sequence encoded by the novel second exon. *Cytokine*. 1996;8(6):439-447.

102. Asensio VC, Lassmann S, Pagenstecher A, Steffensen SC, Henriksen SJ, Campbell IL. C10 is a novel chemokine expressed in experimental inflammatory demyelinating disorders that promotes recruitment of macrophages to the central nervous system. *Am J Pathol*. 1999;154(4):1181-1191.

103. Giles DA, Duncker PC, Wilkinson NM, Washnock-Schmid JM, Segal BM. CNS resident classical DCs play a critical role in CNS autoimmune disease. *J Clin Invest*. September 2018.

104. Sadik CD, Kim ND, Iwakura Y, Luster AD. Neutrophils orchestrate their own recruitment in murine arthritis through C5aR and FcγR signaling. *Proc Natl Acad Sci U S A*. 2012;109(46):E3177-85.

105. Furuichi K, Gao J-L, Horuk R, Wada T, Kaneko S, Murphy PM. Chemokine receptor CCR1 regulates inflammatory cell infiltration after renal ischemia-reperfusion injury. *J Immunol*. 2008;181(12):8670-8676.

106. Elsner J, Dulkys Y, Gupta S, Escher SE, Forssmann W-G, Kapp A, Forssmann U. Differential pattern of CCR1 internalization in human eosinophils: prolonged internalization by CCL5 in contrast to CCL3. *Allergy*. 2005;60(11):1386-1393.

107. Chou RC, Kim ND, Sadik CD, Seung E, Lan Y, Byrne MH, Haribabu B, Iwakura Y, Luster AD. Lipid-cytokine-chemokine cascade drives neutrophil recruitment in a murine model of inflammatory arthritis. *Immunity*. 2010;33(2):266-278.

108. Steinbach K, Piedavent M, Bauer S, Neumann JT, Friese MA. Neutrophils Amplify Autoimmune Central Nervous System Infiltrates by Maturing Local APCs. *J Immunol*. 2013;191(9):4531-4539.

109. Kawakami N, Lassmann S, Li Z, Odoardi F, Ritter T, Ziemssen T, Klinkert WEF, Ellwart JW, Bradl M, Krivacic K, Lassmann H, Ransohoff RM, Volk H-D, Wekerle H, Linington C, Flügel A. The activation status of neuroantigen-specific T cells in the target organ determines the clinical outcome of autoimmune encephalomyelitis. *J Exp Med*. 2004;199(2):185-197.

110. Kroenke MA, Segal BM. Th17 and Th1 responses directed against the immunizing epitope, as opposed to secondary epitopes, dominate the autoimmune repertoire during relapses of experimental autoimmune encephalomyelitis. *J Neurosci Res*. 2007;85(8):1685-1693.

111. Gehrmann J, Banati RB, Kreutzberg GW. Microglia in the immune surveillance of the brain: human microglia constitutively express HLA-DR molecules. *J Neuroimmunol*. 48(2):189-198.

112. Giles DA, Washnock-Schmid JM, Duncker PC, Dahlawi S, Ponath G, Pitt D, Segal BM. Myeloid cell plasticity in the evolution of central nervous system autoimmunity. *Ann Neurol*. 2018;83(1):131-141.

113. Ford AL, Goodsall AL, Hickey WF, Sedgwick JD. Normal adult ramified microglia separated from other central nervous system macrophages by flow cytometric sorting. Phenotypic differences defined and direct ex vivo antigen presentation to myelin basic protein-reactive CD4+ T cells compared. *J Immunol*. 1995;154(9):4309-4321.

114. Miller SD, McMahon EJ, Schreiner B, Bailey SL. Antigen presentation in the CNS by myeloid dendritic cells drives progression of relapsing experimental autoimmune encephalomyelitis. *Ann N Y Acad Sci*. 2007;1103:179-191.

115. Wong GH, Bartlett PF, Clark-Lewis I, Battye F, Schrader JW. Inducible expression of H-2 and Ia antigens on brain cells. *Nature*. 310(5979):688-691.

116. McCarron RM, Wang L, Cowan EP, Spatz M. Class II MHC antigen expression by cultured human cerebral vascular endothelial cells. *Brain Res*. 1991;566(1-2):325-328.

117. Greter M, Heppner FL, Lemos MP, Odermatt BM, Goebels N, Laufer T, Noelle RJ, Becher B. Dendritic cells permit immune invasion of the CNS in an animal model of multiple sclerosis. *Nat Med*. 2005;11(3):328-334.

118. Prinz M, Erny D, Hagemeyer N. Ontogeny and homeostasis of CNS myeloid cells. *Nat Immunol*. 2017;18(4):385-392.

119. McMenamin PG. Distribution and phenotype of dendritic cells and resident tissue macrophages in the dura mater, leptomeninges, and choroid plexus of the rat brain as demonstrated in wholemount preparations. *J Comp Neurol*. 1999;405(4):553-562.

120. Matyszak MK, Perry VH. The potential role of dendritic cells in immune-mediated inflammatory diseases in the central nervous system. *Neuroscience*. 1996;74(2):599-608.

121. Kivisäkk P, Mahad DJ, Callahan MK, Sikora K, Trebst C, Tucky B, Wujek J, Ravid R, Staugaitis SM, Lassmann H, Ransohoff RM. Expression of CCR7 in multiple sclerosis: implications for CNS immunity. *Ann Neurol*. 2004;55(5):627-638.

122. Howell OW, Reeves CA, Nicholas R, Carassiti D, Radotra B, Gentleman SM, Serafini B, Aloisi F, Roncaroli F, Magliozzi R, Reynolds R. Meningeal inflammation is widespread and linked to cortical pathology in multiple sclerosis. *Brain*. 2011;134(Pt 9):2755-2771.

123. Serafini B, Rosicarelli B, Magliozzi R, Stigliano E, Capello E, Mancardi GL, Aloisi F. Dendritic cells in multiple sclerosis lesions: maturation stage, myelin uptake, and interaction with proliferating T cells. *J Neuropathol Exp Neurol*. 2006;65(2):124-141.

124. Quintana E, Fernández A, Velasco P, de Andrés B, Liste I, Sancho D, Gaspar ML, Cano E. DNGR-1(+) dendritic cells are located in meningeal membrane and choroid plexus of the noninjured brain. *Glia*. 2015;63(12):2231-2248.

125. Prodinger C, Bunse J, Krüger M, Schiefenhövel F, Brandt C, Laman JD, Greter M, Immig K, Heppner F, Becher B, Bechmann I. CD11c-expressing cells reside in the juxtavascular parenchyma and extend processes into the glia limitans of the mouse nervous system. *Acta Neuropathol*. 2011;121(4):445-458.

126. Christy AL, Walker ME, Hessner MJ, Brown MA. Mast cell activation and neutrophil recruitment promotes early and robust inflammation in the meninges in EAE. *J Autoimmun*. 2013;42:50-61.

127. Tsuchida M, Hanawa H, Hirahara H, Watanabe H, Matsumoto Y, Sekikawa H, Abo T. Identification of CD4- CD8- alpha beta T cells in the subarachnoid space of rats with experimental autoimmune encephalomyelitis. A possible route by which effector cells invade the lesions. *Immunology*. 1994;81(3):420-427.

128. Reboldi A, Coisne C, Baumjohann D, Benvenuto F, Bottinelli D, Lira S, Uccelli A, Lanzavecchia A, Engelhardt B, Sallusto F. C-C chemokine receptor 6-regulated entry of TH-17 cells into the CNS through the choroid plexus is required for the initiation of EAE. *Nat Immunol*. 2009;10(5):514-523.

129. Bartholomäus I, Kawakami N, Odoardi F, Schläger C, Miljkovic D, Ellwart JW, Klinkert WEF, Flügel-Koch C, Issekutz TB, Wekerle H, Flügel A. Effector T cell interactions with meningeal vascular structures in nascent autoimmune CNS lesions. *Nature*. 2009;462(7269):94-98.

130. Hawiger D, Inaba K, Dorsett Y, Guo M, Mahnke K, Rivera M, Ravetch J V, Steinman RM, Nussenzweig MC. Dendritic cells induce peripheral T cell unresponsiveness under steady state conditions in vivo. *J Exp Med*. 2001;194(6):769-779.

131. Isaksson M, Lundgren BA, Ahlgren KM, Kämpe O, Lobell A. Conditional DC depletion does not affect priming of encephalitogenic Th cells in EAE. *Eur J Immunol*. 2012;42(10):2555-2563.

132. Yogev N, Frommer F, Lukas D, Kautz-Neu K, Karram K, Ielo D, von Stebut E, Probst H-CC, van den Broek M, Riethmacher D, Birnberg T, Blank T, Reizis B, Korn T, Wiendl H, Jung S, Prinz M, Kurschus FC, Waisman A. Dendritic cells ameliorate autoimmunity in the CNS by controlling the homeostasis of PD-1 receptor(+) regulatory T cells. *Immunity*. 2012;37(2):264-275.

133. Deshpande P, King IL, Segal BM. Cutting edge: CNS CD11c+ cells from mice with encephalomyelitis polarize Th17 cells and support CD25+CD4+ T cell-mediated immunosuppression, suggesting dual roles in the disease process. *J Immunol*. 2007;178(11):6695-6699.

134. Anandasabapathy N, Victora GD, Meredith M, Feder R, Dong B, Kluger C, Yao K, Dustin ML, Nussenzweig MC, Steinman RM, Liu K. Flt3L controls the development of radiosensitive dendritic cells in the meninges and choroid plexus of the steady-state mouse brain. *J Exp Med*. 2011;208(8):1695-1705.

135. Whartenby KA, Calabresi PA, McCadden E, Nguyen B, Kardian D, Wang T, Mosse C, Pardoll DM, Small D. Inhibition of FLT3 signaling targets DCs to ameliorate autoimmune disease. *Proc Natl Acad Sci U S A*. 2005;102(46):16741-16746.

136. Norton WT, Poduslo SE. Myelination in rat brain: method of myelin isolation. *J Neurochem*. 1973;21(4):749-757.

137. Miller JC, Brown BD, Shay T, Gautier EL, Jojic V, Cohain A, Pandey G, Leboeuf M, Elpek KG, Helft J, Hashimoto D, Chow A, Price J, Greter M, Bogunovic M, Bellemare-Pelletier A, Frenette PS, Randolph GJ, Turley SJ, Merad M, Immunological Genome Consortium. Deciphering the transcriptional network of the dendritic cell lineage. *Nat Immunol*. 2012;13(9):888-899.

138. Stober CB, Brode S, White JK, Popoff J-F, Blackwell JM. Slc11a1, formerly Nramp1, is expressed in dendritic cells and influences major histocompatibility complex class II expression and antigen-presenting cell function. *Infect Immun*. 2007;75(10):5059-5067.

139. Krause SW, Rehli M, Heinz S, Ebner R, Andreesen R. Characterization of MAX.3 antigen, a glycoprotein expressed on mature macrophages, dendritic cells and blood platelets: identity with CD84. *Biochem J*. 2000;346 Pt 3(Pt 3):729-736.

140. Hussain AM, Lee HC, Chang CF. Modulation of CD157 expression in multi-lineage myeloid differentiation of promyelocytic cell lines. *Eur J Cell Biol*. 2000;79(10):697-706.

141. Széles L, Meissner F, Dunand-Sauthier I, Thelemann C, Hersch M, Singovski S, Haller S, Gobet F, Fuertes Marraco SA, Mann M, Garcin D, Acha-Orbea H, Reith W. TLR3-Mediated CD8+ Dendritic Cell Activation Is Coupled with Establishment of a Cell-Intrinsic Antiviral State. *J Immunol*. 2015;195(3):1025-1033.

142. Bettelli E, Pagany M, Weiner HL, Linington C, Sobel RA, Kuchroo VK. Myelin oligodendrocyte glycoprotein-specific T cell receptor transgenic mice develop spontaneous autoimmune optic neuritis. *J Exp Med*. 2003;197(9):1073-1081.

143. Barnden MJ, Allison J, Heath WR, Carbone FR. Defective TCR expression in transgenic mice constructed using cDNA-based alpha- and beta-chain genes under the control of heterologous regulatory elements. *Immunol Cell Biol*. 1998;76(1):34-40.

144. Sherman MA, Weber DA, Jensen PE. DM enhances peptide binding to class II MHC by release of invariant chain-derived peptide. *Immunity*. 1995;3(2):197-205.

145. Slavin AJ, Soos JM, Stuve O, Patarroyo JC, Weiner HL, Fontana A, Bikoff EK, Zamvil SS. Requirement for endocytic antigen processing and influence of invariant chain and H-2M deficiencies in CNS autoimmunity. *J Clin Invest*. 2001;108(8):1133-1139.

146. Oppmann B, Lesley R, Blom B, Timans JC, Xu Y, Hunte B, Vega F, Yu N, Wang J, Singh K, Zonin F, Vaisberg E, Churakova T, Liu M, Gorman D, Wagner J, Zurawski S, Liu Y, Abrams JS, Moore KW, Rennick D, de Waal-Malefyt R, Hannum C, Bazan JF, Kastelein RA. Novel p19 protein engages IL-12p40 to form a cytokine, IL-23, with biological

activities similar as well as distinct from IL-12. *Immunity*. 2000;13(5):715-725.

147. Langrish CL, Chen Y, Blumenschein WM, Mattson J, Basham B, Sedgwick JD, McClanahan T, Kastelein RA, Cua DJ. IL-23 drives a pathogenic T cell population that induces autoimmune inflammation. *J Exp Med*. 2005;201(2):233-240.

148. Malawista SE, Gee JB, Bensch KG. Cytochalasin B reversibly inhibits phagocytosis: functional, metabolic, and ultrastructural effects in human blood leukocytes and rabbit alveolar macrophages. *Yale J Biol Med*. 1971;44(3):286-300.

149. Immig K, Gericke M, Menzel F, Merz F, Krueger M, Schiefenhövel F, Lösche A, Jäger K, Hanisch U-K, Biber K, Bechmann I. CD11c-positive cells from brain, spleen, lung, and liver exhibit site-specific immune phenotypes and plastically adapt to new environments. *Glia*. 2015;63(4):611-625.

150. Lucchinetti CF, Popescu BFG, Bunyan RF, Moll NM, Roemer SF, Lassmann H, Brück W, Parisi JE, Scheithauer BW, Giannini C, Weigand SD, Mandrekar J, Ransohoff RM. Inflammatory cortical demyelination in early multiple sclerosis. *N Engl J Med*. 2011;365(23):2188-2197.

151. Jung S, Unutmaz D, Wong P, Sano G-I, De los Santos K, Sparwasser T, Wu S, Vuthoori S, Ko K, Zavala F, Pamer EG, Littman DR, Lang RA. In vivo depletion of CD11c+ dendritic cells abrogates priming of CD8+ T cells by exogenous cell-associated antigens. *Immunity*. 2002;17(2):211-220.

152. Pesic M, Bartholomäus I, Kyratsous NI, Heissmeyer V, Wekerle H, Kawakami N. 2-photon imaging of phagocyte-mediated T cell activation in the CNS. *J Clin Invest*. 2013;123(3):1192-1201.

153. Saito Y, Boddupalli CS, Borsotti C, Manz MG. Dendritic cell homeostasis is maintained by nonhematopoietic and T-cell-produced Flt3-ligand in steady state and during immune responses. *Eur J Immunol*. 2013;43(6):1651-1658.

154. Miyazaki T, Wolf P, Tourne S, Waltzinger C, Dierich A, Barois N, Ploegh H, Benoist C, Mathis D. Mice lacking H2-M complexes, enigmatic elements of the MHC class II peptide-loading pathway. *Cell*. 1996;84(4):531-541.

155. Tompkins SM, Padilla J, Dal Canto MC, Ting JP-Y, Van Kaer L, Miller SD. De novo central nervous system processing of myelin antigen is required for the initiation of experimental autoimmune encephalomyelitis. *J Immunol*. 2002;168(8):4173-4183.

156. Martin WD, Hicks GG, Mendiratta SK, Leva HI, Ruley HE, Van Kaer L. H2-M mutant mice are defective in the peptide loading of class II molecules, antigen presentation, and T cell repertoire selection. *Cell*. 1996;84(4):543-550.

157. Braley TJ, Segal BM. B-cell targeting agents in the treatment of multiple sclerosis. *Curr Treat Options Neurol*. 2013;15(3):259-269.

158. Petereit HF, Moeller-Hartmann W, Reske D, Rubbert A. Rituximab in a patient with multiple sclerosis--effect on B cells, plasma cells and intrathecal IgG synthesis. *Acta Neurol Scand*. 2008;117(6):399-403.

159. Serafini B, Rosicarelli B, Magliozzi R, Stigliano E, Aloisi F. Detection of ectopic B-cell follicles with germinal centers in the meninges of patients with secondary progressive multiple sclerosis. *Brain Pathol*. 2004;14(2):164-174.

160. Magliozzi R, Howell O, Vora A, Serafini B, Nicholas R, Puopolo M, Reynolds R, Aloisi F. Meningeal B-cell follicles in secondary progressive multiple sclerosis associate with early onset of disease and severe cortical pathology. *Brain*. 2007;130(Pt 4):1089-1104.

161. Avalos AM, Ploegh HL. Early BCR Events and Antigen Capture, Processing, and Loading on MHC Class II on B Cells. *Front Immunol*. 2014;5:92.

162. Lindert RB, Haase CG, Brehm U, Linington C, Wekerle H, Hohlfeld R. Multiple sclerosis: B- and T-cell responses to the extracellular domain of the myelin oligodendrocyte glycoprotein. *Brain*. 1999;122 (Pt 1:2089-2100.

163. Parker Harp CR, Archambault AS, Sim J, Ferris ST, Mikesell RJ, Koni PA, Shimoda M, Linington C, Russell JH, Wu GF. B cell antigen presentation is sufficient to drive neuroinflammation in an animal model of multiple sclerosis. *J Immunol*. 2015;194(11):5077-5084.

164. Berger T, Rubner P, Schautzer F, Egg R, Ulmer H, Mayringer I, Dilitz E, Deisenhammer F, Reindl M. Antimyelin antibodies as a predictor of clinically definite multiple sclerosis after a first demyelinating event. *N Engl J Med*. 2003;349(2):139-145.

165. Rostami A, Ciric B. Role of Th17 cells in the pathogenesis of CNS inflammatory demyelination. *J Neurol Sci*. 2013;333(1-2):76-87.

166. Croxford AL, Spath S, Becher B. GM-CSF in Neuroinflammation: Licensing Myeloid Cells for Tissue Damage. *Trends Immunol*. 2015;36(10):651-662.

167. Stanley E, Lieschke GJ, Grail D, Metcalff D, Hodgson G, Gall JAM, Maher DW, Cebon J, Sinickas V, Dunn AR. Granulocyte/macrophage colony-stimulating factor-deficient mice show no major perturbation of hematopoiesis but develop a characteristic pulmonary pathology (hematopoletic growth factors/gene targeting/honlus recombtlo/punry dises). *Med Sci*. 1994;91(12):5592-55.

168. Hamilton JA. GM-CSF in inflammation and autoimmunity. *Trends Immunol*. 2002;23(8):403-408.

169. Lacey DC, Achuthan A, Fleetwood AJ, Dinh H, Roiniotis J, Scholz GM, Chang MW, Beckman SK, Cook AD, Hamilton JA. Defining GM-CSF- and Macrophage-CSF-Dependent Macrophage Responses by In Vitro Models. *J Immunol*. 2012;188(11):5752-5765.

170. Roberge CJ, McColl SR, Larochelle B, Gosselin J. Granulocyte-macrophage colony-stimulating factor enhances EBV-induced synthesis of chemotactic factors in human neutrophils. *J Immunol*. 1998;160(5):2442-2448.

171. Miyabe Y, Miyabe C, Murooka TT, Kim EY, Newton GA, Kim ND, Haribabu B, Luscinskas FW, Mempel TR, Luster AD. Complement C5a receptor is the key initiator of neutrophil adhesion igniting immune complex–induced arthritis. *Sci Immunol*. 2017;2(7):eaaj2195.

172. Wolf Y, Shemer A, Levy-Efrati L, Gross M, Kim J-S, Engel A, David E, Chappell-Maor L, Grozovski J, Rotkopf R, Biton I, Eilam-Altstadter R, Jung S. Microglial MHC class II is dispensable for experimental autoimmune encephalomyelitis and cuprizone-induced demyelination. *Eur J Immunol*. 2018;48(8):1308-1318.

173. Ko H-JH-J, Brady JL, Ryg-Cornejo V, Hansen DS, Vremec D, Shortman K, Zhan Y, Lew AM. GM-CSF-Responsive Monocyte-Derived Dendritic Cells Are Pivotal in Th17 Pathogenesis. *J Immunol*. 2014;192(5):2202-2209.

174. Rua R, McGavern DB. Advances in Meningeal Immunity. *Trends Mol Med*. 2018;24(6):542-559.

175. Ye Z, Huang H, Hao S, Xu S, Yu H, Van Den Hurk S, Xiang J. IL-10 has a distinct immunoregulatory effect on naive and active T cell subsets. *J Interferon Cytokine Res*. 2007;27(12):1031-1038.

176. Fleischmann J, Golde DW, Weisbart RH, Gasson JC. Granulocyte-macrophage colony-stimulating factor enhances phagocytosis of bacteria by human neutrophils. *Blood*. 1986;68(3):708-711.

177. Kedzierska K, Mak J, Mijch A, Cooke I, Rainbird M, Roberts S, Paukovics G, Jolley D, Lopez A, Crowe SM. Granulocyte-macrophage colony-stimulating factor augments phagocytosis of Mycobacterium avium complex by human immunodeficiency virus type 1-infected monocytes/macrophages in vitro and in vivo. *J Infect Dis*. 2000;181(1):390-394.

178. Yue F, Cheng Y, Breschi A, Vierstra J, Wu W, Ryba T, Sandstrom R, Ma Z, Davis C, Pope BD, Shen Y, Pervouchine DD, Djebali S, Thurman RE, Kaul R, Rynes E, Kirilusha A, Marinov GK, Williams BA, Trout D, Amrhein H, Fisher-Aylor K, Antoshechkin I, DeSalvo G, See L-H, Fastuca M, Drenkow J, Zaleski C, Dobin A, Prieto P, Lagarde J, Bussotti G, Tanzer A, Denas O, Li K, Bender MA, Zhang M, Byron R, Groudine MT, McCleary D, Pham L, Ye Z, Kuan S, Edsall L, Wu Y-C, Rasmussen MD, Bansal MS, Kellis M, Keller CA, Morrissey CS, Mishra T, Jain D, Dogan N, Harris RS, Cayting P, Kawli T, Boyle AP, Euskirchen G, Kundaje A, Lin S, Lin Y, Jansen C, Malladi VS, Cline MS, Erickson DT, Kirkup VM, Learned K, Sloan CA, Rosenbloom KR, Lacerda de Sousa B, Beal K, Pignatelli M, Flicek P, Lian J, Kahveci T, Lee D, Kent WJ, Ramalho Santos M, Herrero J, Notredame C, Johnson A, Vong S, Lee K, Bates D, Neri F, Diegel M, Canfield T, Sabo PJ, Wilken MS, Reh TA, Giste E, Shafer A, Kutyavin T, Haugen E, Dunn D, Reynolds AP, Neph S, Humbert R, Hansen RS, De Bruijn M, Selleri L, Rudensky A, Josefowicz S, Samstein R, Eichler EE, Orkin SH, Levasseur D, Papayannopoulou T, Chang K-H, Skoultchi A, Gosh S, Disteche

C, Treuting P, Wang Y, Weiss MJ, Blobel GA, Cao X, Zhong S, Wang T, Good PJ, Lowdon RF, Adams LB, Zhou X-Q, Pazin MJ, Feingold EA, Wold B, Taylor J, Mortazavi A, Weissman SM, Stamatoyannopoulos JA, Snyder MP, Guigo R, Gingeras TR, Gilbert DM, Hardison RC, Beer MA, Ren B, Mouse ENCODE Consortium. A comparative encyclopedia of DNA elements in the mouse genome. *Nature*. 2014;515(7527):355-364.

179. Constantinescu CS, Asher A, Fryze W, Kozubski W, Wagner F, Aram J, Tanasescu R, Korolkiewicz RP, Dirnberger-Hertweck M, Steidl S, Libretto SE, Sprenger T, Radue EW. Randomized phase 1b trial of MOR103, a human antibody to GM-CSF, in multiple sclerosis. *Neurol Neuroimmunol neuroinflammation*. 2015;2(4):e117.

180. Gladue RP, Brown MF, Zwillich SH. CCR1 antagonists: what have we learned from clinical trials. *Curr Top Med Chem*. 2010;10(13):1268-1277.

181. Mårdh CK, Root J, Uddin M, Stenvall K, Malmgren A, Karabelas K, Thomas M. Targets of Neutrophil Influx and Weaponry: Therapeutic Opportunities for Chronic Obstructive Airway Disease. *J Immunol Res*. 2017;2017:5273201.

182. Caminschi I, Maraskovsky E, Heath WR. Targeting Dendritic Cells in vivo for Cancer Therapy. *Front Immunol*. 2012;3:13.

183. Macri C, Dumont C, Johnston AP, Mintern JD. Targeting dendritic cells: a promising strategy to improve vaccine effectiveness. *Clin Transl Immunol*. 2016;5(3):e66.